

**A Precision Search for Exotic Scalar and Tensor Couplings in
the Beta Decay of Polarized ^{37}K**

by

Melissa Anholm

A Thesis submitted to the Faculty of Graduate Studies of
The University of Manitoba
in partial fulfillment of the requirements of the degree of

DOCTOR OF PHILOSOPHY

Department of Physics and Astronomy
University of Manitoba
Winnipeg

Abstract

Abstract Goes Here

Acknowledgements

People to acknowledge here include: John Behr, Gerald Gwinner, Dan Melconian.
Also: Spencer Behling, Ben Fenker. Also-also: Alexandre Gorelov, James McNeil.
But additionally: Danny Ashery.

Contents

Abstract	ii
Acknowledgements	iii
Contents	vi
List of Figures	vii
List of Tables	x
Shit To Do	xxxv
1 Background and Introduction	1
1.1 Motivation	1
1.2 The Basics of Beta Decay	3
1.3 Mathematical Formalism	4
1.4 Our Decay	5
1.5 Shake-off Electron Spectrum	7
1.6 Fierz Interference – The Physical Signature	8
1.7 On the Superratio, the Supersum, and the Constructed Asymmetry .	10
2 Considerations and Implementation of Atomic Techniques	11
2.1 An Overview of Magneto-Optical Traps	11
2.1.1 Zeeman Splitting	12
2.1.2 Saturation Spectroscopy	13
2.1.3 Doppler Cooling	14
2.1.4 Atom Trapping with a MOT	15
2.2 Optical Pumping	16
2.3 An Overview of the Double MOT System and Duty Cycle	19
2.4 The AC-MOT and Polarization Setup	22
2.5 Measurement Geometry and Detectors	26
2.6 The Photoionization Laser	29

3	Calibrations and Data Selection	32
3.1	Measurements of the Atom Cloud	32
3.1.1	Measurements with the rMCP	37
3.1.2	Measurements with the eMCP	38
3.2	Data Selection and Preliminary Cuts	39
3.3	Further Cuts Using the DSSD	44
3.4	Further Cuts Using the eMCP	46
4	Simulations	54
4.1	Considerations for Software Upgrade Implementation	55
4.2	The Simple Monte Carlo and Response Function	57
4.3	Simulating the Background	65
4.4	Comparing Simulations with Experimental Data	68
5	Analysis and Estimates of Systematic Effects	71
5.1	Overview	73
5.2	BB1 Radius, Energy Threshold, Agreement	73
5.3	Background Modeling – Decay from Surfaces within the Chamber . .	75
5.4	Quantifying the Effects of Backscatter with Geant4	76
5.5	Lineshape Reconstruction	76
5.5.1	Motivation	76
5.5.2	What is it and how does it work?	77
5.5.3	The Math-Specifics	77
5.5.4	The Results – Things That Got Evaluated This Way	78
5.5.5	The low-energy tail uncertainty, and what it does	79
6	Results and Conclusions	81
6.1	Measured Limits on b_{Fierz}	81
6.2	Discussion of Corrections and Uncertainties	81
6.3	Relation to Other Measurements and New Overall Limits	82
6.4	R_{slow} and Other Possible Future Work for the Collaboration	84
6.4.1	Motivation	84
6.4.2	The Decay Process	85
6.4.3	Current Status	86
6.5	Conclusions	86
Bibliography		87
Appendices		91

A Notable Differences in Data Selection between this and the Previous Result	91
A.1 Polarization Cycle Selection	91
A.2 Leading Edge / Trailing Edge and Walk Correction	92
A.3 TOF Cut + Background Modelling	92
A.4 BB1 Radius	92
B A PDF	93
B.1 JTW	93
B.2 Holstein	95
C Notation	101
C.1 Comparison Guide	101
C.2 Imported from Another Appendix	101
D SuperRatio	111
E Old SuperRatio	114
F Old Super Corrections	116

List of Figures

1.1	A level diagram for the decay of ^{37}K	6
1.2	Levinger TOF	8
1.3	Here's why it's better to extract b_{Fierz} from an asymmetry, in this case.	9
2.1	Components of a magneto-optical trap, including current-carrying magnetic field coils and counterpropagating circularly polarized laser beams. Diagram taken from [2]	17
2.2	An atomic level diagram for the optical pumping of ^{37}K , taken from [1].	18
2.3	The TRINAT experimental set-up, viewed from above. The two MOT system reduces background in the detection chamber. Funnel beams along the atom transfer path keep the atoms focused.	20
2.4	The duty cycle used for transferring, cooling, trapping, and optically pumping ^{37}K during the June 2014 experiment. Not drawn to scale. Question marks indicate timings that varied either as a result of electronic jitter or as a result of variable times to execute the control code. Atoms are transferred during operation of the DC-MOT. Though the push beam laser itself is only on for 30 ms, the bulk of the DC-MOT's operation time afterwards is needed to collect and cool the transferred atoms. After 100 on/off cycles of optical pumping and the AC-MOT, the DC-MOT resumes and the next group of atoms is transferred in. After 16 atom transfers, the polarization of the optical pumping laser is flipped to spin-polarize the atoms in the opposite direction, in order to minimize systematic errors.	22
2.5	One cycle of trapping with the AC-MOT, followed by optical pumping to spin-polarize the atoms. After atoms are transferred into the science chamber, this cycle is repeated 100 times before the next transfer. The magnetic dipole field is created by running parallel (rather than anti-parallel as is needed for the MOT) currents through the two coils. . .	23

2.6	A decay event within the TRINAT science chamber. After a decay, the daughter will be unaffected by forces from the MOT. Positively charged recoils and negatively charged shake-off electrons are pulled towards detectors in opposite directions. Although the β^+ is charged, it is also highly relativistic and escapes the electric field with minimal perturbation.	27
2.7	Inside the TRINAT science chamber. This photo is taken from the vantage point of one of the microchannel plates, looking into the chamber towards the second microchannel plate. The current-carrying copper Helmholtz coils and two beta telescopes are visible at the top and bottom. The metallic piece near the center is one of the electrostatic ‘hoops’ used to generate an electric field within the chamber. The hoop’s central circular hole allows access to the microchannel plate, and the two elongated holes on the sides allow the MOT’s trapping lasers to pass unimpeded at an angle of 45 degrees ‘out of the page’. . .	31
3.1	Photoion Hit Positions in 2D	33
3.2	Photoion Hit Positions at 535 V/cm, as a function of AC-MOT Time	34
3.3	Sumcuts for the rMCP, run 447.	35
3.4	A projection along all three axes for run 447, with various cuts on the rMCP delay line timing sum.	36
3.5	Trap Position along TOF Axis	38
3.6	Trap Position from Camera	39
3.7	Vertical Trap Position from rMCP	40
3.8	rMCP Calibration	41
3.9	Position as measured on the eMCP, after some data cleaning.	47
3.10	Beta-electron TOF, for events with and without eMCP hit position information. A cut will eventually be taken to accept only events sufficiently near the largest peak – in this case the number of events is ‘only’ decreased by a factor of 2.	48
3.11	SOE TOF peaks (eMPC - Scintillator), using the leading edge (LE) and using the trailing edge (TE). Data is sorted according to runset. For each individual runset, the TE peak is broader than the LE peak. The centroid of each runset is also more variable in the TE plots. . .	49
3.12	SOE TOF walk, before (left) and after (right) applying a quartic adjustment to straighten out the effective TOF.	50
3.13	SOE TOF, model and data. In the end, I cut the data to use only events with a TOF between -0.928 ns and +1.416 ns. Max. possible background is like a factor of two too big. Similar quality results no matter how you distribute the Levinger spectra between 4S and 3P, however adding the 0 eV electrons makes a big improvement to the agreement.	51

3.14 Experimental Scintillator Spectra	52
3.15 The superratio asymmetry, averaged over all scintillator energies between 400-4800 keV, is used to compare the experimental data and simulated TOF model as a proxy for the quality of the model to estimate the background. All other cuts have been applied.	53
4.1 Fit to Mono-Energetic Spectrum, 5000 keV	59
4.2 Fit to Mono-Energetic Spectrum, 3000 keV	60
4.3 Fit to Mono-Energetic Spectrum, 1500 keV	61
4.4 Fit to Mono-Energetic Spectrum, 1000 keV	62
4.5 Fit to Mono-Energetic Spectrum, 750 keV	63
4.6 Lineshape Parameter Fits (Part 1)	66
4.7 Lineshape Parameter Fits (Part 2)	67
4.8 Lineshape Parameter Fits (Part 3)	68
4.9 Lineshape Parameter Fits (Part 4)	69
4.10 Goodness of Fit for Modeled Lineshapes	70
5.1 Simulated Beta TOA vs emission angle w.r.t. detector orientation . .	77
5.2 Lineshape Comparison	78
5.3 A_β Position Error	79
5.4 b_{Fierz} Position Error	80
6.1 A superratio asymmetry from the data, and the best fit from simulations.	82
6.2 Some results. I'll want to show at least one of these things. Probably show a separate one for each runset, actually.	83
C.1 "Notes 0"	105
C.2 "Notes 1"	106
C.3 "Notes 2"	107
C.4 "Notes 3"	108
C.5 "Notes 4"	109
C.6 "Notes 5"	110

List of Tables

3.1	Cloud Position and Size	37
3.2	List of Runs	42
3.3	List of Electron Runs	42
5.1	Error Budget	74
C.1	Kinematic Terms Guide	102
C.2	Angular Momentum Notation	102
C.3	Multipole Notation	103
C.4	Selected Integrals from Holstein's Eq. (51)	104

■ John wanted this change (now implemented), but I think the phrasing is unclear now.

...

"and we shall be interested especially in scalar (S) and tensor (T) couplings." -> "our observable is mostly sensitive to scalar (S) and tensor (T) couplings."

2

■ According to present limits, these couplings would have to be pretty small relative to the (V) and (A) couplings.

2

■ Need to figure out how the exotic couplings actually work, mathematically. What the fuck does " $(V - A)$ " even *mean*? IIRC John wants a brief mention of γ_5 's and γ_μ 's, and probably a brief mention of whatever mumble-mumble group is mumble-mumble represented or something.

...

JB says:

the current transforms like a Lorentz scalar or tensor – this does not refer to the angular momentum.

If you write down the Lagrangian for beta decay, that's enough. All these things refer to the structure of the Lagrangian. The theory considers all possible Lorentz transformations of the currents.

Please don't talk about $SU(2) \times U(1)$ for electroweak unification. It's textbook material that's beyond the scope.

2

■ JB on intuitive concepts that are missing:

The SM couples to left-handed neutrinos and right-handed antineutrinos. Since the neutrinos only have weak interactions, there are no right-handed nu's nor left-handed antinu's in nature. The neutrino asymmetry B_ν is a number with no energy dependence.

Similarly, the SM weak interaction only couples to right-handed positrons and left-handed electrons. Since these are massive particles, the average helicity of positrons is not 1, but instead v/c. One can always boost to a frame where the positron keeps its circulation but is moving in the opposite direction. This is why the beta asymmetry is A v/c, not just A.

The Fierz term's additional energy dependence of m/E also comes from helicity arguments, stemming from the fact that it still is coupling to SM nu's and antinu's only, so the beta's are generated with wrong handedness. The details are built at 4th-year undergrad level in Garcia's paper with his student and postdoc [4].

The beta asymmetry dependence on the Fierz term only comes through the normalization of $W(\theta) = 1 + b_{\text{Fierz}}m/E + A_\beta \cos(\theta)$.

i.e.:

$W'(\theta) = 1 + A_\beta/(1 + b_{\text{Fierz}}m/E) \cos(\theta)$. (the angular distribution must be unity where cos(theta) vanishes, by definition).

2

■ Is this even true? The pointlike thing? ...No. No it's not.

3

■ JB says: The title of Holstein's review addresses this "pointlike" issue, and he describes the "impulse approximation" in Section V. The interaction is not pointlike, because all constants are a form factor expansion in q^2 – finite size terms contribute to the Coulomb correction.

3

■ In beta decay, a proton(neutron) within a nucleus decays into a neutron(proton), and emits a positron(electron) and neutrino(anti-neutrino). The new neutron(proton) remains bound within the nucleus. As always, momentum and energy must both be conserved. The distribution of energy and momenta is, of course, probabilistic rather than deterministic, and with three bodies involved, the full probability distribution for the momenta of outgoing particles cannot be written in closed form. However, because the nucleus is significantly more massive than either of the other two outgoing particles, the great majority of the released kinetic energy is distributed between the leptons, while the nucleus receives only a tiny fraction of the total. This feature lends itself to an approximation in which the energy of the recoiling nucleus (recoil) is neglected entirely, and the decay may be described only in terms of the momenta of the outgoing positron(electron) and neutrino(anti-neutrino), as in JTW [5]. The terms that have been neglected in this treatment are sometimes called ‘recoil-order corrections’.

..

Unfortunately, the outgoing (anti-)neutrino is very difficult to detect directly, and we make no attempt to do so in this experiment. Instead, we might look for coincidences between an outgoing beta and a recoiling nucleus, and use that information to reconstruct the kinematics of the neutrino.

4

■ Do it! Do the master equation!

5

■ JB: cut "so we will simply provide the combined master equation here"

Don't. The equation you have is all you need.

5

■ JB: on 2.3 (now 1.4), "Our decay": Just put the comments in. Keep the figure as-is.

MJA: Pretty sure the comments are literally copy-pasted from somewhere I shouldn't just plagiarize from. Need to rephrase it at least. ...No, it's fine, it's just from my old thesis proposal. I think. Removed now from that section, so it can go here.

5

■ Talk about how great ^{37}K is for what we're doing with it. Also, drop all the math-numbers to support those assertions. Reference the level diagram within the text!

6

Also, ^{37}K is a really nice isotope for this, because $98\% + 2\%$, also because it's a mirror decay, also because it's an alkali. Also-also, its big A_β value means we have a big thing to multiply any b_{Fierz} value there might be when we construct the superratio asymmetry to eliminate systematics.

6

JB on 2.4 SOE:

Say what you did, with as little info as possible now. Georg is a theoretical chemist, so he may be very curious about this.

...

"Atomic electrons with kinetic energies 0 to 100 eV are produced as part of the beta decay process. If their energy is below a certain value, our detection process is not perturbed, so we provide physics about the energy spectrum here.

...

Levinger [6], assuming the sudden approximation, calculated the overlap between an electron in the initial atom with an outgoing electron or an electron in the final atom. Levinger approximated everything with hydrogenic wavefunctions, so his calculations become analytic. The collaboration has found that Levinger's formulae fit our measurements of the position and TOF info of our atomic electrons, so they are used in our simulations

OR

but the precise energy spectrum was found to be unimportant, so we used X in our simulations.

whichever is true.

...

This is then fine. You have most of the basics down.

7

Really, just discuss the physics of what happens to cause SOEs to be a thing.

Talk about *our* SOE spectrum in some other chapter later. Should this go in the atomic physics chapter? I can't decide whether it's more atomic or more nuclear.

7

Should I talk about the distribution of how many SOEs come off in a decay?

I have measurements of the recoil charge distribution, which is related but not really the same thing. From a theoretical POV, I don't know how many get shaken off. Thankfully, it doesn't matter very much in the end.

7

█ JB on that missing figure that I've now put in: "A dependence of Abeta on beta energy is also introduced.	
UCNA fits energy spectrum and Abeta[Ebeta] simultaneously now." . . .	8
█ The point is, the presence of either scalar or tensor interactions will produce a b_{Fierz} term in the decay PDF. It has other effects on the PDF, but those come in at higher-order in the tiny scalar and tensor couplings. So, the Fierz term would be by far the biggest thing that changes in the PDF. The PDF describes the energy and momentum of the outgoing beta w.r.t. a variety of other things. Notably, we can write an elegant-ish description of beta momentum w.r.t. nuclear polarization direction, and ignore the neutrino completely after integrating over it. We have a PDF in beta <i>direction</i> (w.r.t. polarization), and beta <i>energy</i> . To lowest order (and lowest order is best order) the distribution w.r.t. polarization direction doesn't change, but the distribution w.r.t. energy does change. Or ... something? The point is, it makes a change in the beta energy spectrum. This change is most pronounced at low energies, because the Fierz term is scaled by $(1/E_\beta)$. However, the asymmetry is also a function of E_β . A different function of E_β . In fact, it is scaled by (p_β/E_β) within the PDF, which is distinctly different than b_{Fierz} . So, one might ask what effect a b_{Fierz} term would produce on a constructed asymmetry spectrum.This explanation has gone way off track.	8
█ Here's a reference to the picture that shows the result of a non-zero b_{Fierz} term. It's Fig. 1.3.	9
█ JB: You need to at some point say that the supersum is the beta energy spectrum. There are experiments trying to do this method better, but they are very difficult. UCNA published a combined energy spectrum and Abeta[Ebeta] analysis on the neutron in March 2020 [8].	10
█ I can't help but also notice the follow-up article from September 2020 [9]. Ugh.	10
█ Possible Supersection: General Considerations of Atomic Techniques Used	11
█ I need to organize the sections/subsections in this chapter better.	11
█ Have I defined TRINAT yet?	11
█ Possibly most of the above paragraph is also written/paraphrased elsewhere. Like in ((Ch.2B)), unless I removed it.	11

■ “In order to understand the mechanism by which a MOT is able to confine atoms, we must first introduce the Zeeman effect (Section 2.1) and a description of an optical molasses (Section 2.2). A functional MOT combines the forces resulting from these two mechanisms to trap and cool atoms.”	12
■ Needs a level diagram. Maybe.	12
■ When this is combined with a circularly polarized laser beam, the effect is to move the atomic resonance closer to- or farther from- the frequency of the laser. The circular polarization, combined with some selection rules, means a circularly polarized laser will only couple to one particular transition, w.r.t. angular momentum. ie, for a σ_+ polarized laser, the atom’s overall angular momentum projection (along some axis) will be incremented by +1. The Zeeman shift means that in a magnetic field, this transition ($M=+1$) not be the same as the $M=-1$ transition. So, if you have a magnetic field that changes linearly across space, you can make it so that in $+B_z$ regions, the laser beam with one certain polarization is closer to resonance and therefore more likely to be absorbed – and similarly, in $-B_z$ regions, a different laser with the opposite polarization will be more likely to be absorbed. Again, if the B-field is linear in space, you can do it so that as the atoms get further and further from the ‘centre’ region, the effect gets progressively stronger. So, if you’ve done this right, you can make it so that the atoms get a stronger “push” back towards the center the farther away they’ve drifted.	
They still get the optical molasses cooling effect for free.	12
■ JB says: Chapter 3 (that’s this chapter) ((Now Ch.2A)): Starting in Ch. 3 around p. 10, "Atom-Photon Interactions with a Laser" (that’s this section – now “Saturation Spectroscopy”): You need to do a careful pass through it and omit everything you don’t understand and don’t need. Sorry, there is no longer time to resolve your questions unless you need them.	13
■ This is a stupid subsection title.	13
■ Also, if the photon is tuned close enough to atomic resonance, with absorption being more likely the smaller the detuning is...	13
■ Fixed description of which lasers are saturated.	14

■ Do I need to mention saturation at all? It's probably not really necessary, and I don't *think* anything else in this section is wrong per se. But maybe better to just cut it.	14
■ ...and opposite polarization. Or something. I have to talk about the selection rules somewhere else.	15
■ Optical molasses equation? Maybe?	15
■ "...This will slow the atom down, at least up to a limit related to the linewidth of the atomic transition and/or the laser. There's something to look up."	15
■ Removed 'Angular Momentum and Selection Rules' section. Because it was super wrong.	15
■ JB: on 3.3 (now 2.3) "Atom Trapping with a MOT" ((that's here!)): The content and scope are ok, but the informal phrasing is going to confuse people. You have to pay some attention and rephrase these sections.	15
■ Do I *have* an equation I can put here? Surely there must be one somewhere, but I really don't want to dig it up, and I don't think it's really necessary.	15
■ Needs work.	16
■ Do I *really* need to bring up the repumper? I don't wanna. Maybe I can just mention it and move on or something.	16
■ Removed 'Photoionization as a Probe' section from the 'Intro to Atomic Physics' section, because John says it's horribly wrong anyhow. Plus, it's redundant with the 'Photoionization Laser' section (2.6).	16
■ Direct quote from John follows below:	16
■ End quote from John. But also!: "...Then you can refer to that (ie, John's red quoted mini-blurb about optical pumping, (which I may relocate to Sec. 2.6? Or not?) in section 3.4 (now 2.4, about the AC-MOT – ie, Sec. 2.4, (even though I might remove that section entirely and put all its content into Sec. 2.4)), where you're trying to now but the phrasing is poor."	16

■ “Until recently, one limitation of such samples was the necessity for the presence of a relatively large magnetic field, which is expected to partially destroy atomic polarization, limiting the precision of many types of measurements. Here we discuss the construction of a newer type of MOT, the AC-MOT, which minimizes residual magnetic fields. The guys in [7] came up with the idea of the AC-MOT. They made it work and did some stuff with it. Good for them.”	16
■ Somewhere later, I can talk about photoionization? Or should it be here, in this chapter? Surely it should at least get a different section though. . .	18
■ Do I need a MOT level diagram too?	18
■ Describe what’s going on here!	18
■ JB says: “I would say you don’t need an atomic level diagram. You could just describe in words the semiclassical picture of atoms absorbing photons until they are nearly fully polarized, then they stop absorbing. The optical pumping + photoionization is then an <i>in situ</i> probe of the polarization. . . You would need to add in words that quantum mechanical corrections to this picture are in the optical Bloch equation approach in B. Fenker et al. The depolarized states still have high nuclear polarization ($1/2$ for $F = 2, M_F = 1$, $5/6$ for $F = 1, M_F = 1$) and determining the ratio of those two populations provides most of the info we need – we model with the O.B.E, measure the optical pumping light polarization, and float an average transverse magnetic field. This is adequate to determine the depolarized fraction to 10% accuracy, which is all that is needed.” . . .	18
■ JB: ...You could call the first half of such a chapter "General considerations of Atomic techniques used" and the 2nd half "Experimental Implementation of Atomic Techniques used"	19
■ Supersection: Experimental Implementation of Atomic Techniques Used . .	19
■ Remember the pulser LED! To evaluate the stability of the scintillator gain!	19
■ JB says: chapter (((this section))) is really good, and in good shape for the committee	19

■ We obtain a sample of neutral, cold, nuclear spin-polarized ^{37}K atoms with a known spatial position, via the TRIUMF accelerator facility, by intermittently running a magneto-optical trap (MOT) to confine and cool the atoms, then cycling the trap off to polarize the atoms. With β detectors placed opposite each other along the axis of polarization, we are able to directly observe the momenta of β^+ particles emitted into 1.4% of the total solid angle nearest this axis. We also are able to extract a great deal of information about the momentum of the recoiling ^{37}Ar daughters by measuring their times of flight and hit positions on a microchannel plate detector with a delay line. Because the nuclear polarization is known to within < 0.1% [1], and we are able to account for many systematic effects by periodically reversing the polarization and by collecting unpolarized decay data while the atoms are trapped within the MOT, we expect to be well equipped to implement a test of ‘handedness’ within the nuclear weak force.	19
■ Surely most of this paragraph goes in an intro chapter somewhere.	19
■ Cite a bunch of papers here.	20
■ Figure was originally created by Alexandre, modified by ... someone else? Or Alexandre? And I got it from ... probably an experimental proposal? I should figure out how to cite a proposal.	20
■ Mumble mumble UHV. Mumble mumble tail end of the Boltzmann distribution.	21
■ discussed ... idk, somewhere else.	21
■ I *do* discuss this, right? Right??	21
■ How to segue here? Do I... Cite myself? Cite Harvey+Murray? Reference the next section? Reference the previous chapter? This is clunky and stupid.	21
■ JB on Ch. 3.4 (now 2.4) ((now Ch. 2.4)) “The AC-MOT” (that’s this section!): The content and scope are ok, but the informal phrasing is going to confuse people. You have to pay some attention and rephrase these sections.	22
■ John suggests that maybe I should just refer directly to his red, quoted OP blurb in the chapter about the AC-MOT.	22
■ How much do we lose? Have we quantified that somewhere? Probably. . .	23
■ begin content of the historical other AC-MOT+Polarization section.	24

■ Probably document things about the waveform and frequency used for the beamtime, since I don't think it's in my MSc.	24
■ John objects to the phrasing of the following paragraph, because you fundamentally need polarized atoms to measure b_{Fierz}	24
■ Plus, it barely makes sense to talk about measuring b_{Fierz} if you don't know A_β	24
■ End paragraph that John hates.	24
■ JB says: "Since you worked hard on the logic triggers, a photoion spectrum with duty cycle would be appropriate if you want."	24
■ Note that because the atoms within a MOT can be treated as following a thermal distribution, some fraction of the fastest atoms continuously escape from the trap's potential well. Even with the most carefully-tuned apparatus, the AC-MOT cannot quite match a similar standard MOT in terms of retaining atoms. The TRINAT AC-MOT has a 'trapping half-life' of around 6 seconds, and although that may not be particularly impressive by the standards of other MOTs, it is more than adequate for our purposes. ^{37}K itself has a radioactive half-life of only 1.6 seconds (cite someone), so our dominant loss mechanism is radioactive decay rather than thermal escape.	25
■ At some point I have to decide if that's going to be a section or a subsection.	25
■ JB says of ((Sec. 2.5)): first few paragraphs are poorly phrased. You have to fix those. Most of the rest looks really good.	26
■ This section is really disorganized.	26
■ Possibly needs more diagrams? Possibly just needs more words.	26
■ ... (shown in Figure 2.7)	26
■ There's gotta be a better way to describe it	28
■ what's the open area of the detector? how big is each pixel?	28
■ Wait. Am I repeating myself?	29
■ Chapter 4.4 (this section! now 3.4) (((2.6))) is very good and complete, showing you understand what is needed about photoionization. A good reason to omit 3.5 'photoionization as a probe' as I said above.	29
■ Probably worth mentioning that we test this stuff offline on stable ^{41}K	29
■ JB: "you could reference the letter for the value of the field 150V/cm."	29

■ As a check: the camera measurements for photons from de-excitation. It's aimed 35 degrees from vertical, with its horizontal axis the same as one of the other axes. I think it's the TOF axis. I can check this when my computer comes back. Also, there's an unknown additional delay between some of our DAQ channels that can't be explained by accounting for cable lengths, so we really like having the check there.	29
■ JB says: "yes, camera x-axis is tof axis."	30
Figure: Show individual beta energy spectra. ...with a variety of different cuts, perhaps?	32
■ I have some tables summarizing which types of data were measured. Presently, that's in Ch-4 (now ch.3), but probably I should move it here.	32
■ Content that previously was in this subsection is now in Section 2.6. But also, see Section ???. Probably in this section here, I need to just jump right in assuming everyone understands the physical principle of how the data works. Then, I can talk about what the data *is*, and how it gets interpreted.	32
■ Trap position – Measured using the same dataset that was used to quantify the polarization. The trap drifts slightly over the course of our data collection. Describe the rMCP calibration needed to extract this info. . .	32
■ Polarization measurement was conducted on a different set of data, collected in between the measurements used for A_β and b_{Fierz} , and at a higher electric field, because we were unable to run both our MCP detectors simultaneously.	32
■ This figure needs to be discussed in text or whatever.	33
Figure: Need pictures of the cloud. Possibly need projections of the cloud as a function of time, for AC/OP cycles.	33
■ This figure needs to be discussed in text or whatever.	34
■ This figure needs to be discussed in text or whatever.	35
■ Also, we noticed the trap drifting after one of the runs, because one of the batteries on one of the thingies adjusting the laser frequency (I think) was failing.	35

■ JB: "If we rejected the data with the MOT moving (indeed a battery determining the voltage controlled oscillator frequency offset between absorption in stable ^{41}K cell and the ^{37}K resonance) then that's all you need to say."	35
■ describe how you'd turn this into a physical description of the cloud, with like a temperature and a sail velocity and shit. with equations.	35
■ This figure needs to be discussed in text or whatever.	36
■ Sig figs here need work.	37
■ Potential new subsection: the camera? Otherwise it has to go here.	37
■ JB: eMCP. You need to describe the timing information obtained. You also need a statement of whether or not you used the position information in your cuts.	39
■ We now consider how to clean up our data. We make some fairly obvious, intuitive cuts, and those are described here. Later, we'll make less intuitively obvious cuts.	39
■ 'The observant reader may find it curious that the listed runsets start at "B" and continue alphabetically. There was initially a "Runset A" collected as well, however it was determined later that this data could not be salvaged for use in the final analysis because one of the scintillators had its hardware threshold set above the compton peak, and without that reference point an accurate calibration could not be performed.'	41
■ MUST check to make sure I didn't use Run 420 in "good runs" in the end!!!	42
■ Ugh. My categorization system is slightly different than Ben's on the later recoils. That's annoying.	42
■ Other things I could list here: Electric field strengths, total runtime.	42
■ This table might eventually go away. Mostly I just want a record of the total 'good' counts. In total, $N = 399,365$	42
■ also discussed: how we decide what counts as an eMCP hit at all	43
■ Awkward stupid phrasing.	43
■ Also, we claim that it doesn't bias the data. Much. Didn't I try to evaluate how much it biased the data at one point?	43
■ change by 0.2% of its value vs change by 0.5% of its value, according to Ben's thesis pg 143.	44
■ Pretty sure I'm repeating myself from Chapter ??	44

■ JB says: To repeat a comment, since the Appendix on analysis changes is being dispersed throughout, when you state somewhere (I think it's in Ch. 6)((5?)) make sure you state clearly that the only change for BB1 cuts is the radius cut, e.g. that you took the same T and E from the waveforms (I'm not even sure whether the waveforms are recorded anyway). You ask 'how can I state this' but there's no reason to be subtle. Just say upfront that Ben and Spencer's theses did all the groundwork on the BB1, and here you include selected details needed to understand the present analysis. If you need to include some redundant material, don't worry too much about that.

...

MJA: In fact, I think the BB1 radius may have been the same. The uniform energy threshold was different though. But I get the point.

...

Also, yes, the waveforms are absolutely recorded in the MIDAS files but they haven't been saved to modern ntuples, because they made the files huge. I think it's probably pretty easy to switch that on/off in the Analyzer though to generate a set of ntuples that has that info included.

44

■ How do I *say* that Ben was the one who did most of the DSSD calibration stuff? I maybe don't need to describe all of it here, but I *could*, and maybe it's needed in order to understand like 4 rows in my error budget.

45

■ JB: "You can describe anything you did differently or improved, but you can and should otherwise defer all details of the scintillator calibration and DSSD calibration to Ben's paper and his thesis and Spencer's. E.g. Section 5.2 "statistical agreement between BB1 X and Y detectors' energies only makes a small effect on results" does not need the technical details beyond that statement."

45

■ JB: "If you have some way of documenting the coding you used, that would be great." ... yeah, it would, wouldn't it?

45

■ I think Ben might have selected 60 keV? That's maybe something for the appendix.

46

■ Did I even mention the collimator? Like, in the previous chapter or something..?

46

█ Also-also (did I mention it already?) look for events with only *one* DSSD hit (two could indicate the beta scattered back out of the detector in another pixel, or alternately an accidental coincidence of two beta decay events. either way, no good for analysis.) Also, only one scint hit, and it has to be the on the same detector with the DSSD. (...A scintillator hit as indicated by a TDC readout, as well as a max. recorded scint energy for the “extra” scintillator at something stupidly tiny, like 10 keV. Probably *actually* 10 keV.)	46
█ After all other cuts – not before!! – we eventually use only events with scint energy between 400 - 4800 keV. High cutoff is because of the low number of events, which makes the observable—the superratio asymmetry—poorly defined and poorly behaved. Low cutoff is because it’s really hard to model what’s going on down there to the required level of precision. The observable depends most heavily on low beta energy events, so it is imperative that the lower energy portion of the spectra be thoroughly understood if they are to be used for analysis.	46
█ Somewhere I should list what the energy cutoff is for this spectrum. Or semi-equivalently, the Q-value.	46
█ I described the HEX-75 somewhere in a previous chapter, right??	46
█ Do I need to describe MCPs and delay lines somewhere? Maybe not...	46
█ This picture is ‘slow’. Need to re-save it as a png.	47
█ Um. Did I for sure get the labels correct on this??? It seems really wrong.	48
█ The LE spectra allows for us to use a more precise model of the SOE TOFs, so that’s nice.	48
█ This goes in that one appendix, if I haven’t already put it there.	49
█ “...removing X fraction of the remaining events.”	49
█ Probably need to put that figure somewhere else.	49
█ “To check the agreement of the model with reality, we compare the averaged superratio asymmetries from both, as in Fig. 3.15.” probably goes in the other section.	50
█ I think I want this picture to go in some other section.	53
Figure: Show simulated spectra separated by scattering category.	54

Figure: Show SimpleMC spectra, show the supersum, show the superratio, show the superratio asymmetry. Maybe do some simple fits to show how much better the superratio asymmetry is than <i>not</i> the superratio asymmetry.	54
■ John says: “I doubt I will have further useful comments on the Ch. ((this chapter)) as they are now.” – Yeah, but *now* he will.	54
■ because for A_β even a BSM interaction will *basically* look like a SM interaction, and I think something somewhere isn’t precise enough to distinguish it.	55
■ which other corrections? coulomb and/or radiative corrections, but somehow when I say that, I’m apparently talking about a different thing than everyone else who uses those terms. also, weak magnetism. also ... ??? .	55
■ Is this true? Does it not include *any* BSM interactions?	55
■ Furthermore, although it is currently understood that the weak interaction is predominantly or perhaps entirely ‘left-handed’, the JTW treatment leaves certain phase angles unfixed, and is therefore able to accurately describe a decay which is, for example, partially ‘right-handed’ – however the latter feature is not directly relevant to the project at hand. [It’s several phase angles in JTW, but maybe it’s fundamentally only like one angle on some level? Also I think it’s not actually a “gauge freedom,” per se. No, I’m pretty sure this ‘phase angle’ description is all wrong.] Also, consider time reversal! Anyway, most of this paragraph probably goes better in Section 1.3.	55
■ Surely I describe what recoil-order corrections even *are* in some appendix somewhere, right? Or, possibly, in Section 1.3. Possibly the paragraphs above need to be moved...	56
■ Things that the G4 simulation did that I kept include: an accurate representation of the complex details of our experimental geometry. Also, the noise spectra on the DSSDs.	57
■ Reference previous section where I discuss this, maybe?	57
■ See: Some other section? Maybe?	58
■ somewhere I have to talk about the empirical noise spectrum etc. on the BB1s. Or maybe I’ve already mentioned it somewhere.	58

- Do I need the angular distribution in the end? I think maybe I put in scattering later, and just used a cone for the first round. I re-did this to do the opposite thing at some point. 58
- It's clear that the model goes to shit at low energies. I don't really get it. Anyway, we'll never even *look* at events with scintillator energy below 400 keV, so at the very lowest energies it doesn't matter. Though, it gets bad before we get that low in the spectrum. Sadly. 58
- Parameters alpha, beta, gamma, delta, W, k, and functions $f_1()$, $f_2()$, $f_3()$, $f_4()$, $f_5()$ are named that way because we're following Clifford. Exact definitions of the functions aren't really identical though, and my parameters don't necessarily have the same normalization. Qualitatively, all the same features are there though. Also, the moyal function isn't from Clifford, because ... reasons.
...
In particular, Clifford's treatment describes the measured energy (which in their case is a sum of scintillator energy and DeltaE energy) for beta particles interacting with a detector with a collimator, much like ours, however in our case, some energy is lost to the intervening SiC mirror and beryllium foil, and as we don't measure that directly, it can't be directly added back in. Although we might add back in the energy from the BB1 detectors, we have to model other energy losses in similar materials anyway, and as previously mentioned, re-introducing the energy from the BB1s invites problems with maintaining a uniform energy threshold over the entire detector. 59
- Obviously, from a physical standpoint, the initial beta energy E_0 must be positive, but the response function still includes several expressions of the form, $|E_0|$. This is not done by accident, but rather is an intentional adjustment used to encourage the parameters to behave well within a fit. 64
- ... Similarly, Clifford doesn't include a compton edge. I think. But I want to. 64
- Needs a picture of the *full* beta energy distributions that come out of the lineshape thing. To compare with (a) data and (b) G4. Probably a superratio in there somewhere too. 64

█ Um. Which of the scattering things did I actually put in at the end? And when did I do it? Like, how did I account for (back-)scattering? I tried with/without scattering, I think? and eventually decided not to do it. for some reason. I think it breaks normalization in some way that's more subtle than you would think.	64
█ Reference Section 3.4	65
█ What even <i>is</i> the thing plotted below E_0 in the ‘residuals’ spot, you ask? It’s ‘PseudoE’, which describes the difference between the original input energy, E_0 , and the energy where the output spectrum is maximal. Or something. To ‘pretty good’ order, it’s a straight line. the ‘PseudoE’ plot shows what’s left after you fit it to a straight line. It’s fucking weird that it’s negative everywhere. Like, what?	66
█ Total good events after all the cuts: Set B: 173,640 Set C: 18,129 Set D: 207,596 – All Runsets: 399,365	68
█ How many DOF for these things? I should put it on the picture.	70
Figure: Show simulated spectra separated by scattering category.	71
Figure: Show SimpleMC spectra, show the supersum, show the superratio, show the superratio asymmetry. Maybe do some simple fits to show how much better the superratio asymmetry is than <i>not</i> the superratio asymmetry.	71
█ John proposes an intro statement for this chapter (by which I really mean that other chapter, but I’m pretty sure it goes here now). But anyway, the following two paragraphs are a direct quote from him:	71
█ JB: “I doubt I will have further useful comments on the Ch. (((this chapter))) as they are now.	72

■ JB:

I've tried to email you the paragraphs on "collaboration determination of uncertainties" for (((Ch. 5)))

My intent of all that other advice was to keep your time spent on Chs 1-4 ((Now Ch. 1-2)) concise, so you could concentrate on these real jobs.
(n.b.: the advice he's already sent was almost all about chapters 1-4, which are the various intros/background info and experimental setup stuff)

...

I can only say that if you have an equal choice between including a detail or not, pick "not." "

72

■ JB: I will try to schedule meeting with Dan for you to show us the final version of (((Ch. 5))) Estimating systematic effects soon.

72

JB says:

A simple estimate from the collaboration that builds intuition for this result: Scatter in the SiC mirrors and DSSD actually produces an efficiency change at low beta energy. Energy loss is not minimally ionizing in these structures, and instead will have a long Landau tail that can take events below energy threshold in the scintillator. The collaboration has modelled explicitly the false asymmetry as a function of Kbeta between 600 and 1300 keV, producing roughly $(K-0.6 \text{ MeV})/(0.7 \text{ MeV})$, i.e. 50% at $K\beta=0.95 \text{ MeV}$. This efficiency degradation would be distributed roughly equally between the SiC and DSSD. If completely ignored, this would introduce by inspection a false bFierz of approximately 0.5. Scattering effects will vary between linear and $\sqrt{\text{thickness}}$, so assuming worst case of linear, the mechanical thickness uncertainty of 5 micron/300 micron and 6 micron /275 micron, an average of 2%, making a random contribution of order 0.01 each. The Be window has larger mechanical thickness uncertainty of 23micron/229 micron, but energy loss and scattering in this material is 5x smaller, so the net effect would be similar.

...

To minimize this systematic for future experiments, the collaboration has implemented pellicle mirrors of negligible thickness, 100 nm Au on 4 micron kapton. The collaboration is also implementing Be-windowed wire chambers in place of the DSSD.

...

MJA:huh?

72

It's actually not nearly as big as I'd originally expected. It's huge in the lineshape thing, but pretty tiny in everything else.

73

from John: "I used Ben's threshold when determining the uncertainty from the lineshape tail (UFTLT). If you're saying the UFTLT depends on the threshold used, ok, of course it does. But if you're claimiing that UFTLT depends on the **uncertainty** of the threshold, that's manifestly smaller than the UFTLT itself, and I'm going to assert it isn't worth evaluating."

73

- █ JB: I hope the discussion is clear in your head. Any effect that relies on scattering computation in G4 should have an uncertainty on order 10% of the correction – hopefully you are keeping a distinction here between the finite geometry acceptance (which I guess is exact) scattering off the collimator. 73
 - █ As per JB's comment in section 3.3: "statistical agreement between BB1 X and Y detectors' energies only makes a small effect on results" does not need the technical details beyond that statement." 74
- Figure: Surely this requires at *least* one image of the pixelated BB1 data. Maybe some of a few waveforms and energy distributions too.Feels like cheating to include some of that stuff, since Ben was the one who actually used it mostly. 74
- █ JB on missing figure: "if you used such an image as part of your uncertainty estimate, yes [include it]" 74
 - █ Remember: There's noise applied to simulated BB1s, matching some spectrum. 74
 - █ JB: The simulations of course include it event-by-event, not just a minimally ionizing average loss. 75
 - █ JB on figures that might go here: Figure 6.4 (currently that picture of the TOF spectrum) could either be here, or you could reference it from here. The TOF histogram is a great start. Adding the asymmetry[TOF] indeed would be vital. 75
- Figure: Show the "average asymmetry" (all energies) as a function of TOF, with real data, best model normalization, and extrema of model normalizations. Show our cut. Turns out, it's a lot of work for a really tiny correction. Oh well. 75
- █ JB on the *actual* figure I had been planning to put here, and my remarks about it: Indeed it will be critical to show a clear compelling version of this figure in thesis and in a paper. It was vital to minimize and determine this background to avoid fitting a polynomial to it from the wings, even more so for the energy dependence of A than for its average – you should say so.
...
The reason the correction is small is because of all your hard work. 75

JB: "I wouldn't call these "scattered" events... that's very misleading."

...

Yeah, I should really stop doing that.

...

Wait no, scattered is what I mean! But fine, my phrasing is really unclear. 75

JB: Please comment on whether or not it was important to have this energy distribution. 75

JB says: I would say you have a well-determined TOF cut to minimize this error— a cut that could not have been done blind without an unreasonably perfect simulation. Thus the exact spot of the cut should not be considered to introduce a systematic. 76

I think I'm going to put most of the content in this section into the 'Simulations' chapter (Section 4.2) instead. I really need to just mention it here (Sec. 5.5) and give an indication of how good the result is. Then evaluate stuff. 76

JB: so it's still critical to write down more of the lineshape work. 78

JB: yes, brems strahlung is 'braking radiation' so gets 2 ss's. the lineshape tail in any scintillator also includes backscattered events – we are not claiming the 2-pixel cut is complete 78

Here is Subsection 9.5.5 "The low-energy tail uncertainty, and what it does" complete. There should be no figure.

Direct quote from John follows in the next two paragraphs. Maybe I should paraphrase, but it's so nicely written! 79

JB: Dan and I independently discussed (((Ch. 6))) yesterday, and he has suggestions to help. So I will also schedule a meeting with Dan and you to discuss (((Ch. 6))) Results and whether the S,T part must be deleted and left to a paper. You don't have enough time, and although this should be quite straightforward, it is not your critical result and it's the only thing that can go. 81

John says to just skip doing the C_S and C_T stuff, for now. No time. Really, C_S is already basically done, but then that'll lead to awkward questions about C_T 81

Just write a blurb to qualitatively summarize a bunch of the stuff in Ch. 5.
Do I want to put my error budget table here? If not, here it is! (5.1). 81

█ Other things to discuss here: which things are dominant error sources, and how viable it would be to improve those for future experiments.	81
█ JB says: To put your work in context, please add at the end of that minimal S,T section, or at the end of "Our Decay" section	
...	
The best existing measurement of b_{Fierz} is in the decay of the neutron [11], $b_{\text{Fierz}} = 0.017 \pm 0.021$, consistent with the Standard Model prediction of zero. Our measurement is strongly related, yet complementary. In terms on non-Standard Model Lorentz current structures, to lowest order in the non-SM currents the same equation applies:	
$b_{\text{Fierz}} = \pm (C_S + C'_S + (C_T - C'_T)\lambda^2)/(1 + \lambda^2)$	
(the plus is for β^- decay and the - for β^+ decay) [5]. [to be continued...]	82
█ [...continued from prev.]	
In our ^{37}K case, $\lambda^2 = M_{\text{GT}} ^2/ M_F ^2$ is close to $3/5$ (the expected value $j/(j+1)$ for a single $j=3/2$ d $3/2$ nucleon) [12], while for the neutron λ^2 is close to 3 (the expected value for an $(j+1)/j$ $j=1/2$ s $1/2$ nucleon). $ M_F $, the Fermi matrix element, is nearly the same for both of these isospin = $1/2$ decays (the largest correction is the larger isospin mixing of ~ 0.01 in ^{37}K). So our observable is relatively less sensitive to Lorentz tensor currents, and will predominantly constrain or discover Lorentz scalar currents.	
...	
Full considerations would require a weighted fit of b_{Fierz} experiments and similar observables [?], and are beyond the scope of this thesis. The info from this thesis, values of A_β and b_{Fierz} with their uncertainties, can together with the known fT value (lifetime and branching ratio) allow the community and/or the collaboration to include the results in a future constraint or discovery of scalar and tensor Lorentz currents contributing to β decay.	82
█ John says the whole R_{slow} thing should go in here somewhere.	84
█ Appendix I keep, it's excellent. It should be moved as is to Conclusions under "Future Experiment for the collaboration"! so people know you worked so hard on it!!	84
█ The citation format I'm using is really stupid. You must force yourself to ignore this right now, Melissa!	90

■ Removed some appendices:	
- Very Obvious Things (on lifetimes and half-lifes)	
- On Beta Endpoint Energies ("notationandprelimintegration")	
- Wong Nuclear	
- HowTo Lifetime	91
■ JB says Appendix A should all go in the analysis section, and not in an appendix at all.	91
■ JB says: Appendix A (ie, *this appendix*) is very important, and should at least be a subsection in the Analysis chapter.	
...	
You could condense the Appendix into a set of bullet points at the end of the intro to the Analysis section (which you still need, badly!), and then its content could be interleaved in the Analysis chapter. E.g. you already have redundancy in the LE and TE discussion vs. the Appendix, and the discussion is more complete in the Analysis chapter, which is good. . . .	91
■ I really want this appendix to stay here. I'll make sure to mention everything in the body of the thesis though, since it *is* important. But at some point, somebody is going to really want to have this info written into a short summary.	91
■ Somebody will surely ask for a justification for why I did this differently, and I don't have one beyond "this seemed more reasonable to me", which is of course nobody will ever accept as a reason.	92
■ John says to keep this appendix, because it's great now.	93
■ We have already specialized to β^+ decay.	93
■ Also, $\xi = G_v^2 \cos \theta_C f_1(E)$	95
■ There was something wrong with this assumption. Something circular. I forgot. Blah.	97
■ Somewhere I have to define q^2 and Δ are.	97
■ Should I just list the values of things that I inherited from Ian Towner's personal communication that one time?	98
■ and also, I think something like that the weak charge is the same distribution as the electric charge	98

■ What is less clear, given the context in the paper, is whether or not when Holstein writes out his simplified expressions for $\Delta F_x(E_\beta, u, v, s)$ he actually means $F_\mp(Z, E_\beta)\Delta F_i(E_\beta, u, v, s)$. These terms are pretty small, so it probably doesn't *really* matter, but it would still be really nice to *know*, damn it.	98
■ Also, pretty sure one of those never gets used. Which one was it? idk.	100
■ Note: It's not the case that $ \vec{J} == J$. It's actually super fucking infuriating notation.	100
■ I see some stuff in my old Appendix D that needs to be moved (in here? Or maybe in Old Appendix E) before it goes away forever.	101
■ JB: Appendix C has some redundancies with B. You will have to sort that out. (n.b.: from context, it's less clear which appendices he's actually talking about, but whatever, there's certainly redundancies all around.	101
■ Appendix KLM you have to pick what you want– I hope that's Appendix K (that's this one!) – and remove the rest as you say they're "old". Appendix K could be moved to the end of Experimental Methods because it's absolutely critical and helpful!! but if you want to reference it there and leave it as an Appendix, it's up to you.	111
■ We could also use this with the Holstein formulation, at least some of it. The point is, we can put *anything* that only depends on beta energy into $W(E_\beta)$. It doesn't matter, because it's already only integrable through numerical methods anyway – so we can't possibly make it worse.	112
■ Not quite true. Some strips are missing.	112
■ This is only true if we neglect (back-)scatter. This is not actually a good approximation. But we have pretty good simulations to give us the real numbers, anyway.	112
■ Is that definitely true, or is it only true to lowest order?	113
■ See content at Appendix (D). After reading that stuff, continue here.	114
■ The trap is *not* centered, but the polarizations in the two states are equal, to a very high level of precision. More than we need for b_{Fierz} anyway, and probably more than we'd need for A_β	114

Chapter 1

Background and Introduction

from JB on the contents of Chapter 1:

...

2) "These couplings all refer to parameters in a Lagrangian that takes the relativistic inner product of a current for the lepton with a current for the proton or neutron. The resulting Lagrangian must be a scalar under Lorentz transformations, so these currents must have transformations like these V,A,S, and T and be combined into a scalar."

...

3) Add one reference to the latest review:

Adam Falkowski, Martín González-Alonso, Oscar Naviliat-Cuncic. Comprehensive analysis of beta decays within and beyond the Standard Model. Journal of High Energy Physics, Springer, 2021, 04, pp.126. 10.1007/JHEP04(2021)126.

Here it is! [3].

...

You have time for nothing else.

1.1 Motivation

The nuclear weak force is one of four fundamental forces described within physics. It mediates the process of beta decay, which is of particular interest to us here. Although beta decay is generally well understood, it presents a unique opportunity to search for physics beyond the Standard Model within the behaviour of the weak coupling. By observing the kinematics and angular correlations involved in the decay process, one gains access to a wealth of information about the precise form of the operators mediating the decay.

According to the predictions of the Standard Model, beta decay involves only so-called vector (V) and axial-vector (A) couplings, with a relative phase angle producing the left-handed “(V–A)” form of the interaction. There exists an extensive body of experimental evidence to demonstrate that this is overall a very good description of the beta decay process. Despite the success of the (V–A) model, the additional presence of certain other “exotic” couplings cannot be entirely ruled out, and our observable is mostly sensitive to scalar (S) and tensor (T) couplings.

According to present limits, these couplings would have to be pretty small relative to the (V) and (A) couplings.

Need to figure out how the exotic couplings actually work, mathematically. What the fuck does “(V – A)” even *mean*? IIRC John wants a brief mention of γ_5 's and γ_μ 's, and probably a brief mention of whatever mumble-mumble group is mumble-mumble represented or something.

...

JB says:

the current transforms like a Lorentz scalar or tensor – this does not refer to the angular momentum.

If you write down the Lagrangian for beta decay, that's eough. All these things refer to the structure of the Lagrangian. The theory considers all possible Lorentz transformations of the currents.

Please don't talk about $SU(2) \times U(1)$ for electroweak unification. It's textbook material that's beyond the scope.

Did I even get this right? Is the phase angle really what makes it left-handed?
JB says:

...
Relative sign. look at the quark-lepton Lagrangian, which has $(1 \pm \gamma_5)$

Cite a bunch of people here. (Who?) Might be nice to have a picture also.

John wanted this change (now implemented), but I think the phrasing is unclear now.

...
"and we shall be interested especially in scalar (S) and tensor (T) couplings."
-> "our observable is mostly sensitive to scalar (S) and tensor (T) couplings."

JB on intuitive concepts that are missing:

The SM couples to left-handed neutrinos and right-handed antineutrinos. Since the neutrinos only have weak interactions, there are no right-handed nu's nor left-handed antinu's in nature. The neutrino asymmetry B_ν is a number with no energy dependence.

Similarly, the SM weak interaction only couples to right-handed positrons and left-handed electrons. Since these are massive particles, the average helicity of positrons is not 1, but instead v/c. One can always boost to a frame where the positron keeps its circulation but is moving in the opposite direction. This is why the beta asymmetry is A v/c, not just A.

The Fierz term's additional energy dependence of m/E also comes from helicity arguments, stemming from the fact that it still is coupling to SM nu's and antinu's only, so the beta's are generated with wrong handedness.

The details are built at 4th-year undergrad level in Garcia's paper with his student and post-doc [4].

The beta asymmetry dependence on the Fierz term only comes through the normalization of $W(\theta) = 1 + b_{\text{Fierz}}m/E + A_\beta \cos(\theta)$.

i.e.:

$W'(\theta) = 1 + A_\beta/(1 + b_{\text{Fierz}}m/E) \cos(\theta)$. (the angular distribution must be unity where cos(theta) vanishes, by definition).

1.2 The Basics of Beta Decay

Standard Model beta decay is well understood. The Fermi description of beta decay can be found in any nuclear physics textbook, but you have to dig slightly harder to understand Gamow-Teller or mixed decays, all of which are relevant here.

via Krane [13] Under the Allowed Approximation, we require that a beta decay may not carry away any orbital angular momentum, because we treat the nucleus as pointlike and work in the CM frame. An Allowed decay can, however, change the total nuclear angular momentum, because the outgoing leptons have spin= 1/2 and therefore carry angular momentum. Therefore, in an allowed decay, the total nuclear angular momentum must always change by either 0 or 1.

Is this even true? The pointlike thing? ...No. No it's not.

JB says: The title of Holstein's review addresses this "pointlike" issue, and he describes the "impulse approximation" in Section V. The interaction is not pointlike, because all constants are a form factor expansion in q^2 – finite size terms contribute to the Coulomb correction.

From a 2006 paper by Severijns et al [14], the selection rules for an allowed transition are:

$$\Delta I = I_f - I_i = \{0, \pm 1\} \quad (1.1)$$

$$\hat{\Pi}_i \hat{\Pi}_f = +1 \quad (1.2)$$

Then, you can separate the allowed transitions into singlet (anti-parallel lepton spins, $S = 0$ – a Fermi transition) and triplet states (parallel lepton spins, $S = 1$ – a Gamow-Teller transition).

Fermi decays are so-called “vector” interactions, and happen when the spin of the two leptons involved are antiparallel, so there can be no change in angular momentum (at least in the case of the Allowed approximation).

Gamow-Teller decays involve two leptons with parallel spins, so the decay must change the projection of the nuclear angular momentum, M_I , by exactly one unit (in the case of the Allowed approximation). They transition may or may not simultaneously change the total nuclear spin, I , by one unit. These are “axial-vector” interactions. (Note that $I = 0 \rightarrow I = 0$ interactions are never Gamow-Teller decays.

Probably everything in this section is yoinked from [15], pg 212.

1.3 Mathematical Formalism

In order to proceed with a measurement, we must find a master equation to describe the probability of beta decay events with any given distribution of energy and momenta among the daughter particles, as a function of the strength of the specific couplings of interest to us. To do this, two sets of formalisms are combined – the older formalism from Jackson, Treiman, and Wyld (JTW) [5], [16], which describes the effects of all types of Standard Model and exotic couplings of interest to us here, but which truncates its expression at first order in the (small) parameter of recoil energy, and a newer formalism from Holstein [17], which includes terms up to several orders higher in recoil energy, but which does not include any description of the exotic couplings of particular interest to us. We note that because any exotic couplings present in nature have already been determined to be either small or nonexistent, it is sufficient to describe these parameters with expressions truncated at first order, despite the fact that it is still necessary to describe the larger Standard Model couplings with higher-order terms.

In beta decay, a proton(neutron) within a nucleus decays into a neutron(proton), and emits a positron(electron) and neutrino(anti-neutrino). The new neutron(proton) remains bound within the nucleus. As always, momentum and energy must both be conserved. The distribution of energy and momenta is, of course, probabilistic rather than deterministic, and with three bodies involved, the full probability distribution for the momenta of outgoing particles cannot be written in closed form. However, because the nucleus is significantly more massive than either of the other two outgoing particles, the great majority of the released kinetic energy is distributed between the leptons, while the nucleus receives only a tiny fraction of the total. This feature lends itself to an approximation in which the energy of the recoiling nucleus (recoil) is neglected entirely, and the decay may be described only in terms of the momenta of the outgoing positron(electron) and neutrino(anti-neutrino), as in JTW [5]. The terms that have been neglected in this treatment are sometimes called ‘recoil-order corrections’.

..

Unfortunately, the outgoing (anti-)neutrino is very difficult to detect directly, and we make no attempt to do so in this experiment. Instead, we might look for coincidences between an outgoing beta and a recoiling nucleus, and use that information to reconstruct the kinematics of the neutrino.

The procedure for combining the two formalisms is described in detail in Appendix B. Integrating the JTW expression over neutrino direction, we find:

$$\begin{aligned} d^3\Gamma dE_\beta d^3\hat{\Omega}_\beta &= \frac{2}{(2\pi)^4} F_{\mp}(Z, E_\beta) p_\beta E_\beta (E_0 - E_\beta)^2 dE_\beta d^3\hat{\Omega}_\beta \xi \\ &\times \left[1 + b_{\text{Fierz}} \frac{m_e c^2}{E_\beta} + A_\beta \left(\frac{\vec{J}}{J} \cdot \frac{\vec{p}_\beta}{E_\beta} \right) \right], \end{aligned} \quad (1.3)$$

Do it! Do the master equation!

JB: cut "so we will simply provide the combined master equation here"
Don't. The equation you have is all you need.

where

$$\xi = G_v^2 \cos \theta_C f_1(E). \quad (1.4)$$

1.4 Our Decay

JB: on 2.3 (now 1.4), "Our decay": Just put the comments in. Keep the figure as-is.

MJA: Pretty sure the comments are literally copy-pasted from somewhere I shouldn't just plagiarize from. Need to rephrase it at least. ...No, it's fine, it's just from my old thesis proposal. I think. Removed now from that section, so it can go here..

Here, we focus on the decay $^{37}\text{K} \rightarrow ^{37}\text{Ar} + \beta^+ + \nu_e$. The angular correlations between the emerging daughter particles provide a rich source of information about

the type of interaction that produced the decay. Among other useful properties, this is a ‘mirror’ decay, meaning that the nuclear wavefunctions of the parent and daughter are identical up to their isospin quantum number. This property allows us to place strong constraints on the size of the theoretical uncertainties for this decay process within the Standard Model.

Talk about how great ^{37}K is for what we’re doing with it. Also, drop all the math-numbers to support those assertions. Reference the level diagram within the text!

Also, ^{37}K is a really nice isotope for this, because 98% + 2%, also because it’s a mirror decay, also because it’s an alkali. Also-also, its big A_β value means we have a big thing to multiply any b_{Fierz} value there might be when we construct the superratio asymmetry to eliminate systematics.

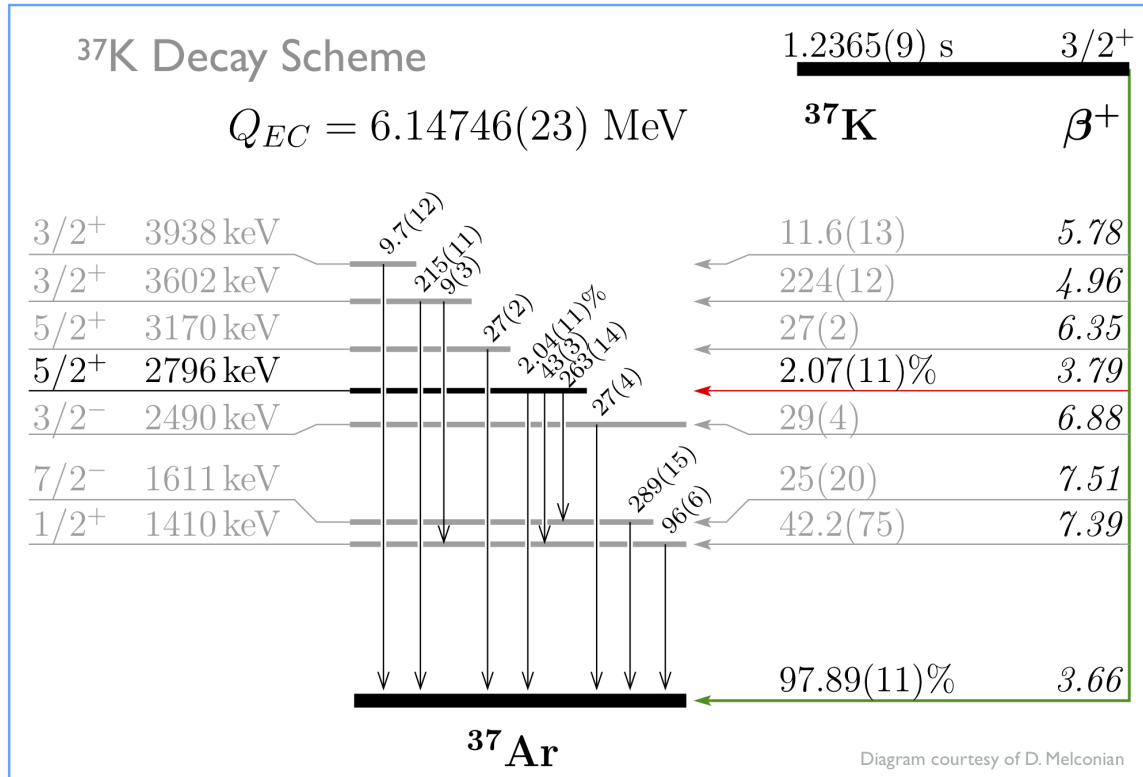


Figure 1.1: A level diagram for the decay of ^{37}K .

1.5 Shake-off Electron Spectrum

JB on 2.4 SOE:

Say what you did, with as little info as possible now. Georg is a theoretical chemist, so he may be very curious about this.

...

"Atomic electrons with kinetic energies 0 to 100 eV are produced as part of the beta decay process. If their energy is below a certain value, our detection process is not perturbed, so we provide physics about the energy spectrum here.

...

Levinger [6], assuming the sudden approximation, calculated the overlap between an electron in the initial atom with an outgoing electron or an electron in the final atom. Levinger approximated everything with hydrogenic wavefunctions, so his calculations become analytic. The collaboration has found that Levinger's formulae fit our measurements of the position and TOF info of our atomic electrons, so they are used in our simulations

OR

but the precise energy spectrum was found to be unimportant, so we used X in our simulations. whichever is true.

...

This is then fine. You have most of the basics down.

Shake-off electrons: where do they come from, and where do they go? [6].

Really, just discuss the physics of what happens to cause SOEs to be a thing. Talk about *our* SOE spectrum in some other chapter later. Should this go in the atomic physics chapter? I can't decide whether it's more atomic or more nuclear.

John made some nice plots of these from the eMCP data. I did *not* use it to make a cut on eMCP hit position in the end, despite the fact that it makes the spectrum more clean, because a lot of good events don't have full hit position information, and you lose an awful lot of statistics by making the cut. I used this for modeling the background spectrum, but in the end it wasn't as elegant a result as I might have hoped. Also, it's still an open question exactly which fraction of SOEs come from which atomic shell, but it doesn't change the resulting spectrum very much.

Should I talk about the distribution of how many SOEs come off in a decay? I have measurements of the recoil charge distribution, which is related but not really the same thing. From a theoretical POV, I don't know how many get shaken off. Thankfully, it doesn't matter very much in the end.

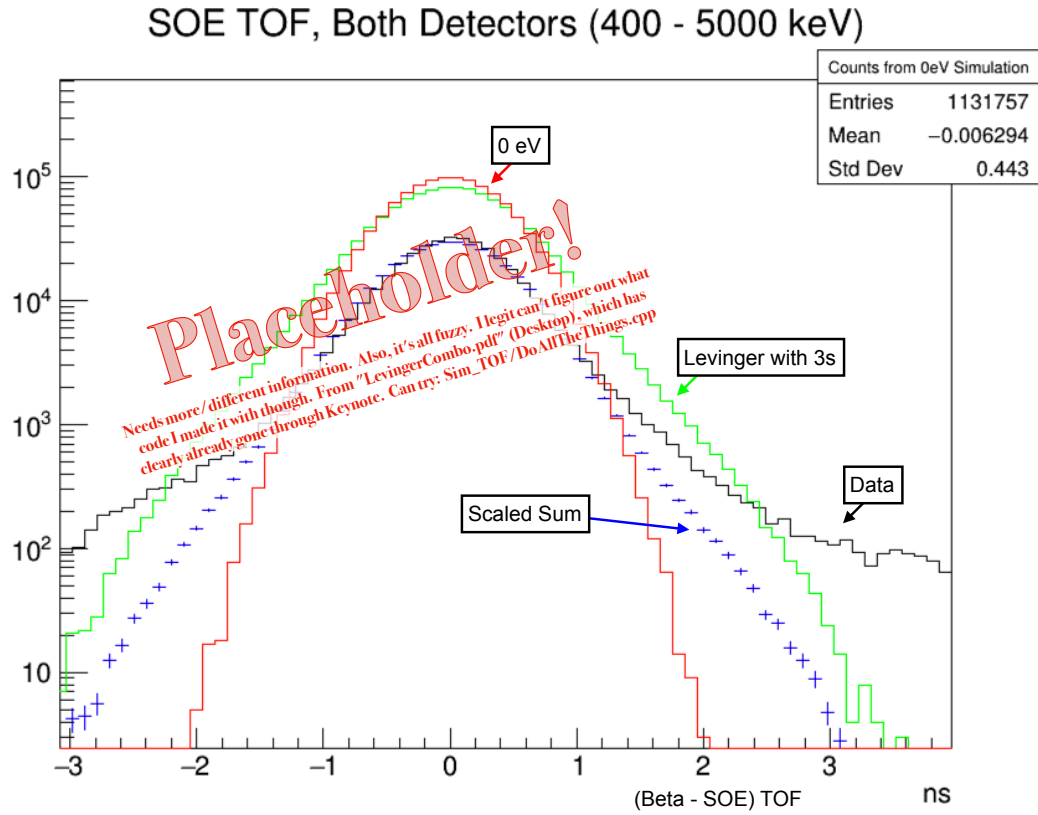


Figure 1.2: Shake-off electron TOF (w.r.t. beta TOA) spectrum, showing how the spectrum is different if one includes different sets of initial electrons to be shaken off. I forgot why some of them have 0 eV. Maybe those are the ones from the $^{37}\text{Ar}^+$ Levinger TOF spectra for some different sets of SOE initial orbitals before shake-off. (At least that's what it's supposed to be, after I fix the picture). It's reconstructed event-by-event with beta times-of-flight that would pass some basic 'good event' cuts. Anyway, it turns out, it doesn't much matter what orbitals you lose SOEs from. That's nice. In the end, I used 85+15. ([Need to re-plot this.](#))

1.6 Fierz Interference – The Physical Signature

The physical effects resulting from the presence of scalar or tensor couplings include a small perturbation to the energy spectrum of betas produced by radioactive decay.

JB on that missing figure that I've now put in: "A dependence of A_{β} on beta energy is also introduced.

UCNA fits energy spectrum and $A_{\beta}[E_{\beta}]$ simultaneously now."

The point is, the presence of either scalar or tensor interactions will produce a b_{Fierz} term in the decay PDF. It has other effects on the PDF, but those come in at higher-order in the tiny scalar and tensor couplings. So, the Fierz term would be by far the biggest thing that changes in the PDF. The PDF describes the energy and momentum of the outgoing beta w.r.t. a variety of other things. Notably, we can write an elegant-ish description of beta momentum w.r.t. nuclear polarization direction, and ignore the neutrino completely after integrating over it. We have a PDF in beta *direction* (w.r.t. polarization), and beta *energy*. To lowest order (and lowest order is best order) the distribution w.r.t. polarization direction doesn't change, but the distribution w.r.t. energy does change. Or ... something? The point is, it makes a change in the beta energy spectrum. This change is most pronounced at low energies, because the Fierz term is scaled by $(1/E_\beta)$. However, the asymmetry is also a function of E_β . A different function of E_β . In fact, it is scaled by (p_β/E_β) within the PDF, which is distinctly different than b_{Fierz} . So, one might ask what effect a b_{Fierz} term would produce on a constructed asymmetry spectrum.This explanation has gone way off track.

Here's a reference to the picture that shows the result of a non-zero b_{Fierz} term. It's Fig. 1.3.

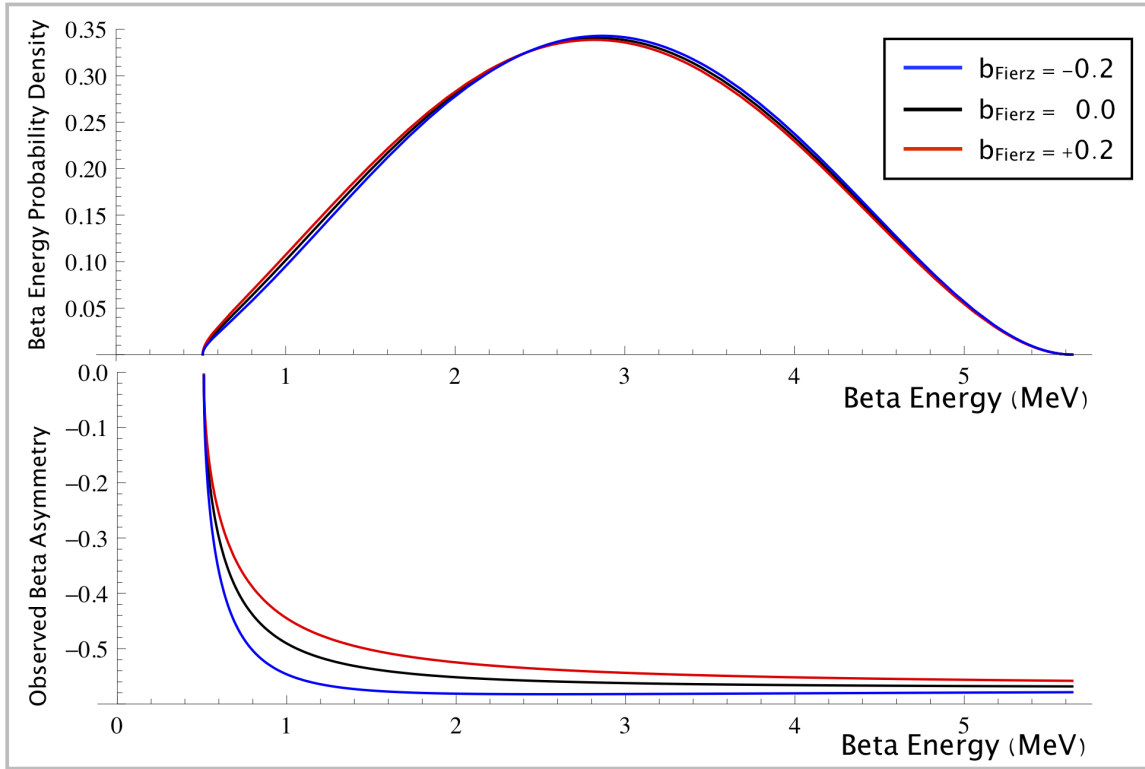


Figure 1.3: Here's why it's better to extract b_{Fierz} from an asymmetry, in this case.

1.7 On the Superratio, the Supersum, and the Constructed Asymmetry

JB: You need to at some point say that the supersum is the beta energy spectrum. There are experiments trying to do this method better, but they are very difficult. UCNA published a combined energy spectrum and Abeta[Ebeta] analysis on the neutron in March 2020 [8].

I can't help but also notice the follow-up article from September 2020 [9]. Ugh.

The data can be combined into a superratio asymmetry. This has the benefit of causing many systematics to cancel themselves out at leading order. It also will increase the fractional size of the effects we're looking for. This can be shown by using math.

Not all systematics effects are eliminated. We'll want to be careful to propagate through any effects that are relevant. Using the superratio asymmetry as our physical observable makes this process a bit messier for the things that don't cancel out, but it's all just math. Some other groups have performed similar measurements using the supersum as the physical observable. There are pros and cons to both methods. I can show, using a back-of-the-envelope calculation, that for this particular dataset, the superratio asymmetry method produces a better result.

Chapter 2

Considerations and Implementation of Atomic Techniques

Possible Supersection: General Considerations of Atomic Techniques Used

2.1 An Overview of Magneto-Optical Traps

I need to organize the sections/subsections in this chapter better...

Since its initial description by Raab et. al. in 1987 [18], the magneto-optical trap (MOT) has become a widely used technique in many atomic physics laboratories. The MOT produces confined samples of cold, electrically neutral and isotopically pure atoms confined within a small spatial region. It is these properties that make the MOT a valuable tool not only in atomic physics, but for precision measurements in nuclear physics as well, and the TRINAT lab has adopted the technique wholeheartedly.

The technique is used predominantly with alkalis due to their simple orbital electron structure, and once set up it is quite robust. The MOT's trapping force is specific to the isotope for which the trap has been tuned. This feature makes it ideal for use in precision radioactive decay experiments, since the daughters are unaffected by the trapping forces keeping the parent confined.

Have I defined TRI-NAT yet?

Possibly most of the above paragraph is also written/paraphrased elsewhere. Like in ((Ch.2B)), unless I removed it...

A typical MOT can be created from relatively simple components: a quadrupole-shaped magnetic field, typically generated by two current-carrying coils of wire, and a

circularly polarized laser tuned to match one or more atomic transitions in the isotope of interest. Because a MOT is easily disrupted by interactions with untrapped atoms, the trap must be created within a vacuum system. Finally, a source of atoms to be trapped is required. [See Fig. 2.1.]

The laser, which must be circularly polarized in the appropriate directions and tuned slightly to the red of an atomic resonance, is split into three perpendicular retroreflected beams, doppler cooling the atoms and (with the appropriate magnetic field) confining them in all three dimensions (see Figure 2.1).

“In order to understand the mechanism by which a MOT is able to confine atoms, we must first introduce the Zeeman effect (Section 2.1) and a description of an optical molasses (Section 2.2). A functional MOT combines the forces resulting from these two mechanisms to trap and cool atoms.”

2.1.1 Zeeman Splitting

In the presence of an external magnetic field \vec{B} , the Hamiltonian associated with an atom’s orbital electrons will acquire an additional “Zeeman Shift” term, given by [19]

$$H_{\text{Zeeman}} = -\vec{\mu} \cdot \vec{B}, \quad (2.1)$$

where $\vec{\mu}$ is the magnetic moment associated with the orbital under consideration. In the limit where the magnetic field is too weak to significantly disrupt the coupling between the electron’s spin- and orbital angular momenta, $\vec{\mu}$ may be treated as being fixed with respect to changes in the magnetic field. It is this weak field regime which will be primarily of interest to us in work with magneto-optical traps.

With $\vec{\mu}$ fixed, it is clear that the magnitude of the energy shift must scale linearly with the strength of the magnetic field. In considering the perturbation to the energy of a particular *transition*, the perturbations to the initial and final states must of course be subtracted:

$$\Delta E_{\text{transition}} = -(\vec{\mu}_f - \vec{\mu}_i) \cdot \vec{B}. \quad (2.2)$$

Needs a level diagram. Maybe.

When this is combined with a circularly polarized laser beam, the effect is to move the atomic resonance closer to- or farther from- the frequency of the laser. The circular polarization, combined with some selection rules, means a circularly polarized laser will only couple to one particular transition, w.r.t. angular momentum. ie, for a σ_+ polarized laser, the atom's overall angular momentum projection (along some axis) will be incremented by +1. The Zeeman shift means that in a magnetic field, this transition ($M+=1$) not be the same as the $M=1$ transition. So, if you have a magnetic field that changes linearly across space, you can make it so that in $+B_z$ regions, the laser beam with one certain polarization is closer to resonance and therefore more likely to be absorbed – and similarly, in $-B_z$ regions, a different laser with the opposite polarization will be more likely to be absorbed. Again, if the B-field is linear in space, you can do it so that as the atoms get further and further from the ‘centre’ region, the effect gets progressively stronger. So, if you’ve done this right, you can make it so that the atoms get a stronger “push” back towards the center the farther away they’ve drifted.

They still get the optical molasses cooling effect for free.

2.1.2 Saturation Spectroscopy

JB says: Chapter 3 (that’s this chapter) ((Now Ch.2A)): Starting in Ch. 3 around p. 10, "Atom-Photon Interactions with a Laser" (that’s this section – now “Saturation Spectroscopy”): You need to do a careful pass through it and omit everything you don’t understand and don’t need.

Sorry, there is no longer time to resolve your questions unless you need them.

This is a stupid subsection title.

Consider a single two-level atom in its ground state interacting with a single photon with the same energy as that of a the atomic transition between the ground and excited states. If angular momentum selection rules allow it, the photon will be absorbed and the atom will receive a “push” from the incident photon’s momentum. After a time, the atom will spontaneously de-excite by emitting a photon in a random direction. Conservation of momentum results in the atom receiving a second push from the emitted photon.

Also, if the photon is tuned close enough to atomic resonance, with absorption being more likely the smaller the detuning is...

If one considers a cloud of many such atoms within the path of a correctly-tuned (low intensity) laser beam, then provided the atoms are constrained to remain within the beam path, the result of many such interactions is a biased random walk in physical space for each individual atom, and a net velocity change for the cloud as a whole.

In contrast to the above description of absorption followed by spontaneous emis-

sion, a photon interacting with an atom in the excited state may cause the atom to de-excite by emitting a second photon. This mechanism is negligible in the case of a sufficiently low intensity laser beam. However, as the laser intensity increases, so too will the fraction of atoms in the excited state at any given time. As it is only the excited state atoms that are able undergo stimulated emission, this effect becomes increasingly dominant as the intensity of the incident laser increases. In the limit of infinite intensity, stimulated emission and absorption are equally likely to occur, and therefore the population is split evenly between the ground and excited states.

To describe the regime change between atomic interactions with low intensity- and high intensity lasers, we introduce the (on-resonance) saturation intensity, I_{sat} , where

$$I_{\text{sat}} = \frac{\hbar\omega_0^3\gamma}{12\pi c^2} \quad (2.3)$$

is the laser intensity at which the rates of decay by stimulated- and spontaneous emission are equal, $\hbar\omega_0$ is the energy of both the atomic transition and γ describes the linewidth of the atomic transition and equivalently its rate of spontaneous decay from its excited state. We may further define the on-resonance saturation parameter s_0 , for a laser of intensity I as,

$$s_0 := \frac{I}{I_{\text{sat}}} \quad (2.4)$$

In practice, for the project that is the topic of this thesis, the MOT laser operates at about 1/2 of saturation intensity, while the optical pumping and photoionization lasers operate at considerably lower than saturation intensity. However, one can gain a qualitative understanding of many aspects of atom-laser interaction while neglecting saturation concerns.

Fixed description of which lasers are saturated.

Do I need to mention saturation at all? It's probably not really necessary, and I don't *think* anything else in this section is wrong per se. But maybe better to just cut it.

2.1.3 Doppler Cooling

We now consider a somewhat more general case in which a cloud of two-level atoms lies along the path of two counter-propagating laser beams, both detuned slightly to

the red of resonance. For simplicity, this cloud will be treated as being constrained in the other two dimensions such that it must within the laser's path. With two counter-propagating laser beams of equal intensity and detuning, the “push” from interaction with one beam is exactly counteracted by the push from the opposite-propagating beam, and there is no net velocity transfer to the cloud.

...and opposite polarization. Or something. I have to talk about the selection rules somewhere else.

Detuning the laser from resonance will of course decrease absorption upon interacting with an atom at rest – however the atoms within the cloud are not at rest, but rather are undergoing thermal motion. As such, within the rest frame of each individual atom, the two laser beams will appear to be Doppler shifted in opposite directions, with the sign dependent on atomic motion. In particular, atoms moving against a laser's direction of propagation will see that laser beam as being blueshifted. Since the laser has been red-detuned within the lab frame, the blueshift moves the laser frequency as seen by the atom back toward resonance, and makes its photons more likely to be absorbed. Similarly, for an atom moving in the same direction as a red-detuned laser beam, this laser will be seen as further red-shifted, and absorption likelihood is decreased. Because of the difference in absorption, such an atom becomes more likely to receive a push back against its (lab frame) direction of motion, slowing it down, and less likely to receive a push to increase its lab frame speed.

The overall effect on a one-dimensional cloud of atoms in the path of two counter-propagating red-detuned lasers is that the atoms will be slowed and cooled. Such a setup is sometimes referred to as a one-dimensional “optical molasses” due to the viscous drag force induced on atomic motion. It is straightforward to extend this model to three dimensions. Although this setup will decrease atomic velocity, it does not include a confining force, so the atoms are still free to move out of the lasers' path, albeit at a decreased speed.

Optical molasses equation? Maybe?

“...This will slow the atom down, at least up to a limit related to the linewidth of the atomic transition and/or the laser. There's something to look up.”

Removed ‘Angular Momentum and Selection Rules’ section. Because it was super wrong.

2.1.4 Atom Trapping with a MOT

JB: on 3.3 (now 2.3) “Atom Trapping with a MOT” ((that's here!)):

The content and scope are ok, but the informal phrasing is going to confuse people. You have to pay some attention and rephrase these sections.

Do I *have* an equation I can put here? Surely there must be one somewhere, but I really don't want to dig it up, and I don't think it's really necessary.

Needs work.

Really, at the end of the previous section, I described the MOT's trapping mechanism. That's literally what it is. You just need to do it in 3 dimensions, rather than only one. Fortunately, an anti-helmholz(sp?) coil gives us a quadrupole-shaped magnetic field, which *actually* has a magnetic field that changes linearly along any axis in the region near the center.

Optical molasses + zeeman splitting = magneto-optical trap. Anyway, see Fig. 2.1.

Do I *really* need to bring up the repumper? I don't wanna. Maybe I can just mention it and move on or something.

Removed 'Photoionization as a Probe' section from the 'Intro to Atomic Physics' section, because John says it's horribly wrong anyhow. Plus, it's redundant with the 'Photoionization Laser' section (2.6).

2.2 Optical Pumping

Direct quote from John follows below:

The optical pumping process is described in detail in our collaboration's Ref. [1]. The main detail described here is that the optical pumping is disturbed by any component of magnetic field not along the quantization axis. (Ours is the vertical axis, defined by the direction of the optical pumping light, and along which the detectors are placed.) This required sophistication with an AC MOT described below.

End quote from John. But also!:

"..Then you can refer to that (ie, John's red quoted mini-blurb about optical pumping, (which I may relocate to Sec. 2.6? Or not?) in section 3.4 (now 2.4, about the AC-MOT – ie, Sec. 2.4, (even though I might remove that section entirely and put all its content into Sec. 2.4)), where you're trying to now but the phrasing is poor."

"Until recently, one limitation of such samples was the necessity for the presence of a relatively large magnetic field, which is expected to partially destroy atomic polarization, limiting the precision of many types of measurements. Here we discuss the construction of a newer type of MOT, the AC-MOT, which minimizes residual magnetic fields. The guys in [7] came up with the idea of the AC-MOT. They made it work and did some stuff with it. Good for them."

Need a nice, uniform, constant magnetic field for your polarization to larmor precess around. Then, however depolarized (from the axis of the magnetic field) you

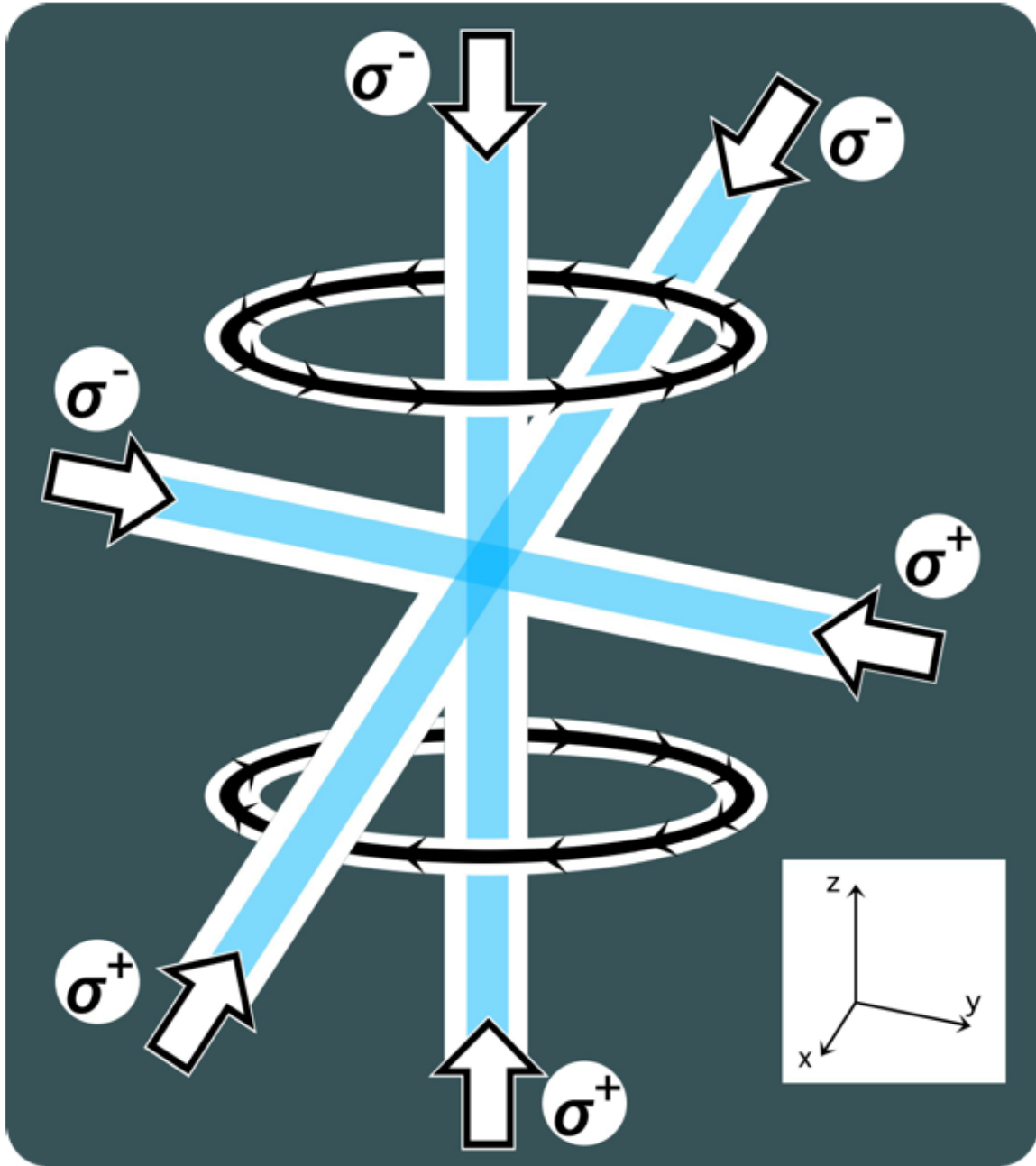


Figure 2.1: Components of a magneto-optical trap, including current-carrying magnetic field coils and counterpropagating circularly polarized laser beams. Diagram taken from [2]

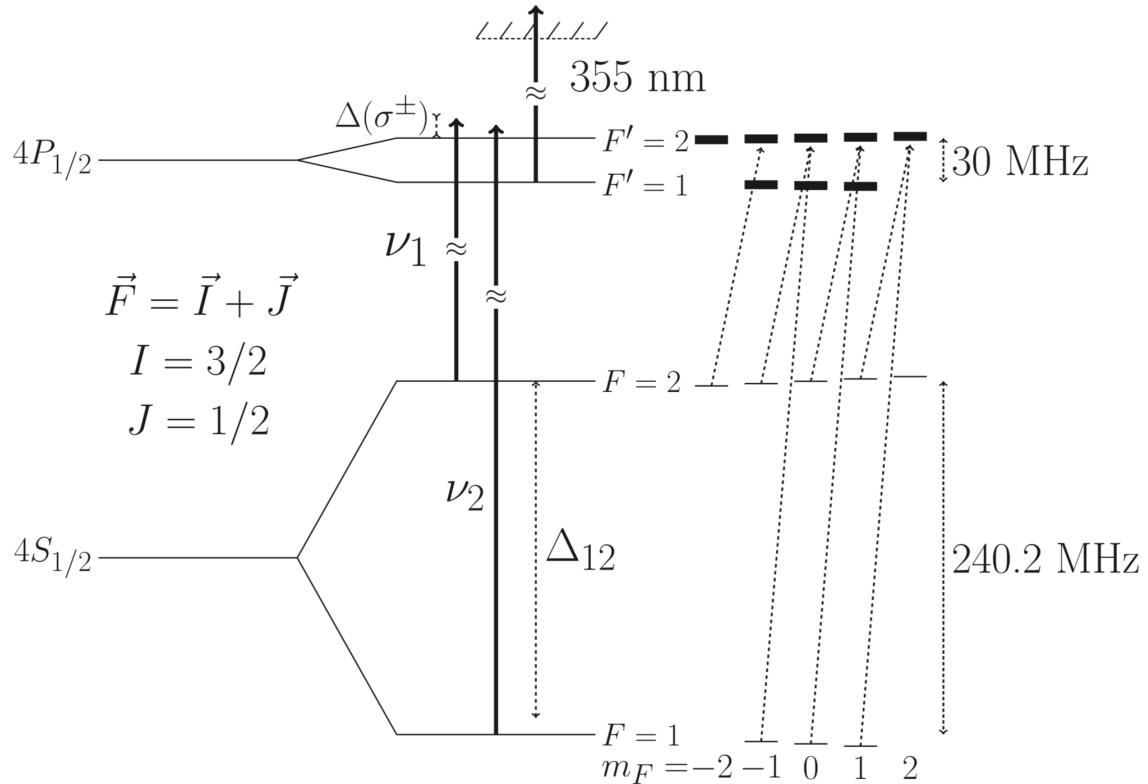
were to start out, you don't like precess in a way that changes the projection you care about.

But also, I should actually describe the optical pumping, too. And point at Ben's OP paper that we did [1].

Somewhere later, I can talk about photoionization? Or should it be here, in this chapter?

Surely it should at least get a different section though.

Do I need a MOT level diagram too?



Describe what's going on here!

Figure 2.2: An atomic level diagram for the optical pumping of ^{37}K , taken from [1].

JB says: "I would say you don't need an atomic level diagram. You could just describe in words the semiclassical picture of atoms absorbing photons until they are nearly fully polarized, then they stop absorbing. The optical pumping + photoionization is then an in situ probe of the polarization. ... You would need to add in words that quantum mechanical corrections to this picture are in the optical Bloch equation approach in B. Fenker et al. The depolarized states still have high nuclear polarization (1/2 for $F = 2, M_F = 1$, 5/6 for $F = 1, M_F = 1$) and determining the ratio of those two populations provides most of the info we need – we model with the O.B.E, measure the optical pumping light polarization, and float an average transverse magnetic field. This is adequate to determine the depolarized fraction to 10% accuracy, which is all that is needed."

2.3 An Overview of the Double MOT System and Duty Cycle

JB: ...You could call the first half of such a chapter "General considerations of Atomic techniques used" and the 2nd half "Experimental Implementation of Atomic Techniques used"

Supersection: Experimental Implementation of Atomic Techniques Used

Remember the pulser LED! To evaluate the stability of the scintillator gain!

JB says: chapter (((this section))) is really good, and in good shape for the committee

We obtain a sample of neutral, cold, nuclear spin-polarized ^{37}K atoms with a known spatial position, via the TRIUMF accelerator facility, by intermittently running a magneto-optical trap (MOT) to confine and cool the atoms, then cycling the trap off to polarize the atoms. With β detectors placed opposite each other along the axis of polarization, we are able to directly observe the momenta of β^+ particles emitted into 1.4% of the total solid angle nearest this axis. We also are able to extract a great deal of information about the momentum of the recoiling ^{37}Ar daughters by measuring their times of flight and hit positions on a microchannel plate detector with a delay line. Because the nuclear polarization is known to within < 0.1% [1], and we are able to account for many systematic effects by periodically reversing the polarization and by collecting unpolarized decay data while the atoms are trapped within the MOT, we expect to be well equipped to implement a test of 'handedness' within the nuclear weak force.

The experimental subject matter of this thesis was conducted at TRIUMF using the apparatus of the TRIUMF Neutral Atom Trap (TRINAT) collaboration. The TRINAT laboratory offers an experimental set-up which is uniquely suited to precision tests of Standard Model beta decay physics, by virtue of its ability to produce highly localized samples of cold, isotopically pure atoms within an open detector geometry. Although the discussion in this chapter will focus on the methodologies used to collect

Surely most of this paragraph goes in an intro chapter somewhere.

one particular dataset, taken over approximately 7 days of beamtime in June 2014, the full apparatus and the techniques used are fairly versatile, and can be (and have been) applied to several related experiments using other isotopes.

Cite a bunch of papers here.

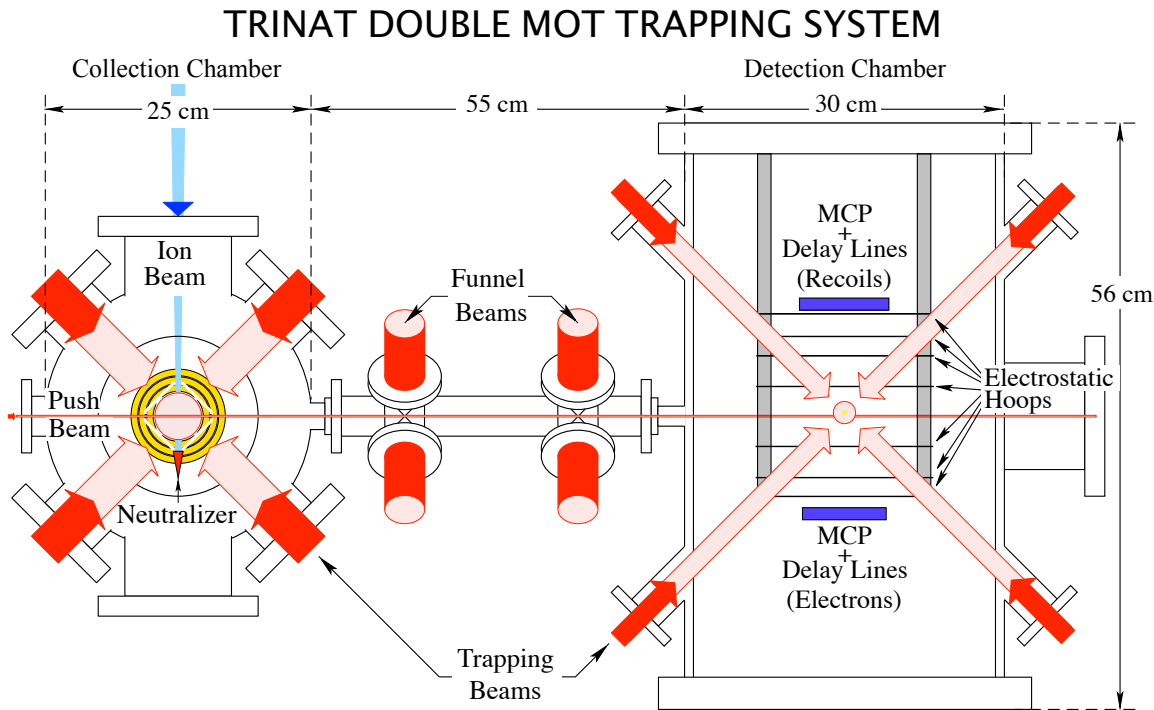


Figure 2.3: The TRINAT experimental set-up, viewed from above. The two MOT system reduces background in the detection chamber. Funnel beams along the atom transfer path keep the atoms focused.

Figure was originally created by Alexandre, modified by ... someone else? Or Alexandre? And I got it from ... probably an experimental proposal? I should figure out how to cite a proposal...

The TRINAT lab accepts radioactive ions delivered by the ISAC beamline at TRIUMF. These ions are collected on the surface of a hot zirconium foil where they are electrically neutralized, and subsequently escape from the foil into the first of two experimental chambers (the “collection chamber”). Further details on the neutralization process are presented in a previous publication [20]. Within the collection chamber, atoms of one specific isotope – for the purposes of this thesis, ^{37}K – are continuously collected into a magneto-optical trap from the tail end of the thermal distribution. Although this procedure preferentially traps only the slowest atoms, once trapped, atoms will be cooled further as a side-effect of the MOT’s trapping mechanism. The

result is a small (~ 1 mm diameter), cold (~ 1 mK) cloud of atoms of a particular isotope.

Mumble mumble UHV. Mumble mumble tail end of the Boltzmann distribution.

These properties of the atomic cloud allow for a relatively clean transfer of linear momentum from an appropriately tuned laser beam to the atoms within the cloud, and we use this mechanism to “push” the atoms out of the collection MOT and into the “detection chamber”, where they are loaded into a second MOT (see Fig. 2.3). During regular operation, atoms are transferred approximately once per second.

There is no need to release previously trapped atoms in the second MOT when a new group of atoms is loaded. Although the trap loses atoms over time as a result of a variety of physical processes, during typical operation the majority of atoms loaded in a given transfer will still be trapped at the time the next set of atoms is loaded, and after several transfer cycles, something like a steady state is obtained.

discussed ... idk, somewhere else.

Because the transfer and trapping mechanisms rely on tuning laser frequencies to specific atomic resonances, these mechanisms act on only a single isotope, and all others remain unaffected. The result is a significant reduction of background contaminants within the detection chamber relative to initial beamline output. The transfer methodology is discussed in some detail within another publication [21].

We now turn our attention to what happens to the atom cloud in the detection chamber between loading phases (see Fig. 2.4). One of the goals for the 2014 ^{37}K beamtime required that the atom cloud must be spin-polarized, as well as being cold and spatially confined. Although the MOT makes it straightforward to produce a cold and well confined cloud of atoms, it is fundamentally incompatible with techniques to polarize these atoms. The physical reasons behind this are discussed in Section 2.4.

Once the newly transferred set of ^{37}K atoms has been collected into the cloud, the entire MOT apparatus cycles 100 times between a state where it is ‘on’ and actively confining atoms, and a state where it is ‘off’ and instead the atoms are spin-polarized by optical pumping while the atom cloud expands ballistically before being re-trapped. These 100 on/off cycles take a combined total of 488 ms. The laser components of the trap are straightforward to cycle on and off on these timescales, but the magnetic field is much more challenging to cycle in this manner.

I *do* discuss this, right? Right??

How to segue here? Do I... Cite myself? Cite Harvey+Murray? Reference the next section?
Reference the previous chapter? This is clunky and stupid.

Immediately following each set of 100 optical pumping cycles, another set of atoms

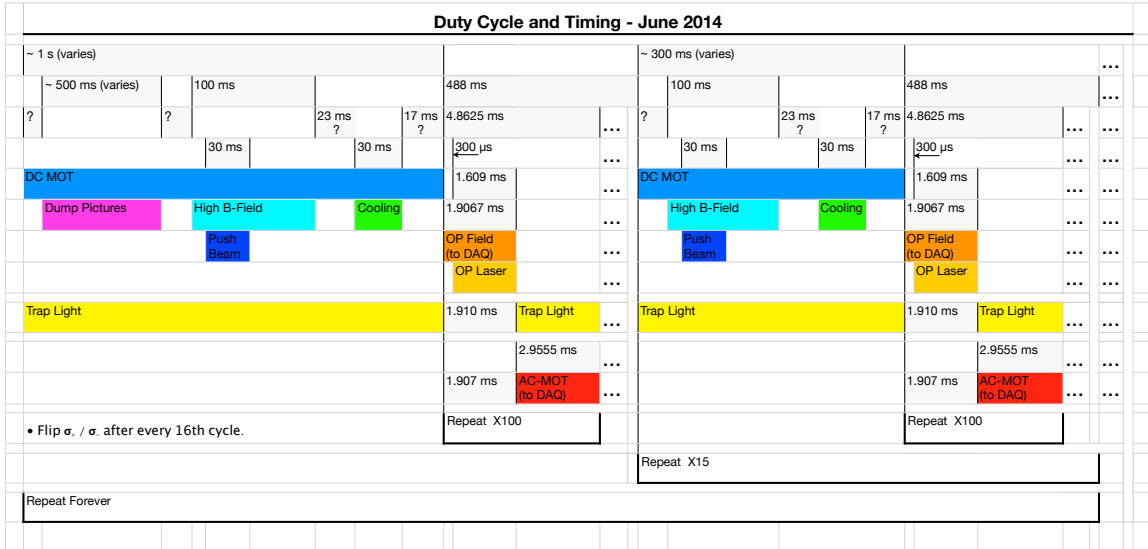


Figure 2.4: The duty cycle used for transferring, cooling, trapping, and optically pumping ^{37}K during the June 2014 experiment. Not drawn to scale. Question marks indicate timings that varied either as a result of electronic jitter or as a result of variable times to execute the control code. Atoms are transferred during operation of the DC-MOT. Though the push beam laser itself is only on for 30 ms, the bulk of the DC-MOT's operation time afterwards is needed to collect and cool the transferred atoms. After 100 on/off cycles of optical pumping and the AC-MOT, the DC-MOT resumes and the next group of atoms is transferred in. After 16 atom transfers, the polarization of the optical pumping laser is flipped to spin-polarize the atoms in the opposite direction, in order to minimize systematic errors.

is transferred in from the collection chamber to the detection chamber, joining the atoms that remain in the trap (see Fig. 2.4). The details of the trapping and optical pumping cycles are described further in Section 2.4, and the optical pumping technique and its results for this beamtime are the subject of a recent publication [1].

2.4 The AC-MOT and Polarization Setup

JB on Ch. 3.4 (now 2.4) ((now Ch. 2.4)) “The AC-MOT” (that’s this section!): The content and scope are ok, but the informal phrasing is going to confuse people. You have to pay some attention and rephrase these sections.

John suggests that maybe I should just refer directly to his red, quoted OP blurb in the chapter about the AC-MOT.

Citation for Harvey and Murray goes here [7]. Also, myself [2].

Here's a diagram of our AC-MOT running one AC-MOT/OP cycle, in Fig. 2.5.

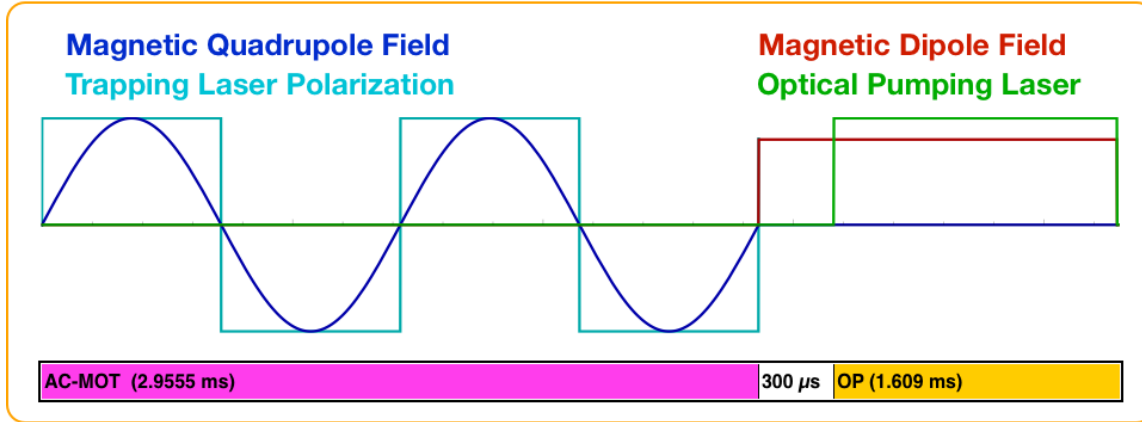


Figure 2.5: One cycle of trapping with the AC-MOT, followed by optical pumping to spin-polarize the atoms. After atoms are transferred into the science chamber, this cycle is repeated 100 times before the next transfer. The magnetic dipole field is created by running parallel (rather than anti-parallel as is needed for the MOT) currents through the two coils.

Normal MOTs are DC-MOTs. They just sort-of go. It's continuous. We used an AC-MOT though! The point of an AC-MOT is to shut off the magnetic field as quickly as possible. With a well-controlled and uniform magnetic field, we can optically pump the atoms, which I think I'm going to describe in the upcoming section (2.2).

Sadly, this also removes our trapping mechanism. We could keep the optical molasses after the field is off if we wanted to, but we don't, because we wouldn't be able to optically pump the atoms then. But at least the atoms are cold-ish (we can measure! I think it's done indirectly in that one table, or for realsies in Ben's thesis), so we can let them just chill for a little while before we have to re-trap them. Don't lose too much.

Anyway, the idea of the AC-MOT is to run a sinusoidal current through your anti-Helmholtz coils. You'll get eddy currents in your nearby metal *stuff* when you have a changing current, and those will *also* make a magnetic field. So, the idea with an AC-MOT is that with a sinusoid, you have clear control over what the eddy currents are actually doing, and you can just shut the current off when the eddy currents are zero (current in the anti-Helmholtz coils will be close to zero at this time too, depending on frequency of the sinusoid...), so you can reduce the size of the eddy

How much do we lose? Have we quantified that somewhere? Probably.

currents by like an order of magnitude. Eddy currents in general take a while to die away, so it's good to make them as small as possible. ...Also, eddy currents making a magnetic field will screw up your optical pumping, because um, reasons? I think it's not just the detuning, it's also something about the Larmor precession.

begin content of the historical other AC-MOT+Polarization section.

Probably document things about the waveform and frequency used for the beamtime, since I don't think it's in my MSc.

John objects to the phrasing of the following paragraph, because you fundamentally need polarized atoms to measure b_{Fierz} .

As alluded to in the previous section (2.3), the measurement in question required a spin-polarized sample of atoms, and a precise knowledge of what that polarization was. This was primarily needed in order to facilitate a measurement of A_β that was performed on the same data that is the subject of discussion here. [22] While this is arguably less critical to a measurement of b_{Fierz} , it can still be an asset for eliminating systematic effects. We use only the polarized portion of the duty cycle in order to minimize other systematic errors, such as the scintillator energy calibration and overall trap position. It also makes for a more straightforward interpretation of the relationship of the measured values of A_β and b_{Fierz} when the systematic effects are the same for both measurements. Finally, using only polarized data allows us to make use of the ‘superratio’ construction in data analysis, a powerful tool for reducing (many) systematic errors at the expense of statistical precision (see Chapter 1.6).

End paragraph that John hates.

Plus, it barely makes sense to talk about measuring b_{Fierz} if you don't know A_β .

The Magneto-Optical Trap is a well-known technique from atomic physics, used to confine and cool neutral atoms [18], and it is also discussed in more detail in Chapter 2.

The TRINAT science chamber includes 6 ‘viewports’ specifically designed to be used for the trapping laser (see Fig. 2.7.).

JB says: “Since you worked hard on the logic triggers, a photoion spectrum with duty cycle would be appropriate if you want.”

A MOT also requires a quadrupolar magnetic field, which we generate with two current-carrying anti-Helmholtz coils located within the vacuum chamber itself. The coils themselves are hollow, and are cooled continuously by pumping temperature-controlled water through them.

One feature which makes our MOT unusual has been developed as a result of our

need to rapidly cycle the MOT on and off – that is, it is an “AC-MOT”. Rather than running the trap with one particular magnetic field and one set of laser polarizations to match, we run a sinusoidal AC current in the magnetic field coils, and so the sign and magnitude of the magnetic field alternate smoothly between two extrema, and the trapping laser polarizations are rapidly swapped to remain in sync with the field [7][2]. See Figure 2.5.

Note that because the atoms within a MOT can be treated as following a thermal distribution, some fraction of the fastest atoms continuously escape from the trap’s potential well. Even with the most carefully-tuned apparatus, the AC-MOT cannot quite match a similar standard MOT in terms of retaining atoms. The TRINAT AC-MOT has a ‘trapping half-life’ of around 6 seconds, and although that may not be particularly impressive by the standards of other MOTs, it is more than adequate for our purposes. ^{37}K itself has a radioactive half-life of only 1.6 seconds (cite someone), so our dominant loss mechanism is radioactive decay rather than thermal escape.

We spin-polarize ^{37}K atoms within the trapping region by optical pumping [1]. A circularly polarized laser is tuned to match the relevant atomic resonances, and is directed through the trapping region along the vertical axis in both directions. When a photon is absorbed by an atom, the atom transitions to an excited state and its total angular momentum (electron spin + orbital + nuclear spin) along the vertical axis is incremented by one unit. When the atom is de-excited a photon is emitted isotropically, so it follows that if there are available states of higher and lower angular momentum, the *average* change in the angular momentum projection is zero. If the atom is not yet spin-polarized, it can absorb and re-emit another photon, following a biased random walk towards complete polarization.

In order to optimally polarize a sample of atoms by this method, it is necessary to have precise control over the magnetic field. This is because absent other forces, a spin will undergo Larmor precession about the magnetic field lines. In particular, the magnetic field must be aligned along the polarization axis (otherwise the tendency will be to actually depolarize the atoms), and it must be uniform in magnitude over the region of interest (otherwise its divergencelessness will result in the field also having a non-uniform direction, which results in a spatially-dependent depolarization mechanism). Note that this type of magnetic field is not compatible with the MOT, which requires a linear magnetic field gradient in all directions (characteristic of a quadrupolar field shape), and has necessitated our use of the AC-MOT as described in (Sub-)Section 2.4.

At some point I have to decide if that's going to be a section or a subsection.

2.5 Measurement Geometry and Detectors

JB says of ((Sec. 2.5)): first few paragraphs are poorly phrased. You have to fix those. Most of the rest looks really good.

This section is really disorganized.

Possibly needs more diagrams? Possibly just needs more words.

MCPs. Hoops. Only one MCP works at a time! Blarg. Upon decay, atoms literally aren't trapped anymore by the trap. No trapping forces, no slowing forces, because it's all isotope-specific.

Back-to-back MCPs in an electric field to tag events from the trap, and to measure the trap position and polarization. Hoops to produce the electric field. The electric field sucks negatively charged electrons into one MCP, and positively charged ions into the other. See Fig. 2.6

Back-to-back beta detectors along the polarization axis.

Many laser ports to make the MOT functional, and for optical pumping. Fancy mirror geometry to combine optical pumping and trapping light along the vertical axis. Water-cooled (anti-)Helmholz coils within the chamber for the AC-MOT, fast switching to produce an optical pumping field.

Detectors are positioned about the second MOT for data collection. The detection chamber operates at ultra-high vacuum (UHV) and provides not only the apparatus necessary to intermittently confine and then spin-polarize atoms, but also the variety of detectors and implements required to quantify their position, temperature, and polarization. The detection chamber further boasts an array of electrostatic hoops to collect both positively and negatively charged low energy particles into two microchannel plates (MCPs), and a further set of two beta detectors positioned along the polarization axis, each of which consists of a 40x40 pixel double-sided silicon strip detector (DSSD) and a scintillator and photomultiplier tube (PMT).

... (shown in Figure 2.7) ...

The beta detectors, located above and below the atom cloud along the axis of polarization (see Figure 2.6), are each the combination of a plastic scintillator and a set of silicon strip detectors. Using all of the available information, these detectors are able to reconstruct the energy of an incident beta, as well as its hit position, and provide a timestamp for the hit's arrival. Together the upper and lower beta detectors subtend approximately 1.4% of the total solid angle as measured with respect to the

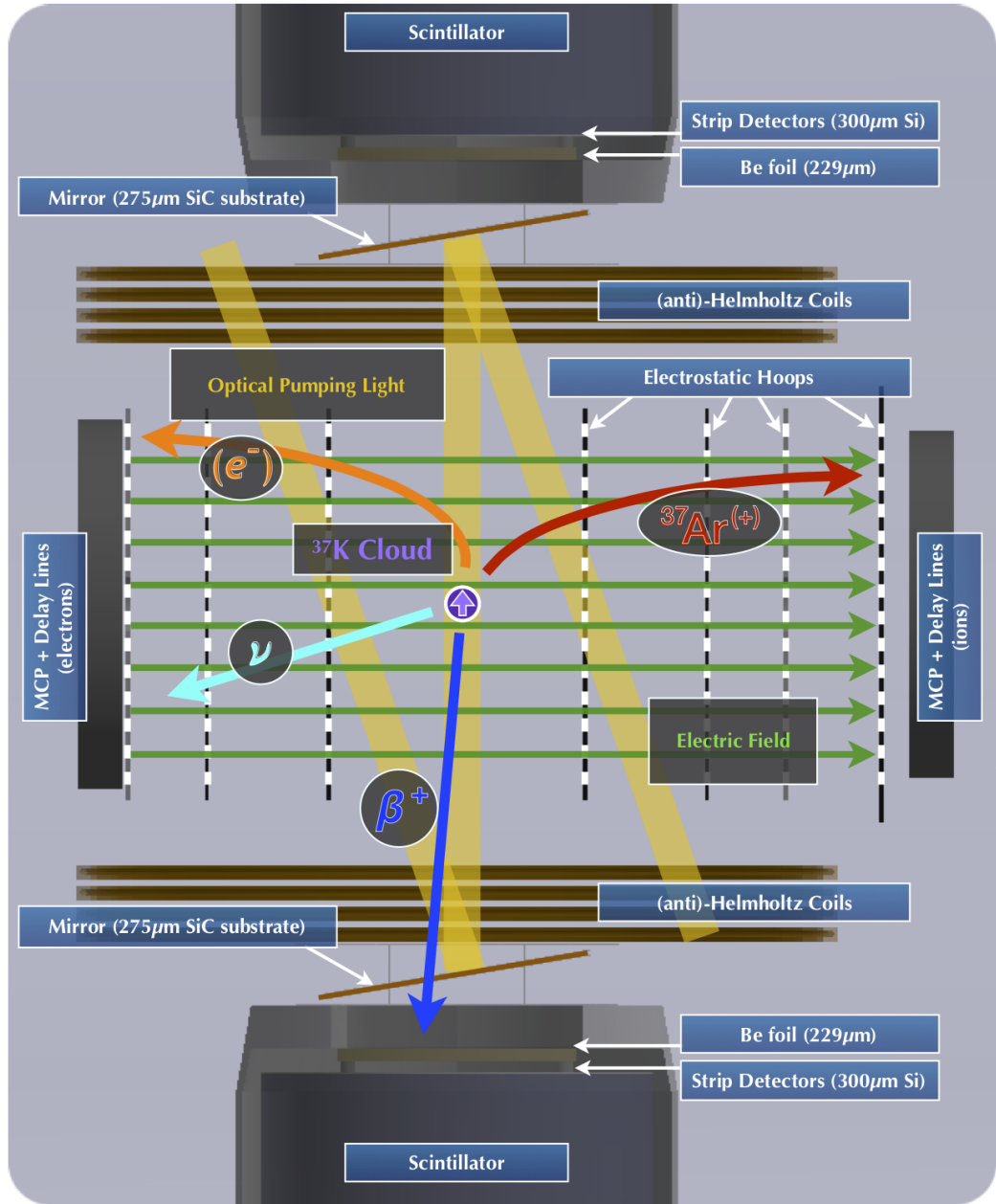


Figure 2.6: A decay event within the TRINAT science chamber. After a decay, the daughter will be unaffected by forces from the MOT. Positively charged recoils and negatively charged shake-off electrons are pulled towards detectors in opposite directions. Although the β^+ is charged, it is also highly relativistic and escapes the electric field with minimal perturbation.

cloud position.

The two sets of beta detectors were positioned directly along the axis of polar-

ization. Each beta detector consists of a plastic scintillator and photo-multiplier tube (PMT) placed directly behind a 40×40 -pixel double-sided silicon strip detector (DSSD). The scintillator is used to measure the overall energy of the incoming particles, as well as to assign a timestamp to these events, while the DSSD is used both to localize the hit position to one (or in some cases, two) individual pixel(s), and also to discriminate between different types of incoming particles. In particular, though the scintillator will measure the energy of an incoming beta or an incoming gamma with similar efficiency, the beta will lose a portion of its kinetic energy as it passes through the DSSD into the scintillator. By contrast, an incident gamma will deposit only a very small amount of energy in the DSSD layer, making it possible to reject events with insufficient energy deposited in the DSSD as likely gamma ray events. Given that the decay of interest to us emits positrons, we expect a persistent background 511 keV gamma rays that are not of interest to us, so it is extremely important that we are able to clean these background events from our spectrum.

There's gotta be a better way to describe it

what's the open area of the detector? how big is each pixel?

It must be noted that the path between the cloud of trapped atoms and either beta detector is blocked by two objects: a $275\text{ }\mu\text{m}$ silicon carbide mirror (necessary for both trapping and optical pumping), and a $229\text{ }\mu\text{m}$ beryllium foil (separating the UHV vacuum within the chamber from the outside world). In order to minimize beta scattering and energy attenuation, these objects have had their materials selected to use the lightest nuclei with the desired material properties, and have been manufactured to be as thin as possible without compromising the experiment. As the $^{37}\text{K} \rightarrow ^{37}\text{Ar} + \beta^+ + \nu_e$ decay process releases $Q = 5.125$ MeV of kinetic energy [23], the great majority of betas are energetic enough to punch through both obstacles without significant energy loss before being collected by the beta detectors.

On opposing sides of the chamber, and perpendicular to the axis of polarization, two stacks of ~ 80 mm diameter microchannel plates (MCPs) have been placed (see Figure 2.7) as detectors, providing a time stamp when a particle is incident on their surfaces. Behind each stack of MCPs there is a set of delay lines, which provide position sensitivity for these detectors.

In order to make best use of these MCPs, we create an electric field in order to draw positively charged particles into one MCP, while drawing negatively charged electrons into the other MCP. Seven electrostatic hoops have been placed within the chamber (see Figure 2.7), and are connected to a series of high voltage power supplies. See Sections 2.6 and 6.4.2 for a discussion of what sort of charged particles we expect

to observe in these detectors and how they are created.

Wait. Am I repeating myself?

Scientific data has been collected at field strengths of 66.7 V/cm, 150 V/cm, 395 V/cm, 415 V/cm, and 535 V/cm. It should be noted that these field strengths are too low to significantly perturb any but the least energetic of the (positively charged) betas from the decay process, and these low energy betas would already have been unable to reach the upper and lower beta detectors due to interactions with materials in the SiC mirror and Be foil vacuum seal.

2.6 The Photoionization Laser

Chapter 4.4 (this section! now 3.4) (((2.6))) is very good and complete, showing you understand what is needed about photoionization. A good reason to omit 3.5 ‘photoionization as a probe’ as I said above.

In order to measure properties of the trapped ^{37}K cloud, a 10 kHz pulsed laser at 355 nm is directed towards the cloud. These photons have sufficient energy to photoionize neutral ^{37}K from its excited atomic state, which is populated by the trapping laser when the MOT is active, releasing 0.77 eV of kinetic energy, but do not interact with ground state ^{37}K atoms. The laser is of sufficiently low intensity that only $\sim 1\%$ of excited state atoms are photoionized, so the technique is only very minimally destructive.

Probably worth mentioning that we test this stuff offline on stable ^{41}K .

Because an electric field has been applied within this region (see Section ??) the $^{37}\text{K}^+$ ions are immediately pulled into the detector on one side of the chamber, while the freed e^- is pulled towards the detector on the opposite side of the chamber. Because $^{37}\text{K}^+$ is quite heavy relative to its initial energy, it can be treated as moving in a straight line directly to the detector, where its hit position on the microchannel plate is taken as a 2D projection of its position within the cloud. Similarly, given a sufficient understanding of the electric field, the time difference between the laser pulse and the microchannel plate hit allows for a calculation of the ion’s initial position along the third axis.

JB: “you could reference the letter for the value of the field 150V/cm.”

As a check: the camera measurements for photons from de-excitation. It's aimed 35 degrees from vertical, with its horizontal axis the same as one of the other axes. I think it's the TOF axis. I can check this when my computer comes back. Also, there's an unknown additional delay between some of our DAQ channels that can't be explained by accounting for cable lengths, so we really like having the check there.

JB says: "yes, camera x-axis is tof axis."

With this procedure, it is possible to produce a precise map of the cloud's position and size, both of which are necessary for the precision measurements of angular correlation parameters that are of interest to us here. However, it also allows us to extract a third measurement: the cloud's polarization.

The key to the polarization measurement is that only atoms in the excited atomic state can be photoionized via the 355 nm laser. While the MOT runs, atoms are constantly being pushed around and excited by the trapping lasers, so this period of time provides a lot of information for characterizing the trap size and position. When the MOT is shut off, the atoms quickly return to their ground states and are no longer photoionized until the optical pumping laser is turned on. As described in Section ??, and in greater detail in [1], the optical pumping process involves repeatedly exciting atoms from their ground states until the atoms finally cannot absorb any further angular momentum and remain in their fully-polarized (ground) state until they are perturbed. Therefore, there is a sharp spike in excited-state atoms (and therefore photoions) when the optical pumping begins, and none if the cloud has been fully polarized. The number of photoion events that occur once the sample has been maximally polarized, in comparison with the size and shape of the initial spike of photoions, provides a very precise characterization of the cloud's final polarization [1].

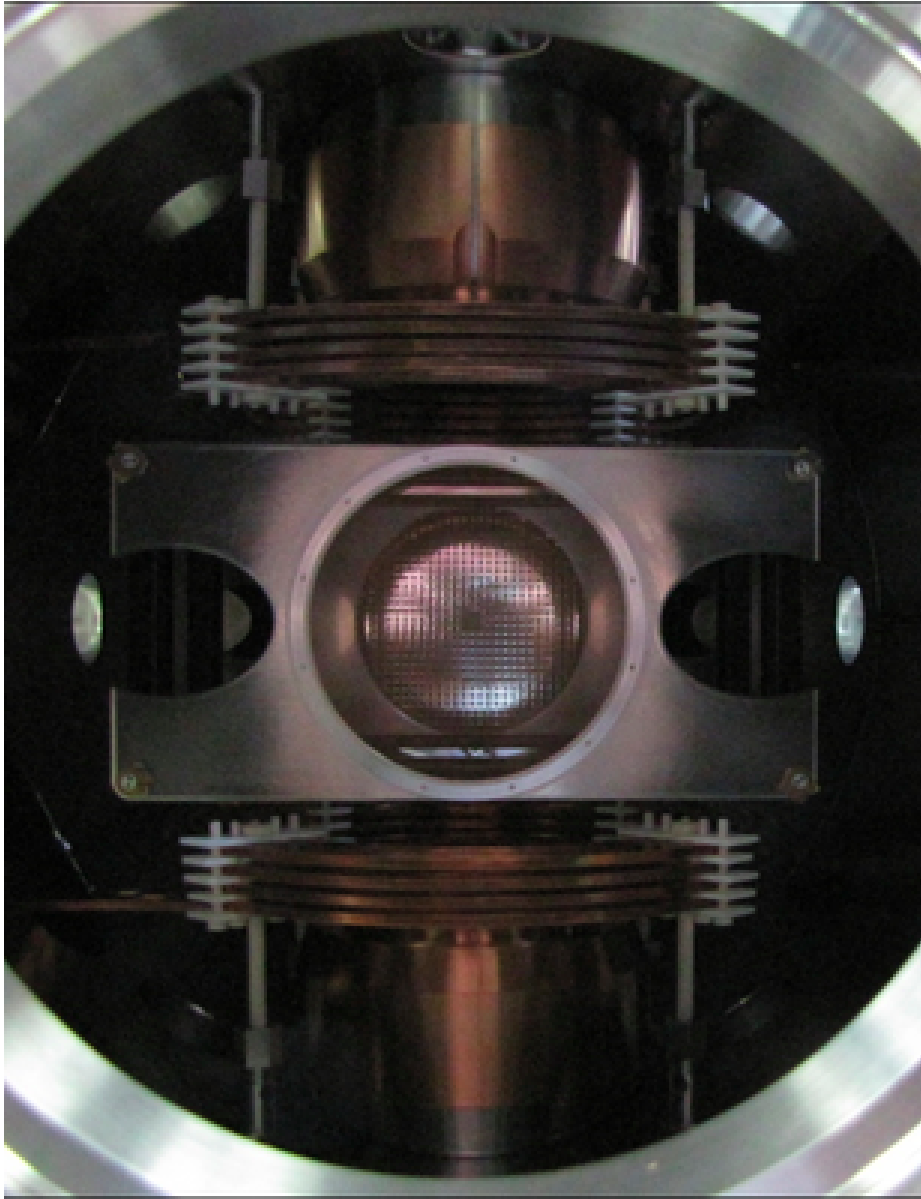


Figure 2.7: Inside the TRINAT science chamber. This photo is taken from the vantage point of one of the microchannel plates, looking into the chamber towards the second microchannel plate. The current-carrying copper Helmholtz coils and two beta telescopes are visible at the top and bottom. The metallic piece near the center is one of the electrostatic ‘hoops’ used to generate an electric field within the chamber. The hoop’s central circular hole allows access to the microchannel plate, and the two elongated holes on the sides allow the MOT’s trapping lasers to pass unimpeded at an angle of 45 degrees ‘out of the page’.

Chapter 3

Calibrations and Data Selection

I really need an excuse to include more pictures of data. Also, more pictures of simulations.

Missing figure

Show individual beta energy spectra. ...with a variety of different cuts, perhaps?

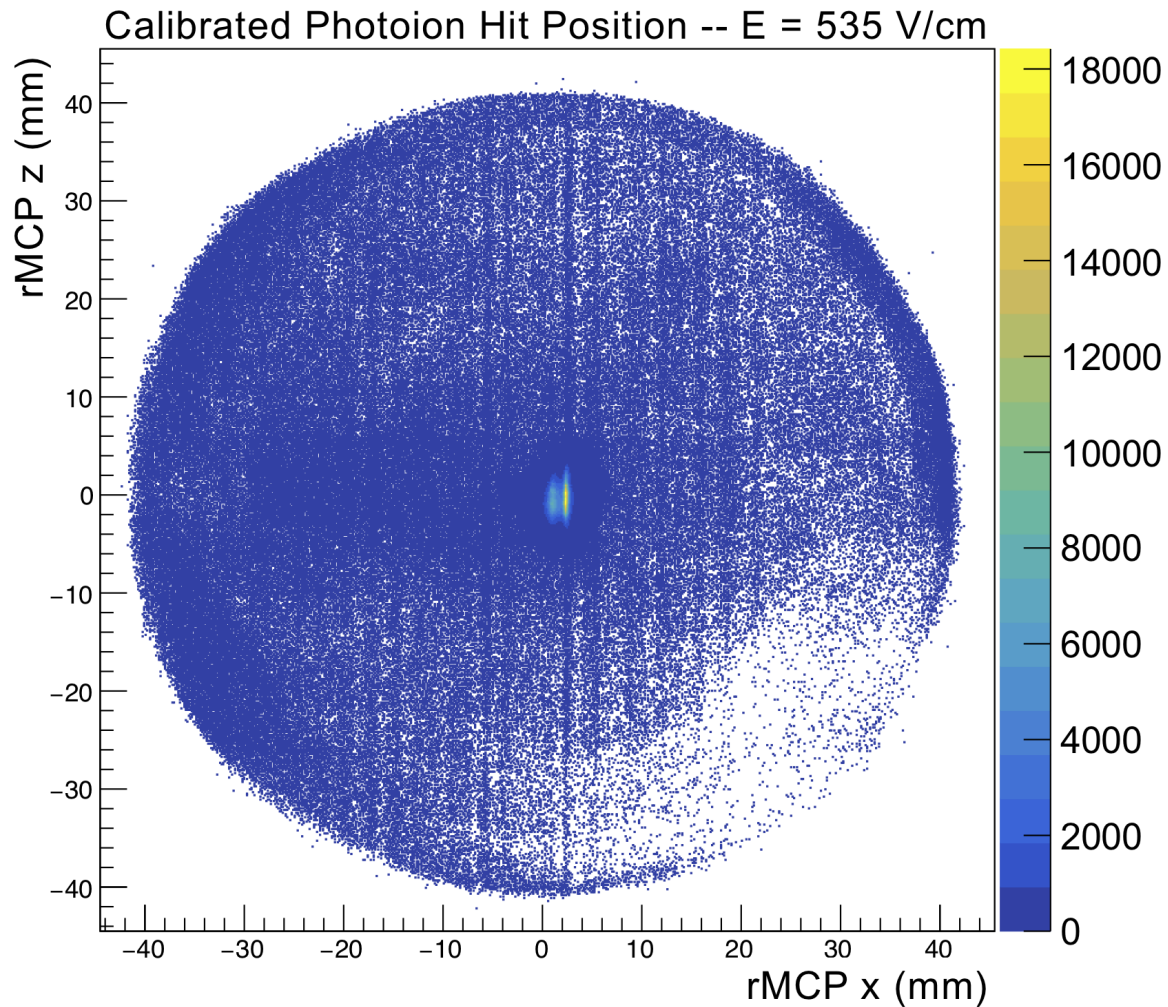
Without further ado, I'm just going to put in several pictures. Right here, right now. They're likely to **actually** show up on subsequent pages mixed in with the other content. I'll have to fix that at some point.

I have some tables summarizing which types of data were measured. Presently, that's in Ch-4 (now ch.3), but probably I should move it here.

3.1 Measurements of the Atom Cloud

Content that previously was in this subsection is now in Section 2.6. But also, see Section ???. Probably in this section here, I need to just jump right in assuming everyone understands the physical principle of how the data works. Then, I can talk about what the data **is**, and how it gets interpreted.

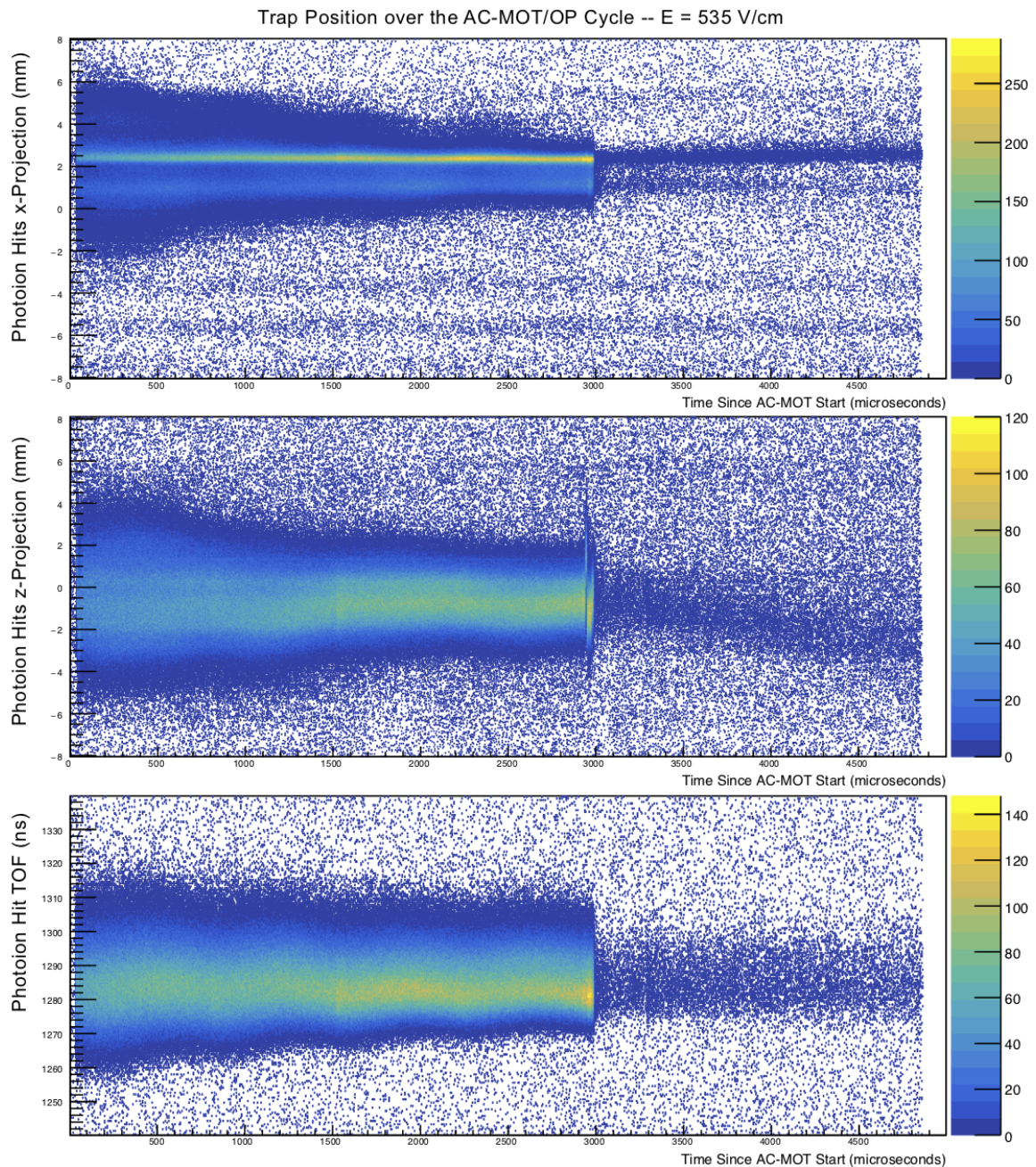
Trap position – Measured using the same dataset that was used to quantify the polarization. The trap drifts slightly over the course of our data collection. Describe the rMCP calibration needed to extract this info.



This figure needs to be discussed in text or whatever.

Figure 3.1: Photoion Hit Positions in 2D. This is all of the data taken at 535 V/cm.

Polarization measurement was conducted on a different set of data, collected in between the measurements used for A_β and b_{Fierz} , and at a higher electric field, because we were unable to run both our MCP detectors simultaneously.

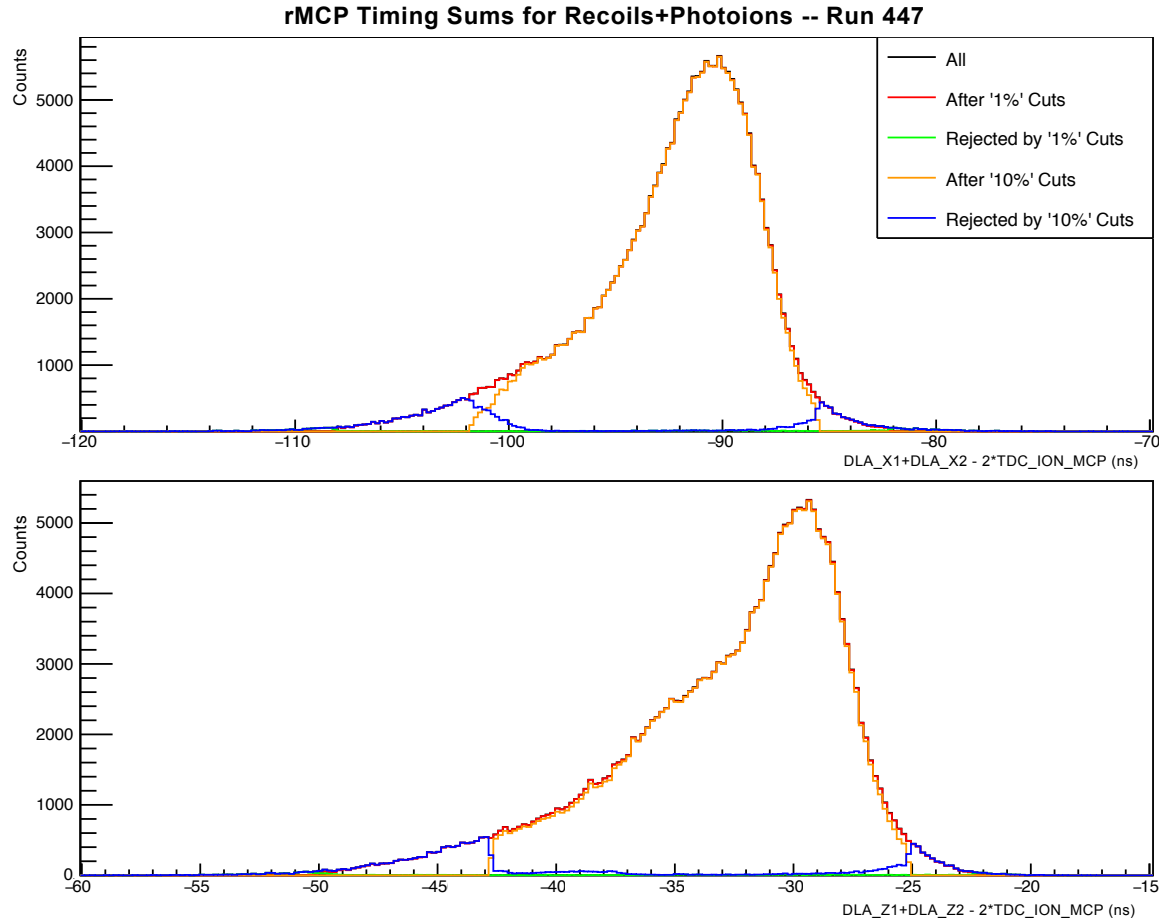


This figure needs to be discussed in text or whatever.

Figure 3.2: Photoion Hit Positions at 535 V/cm, as a function of AC-MOT Time

Missing
figure

Need pictures of the cloud. Possibly need projections of the cloud as a function of time, for AC/OP cycles.



This figure needs to be discussed in text or whatever.

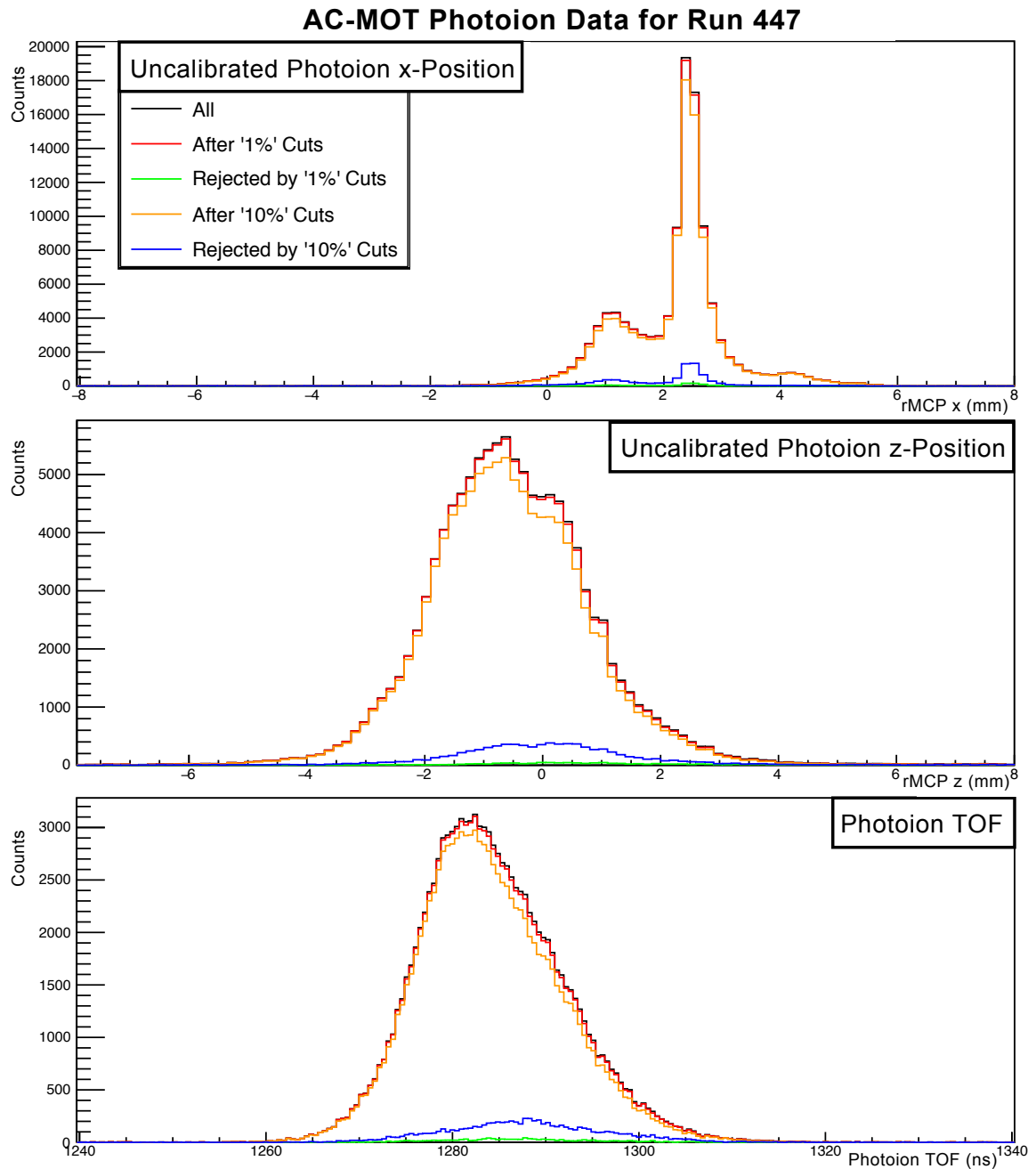
Figure 3.3: Sumcuts for the rMCP, run 447.

Anyway, here is a nice table describing the atom cloud, for each of 3 runsets, and I'll immediately reference it right now, as Table 3.1:

Also, we noticed the trap drifting after one of the runs, because one of the batteries on one of the thingies adjusting the laser frequency (I think) was failing.

JB: "If we rejected the data with the MOT moving (indeed a battery determining the voltage controlled oscillator frequency offset between absorption in stable ^{41}K cell and the ^{37}K resonance) then that's all you need to say."

describe how you'd turn this into a physical description of the cloud, with like a temperature and a sail velocity and shit. with equations.



This figure needs to be discussed in text or whatever.

Figure 3.4: A projection along all three axes for run 447, with various cuts on the rMCP delay line timing sum.

		Initial Position	Final Position	Initial Size	Final Size
Runset B	x	1.77 ± 0.03	2.06 ± 0.08	0.601 ± 0.013	1.504 ± 0.047
	y	-3.51 ± 0.04	-3.33 ± 0.05	1.009 ± 0.013	1.551 ± 0.018
	z	-0.661 ± 0.005	-0.551 ± 0.021	0.891 ± 0.004	1.707 ± 0.015
Runset C	x	2.22 ± 0.05	2.33 ± 0.11	1.18 ± 0.04	1.538 ± 0.087
	y	-3.68 ± 0.04	-3.31 ± 0.06	0.965 ± 0.012	1.460 ± 0.030
	z	-0.437 ± 0.09	-0.346 ± 0.037	0.927 ± 0.007	1.797 ± 0.026
Runset D	x	2.274 ± 0.012	2.46 ± 0.06	0.386 ± 0.016	1.382 ± 0.046
	y	-4.54 ± 0.04	-4.28 ± 0.04	0.986 ± 0.08	1.502 ± 0.013
	z	-0.587 ± 0.04	-0.481 ± 0.018	0.969 ± 0.003	1.861 ± 0.013

Sig figs here need work.

Table 3.1: Cloud Positions and Sizes – Measured immediately before and immediately following the optical pumping phase of the trapping cycle. All entries are expressed in units of mm, and the “size” parameters describe the gaussian width.

3.1.1 Measurements with the rMCP

Potential new subsection: the camera? Otherwise it has to go here.

I did this, and they’re absolutely needed to make any sense of the trap position data. These calibrations are done during AC-MOT time, and we’re actually interested in the rMCP data taken during OP time. Can I find pictures to estimate the size of the change resulting from the magnetic field? In any case, the change is pretty small.

Now, the unsorted bullet points for the rMCP stuff!

Using the “other” data set with the rMCP: Measure the trap position/size/velocity/expansion with the rMCP and with the camera. Necessitates calibrating the rMCP, which is its own whole thing. Also measure polarization.

- rMCP calibration probably gets its own section, if not its own chapter..
- We took the mask off before the 2014 run, to give us more detector area. Use previous reference calibration *with the mask* during the test run in Nov 2013. The delay line’s non-linearities should be the same, assuming we can get the centering the same. Cables have changed and stuff, so we have to re-center the pre-calibration image to where the old pre-calibration image was. ... So, center the new runs w.r.t the old run.
- We’ll want to make some sum cuts for these things. We might like them to be

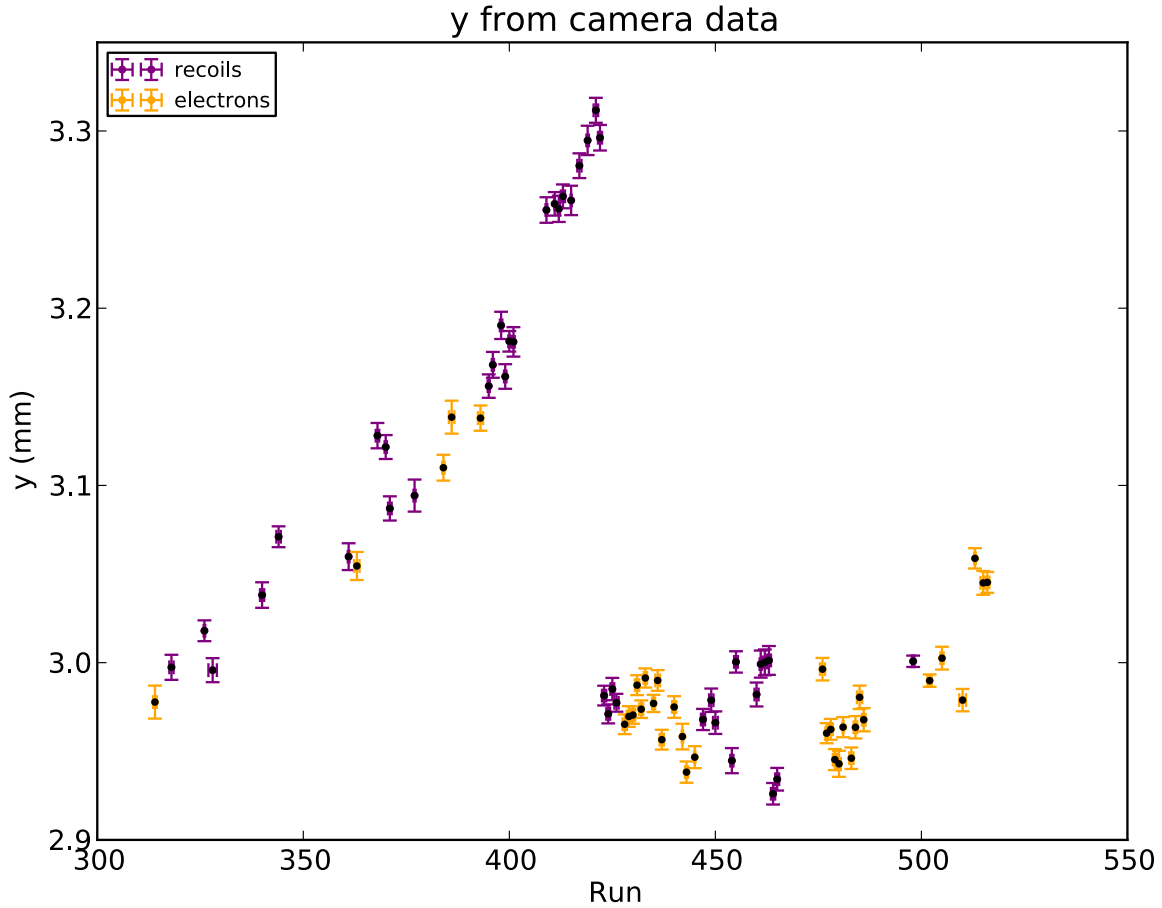


Figure 3.5: Trap Position along the “Time-of-Flight” Axis. Electron runs and recoil runs plotted by run number. (I should probably re-plot this. Maybe combine info with Fig. (3.6).)

identical, or at least identical-ish, but the peaks don’t really look the same. So we’ll settle for “decent sum cuts for all!”. ... So, apply sum cuts to the new runs and old run.

- Calibrate the old run, with the mask. In fact, I don’t remember which order I did things in. But I have a record of it here, somewhere...

3.1.2 Measurements with the eMCP

I can describe the eMCP calibration here, even though it mostly wasn’t implemented by me. It is tangentially relevant to data selection and background estimation by providing an experimental energy spectrum for shake-off electrons. It’s actually a

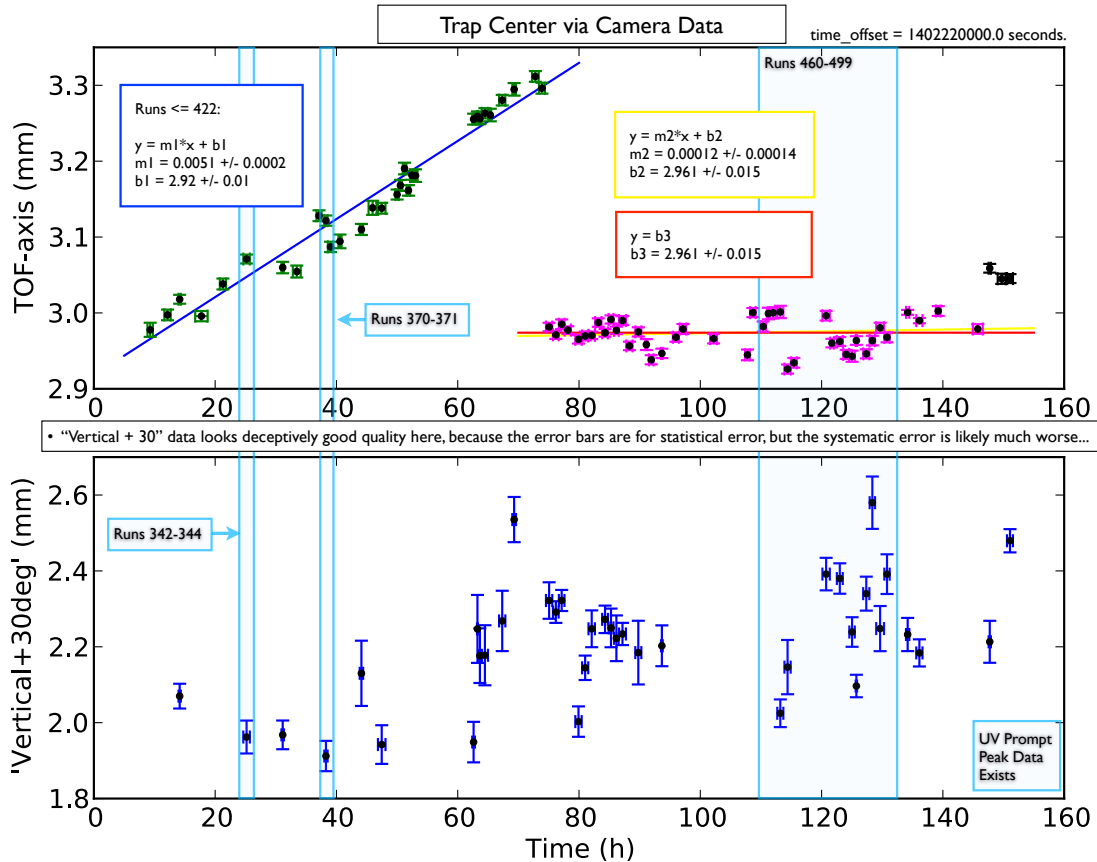


Figure 3.6: Trap Position along the “Time-of-Flight” Axis and the “Vertical+30” Axis. All runs plotted by time of run. (Need to re-plot this.)

pretty neat algorithm that I basically wasn’t involved with.

JB: eMCP. You need to describe the timing information obtained. You also need a statement of whether or not you used the position information in your cuts.

3.2 Data Selection and Preliminary Cuts

We now consider how to clean up our data. We make some fairly obvious, intuitive cuts, and those are described here. Later, we’ll make less intuitively obvious cuts.

Although the detection chamber was designed to feature two MCP detectors on opposing sides of an applied electric field intended for simultaneous use (see Section 2.5), in practice the two detectors produced quite a bit of feedback when operated at the same time. In order to salvage usable data from the beamtime, we ended up running

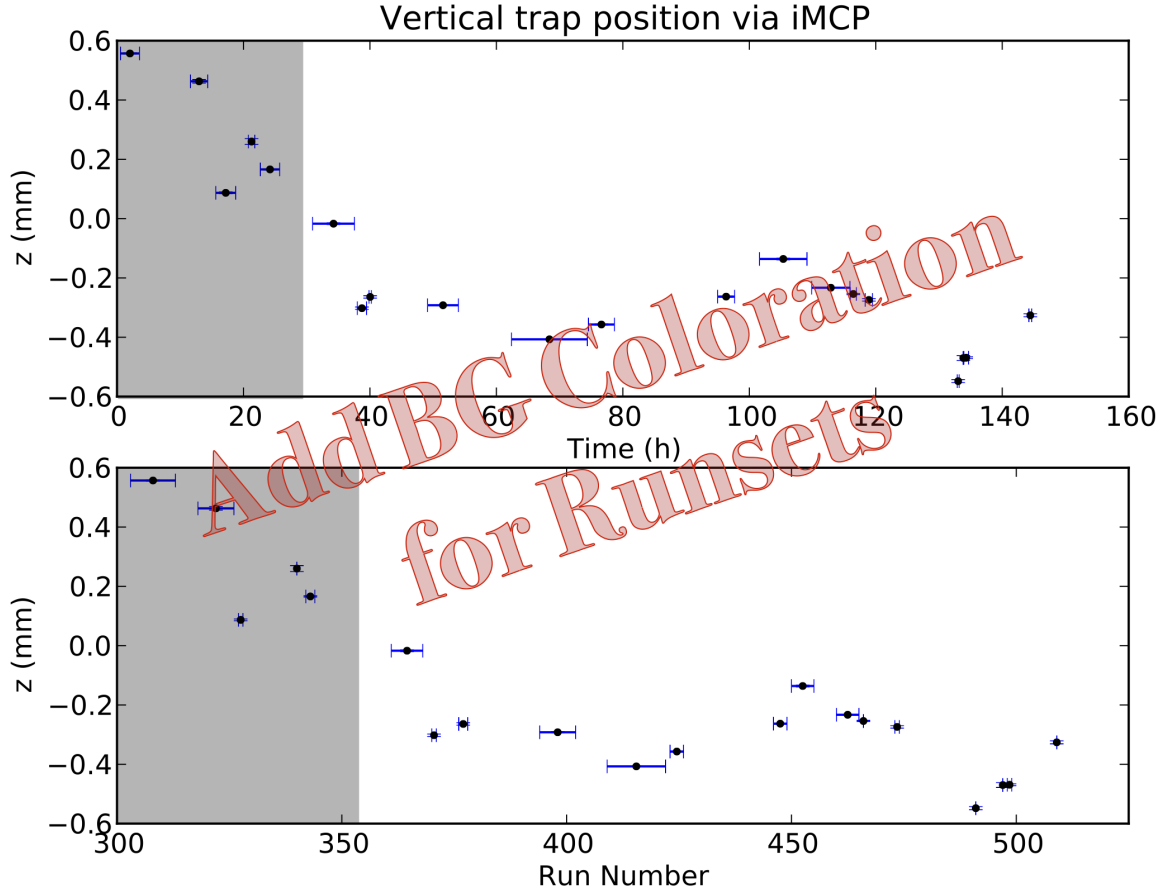


Figure 3.7: Trap Position along the Vertical Axis, plotted as a function of time of run (top) and run number (bottom).

only one detector at a time, but switched which detector was in use every few hours, collecting approximately the same amount of data with each detector. Thus, the runs are sorted into ‘electron’ and ‘recoil’ runs, depending on what the detector in use was intended to detect.

While the beta asymmetry and Fierz interference are best evaluated using the electron runs, the recoil runs are best for evaluating the polarization (a dominant uncertainty in the beta asymmetry measurement) and the cloud position. The polarization measurement is the subject of a recent publication (see [1]), and the cloud position evaluation is discussed in more detail in Chapter 3.

The data is further split up into four runsets: A, B, C, and D based on when certain detection settings were adjusted, and each of these runsets contains both electron and recoil runs. These four runsets were then treated separately for nearly

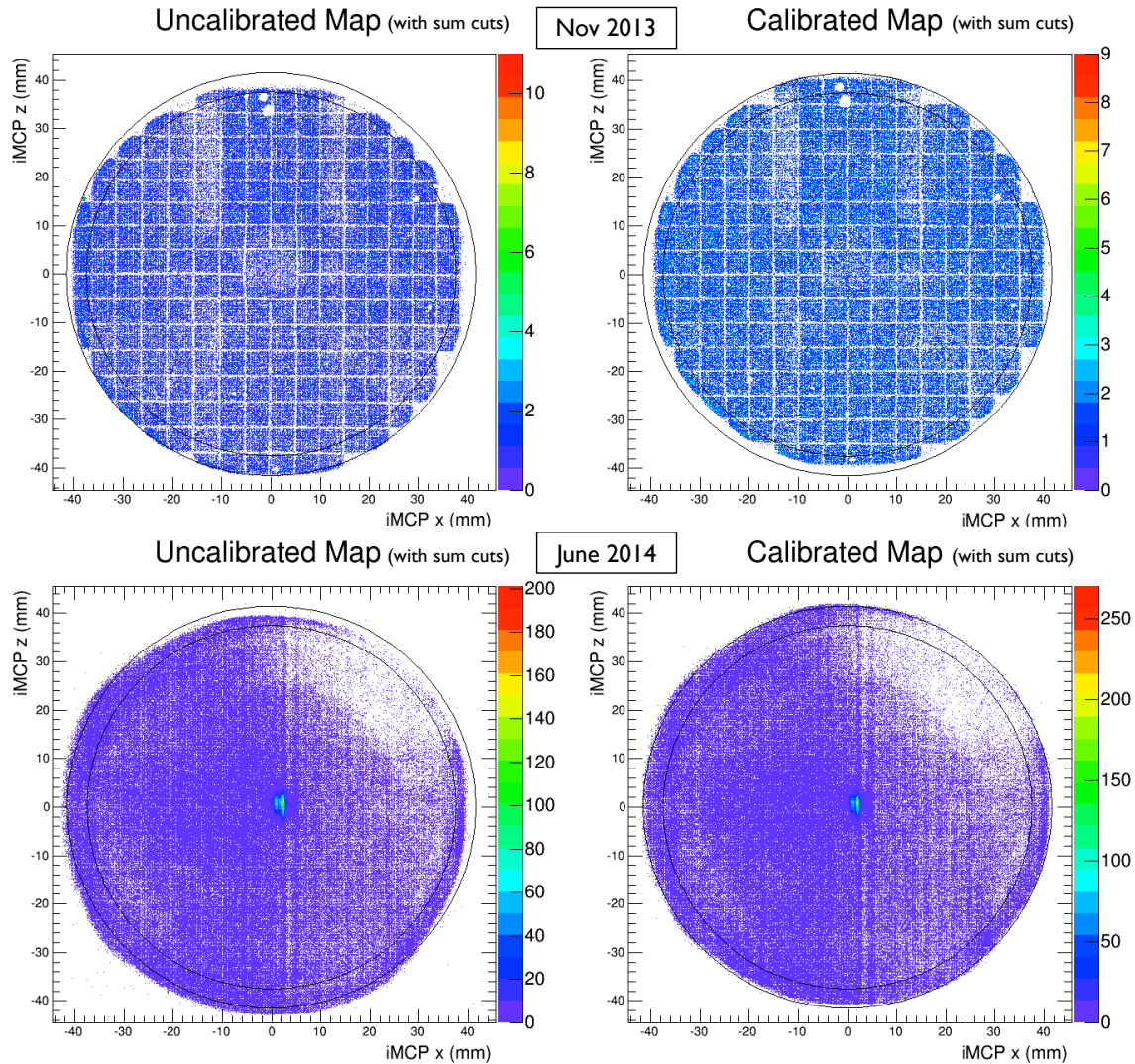


Figure 3.8: rMCP Calibration. Definitely comment about how this calibration went here, in the figure caption. (Do I definitely want a picture with the stupid line-y runs? Maybe it's better to just *not*...)

all parts of the analysis. In particular, Data Set A was neglected completely during analysis after it was determined that one scintillator had an improperly set hardware threshold such that lower energy betas weren't being detected at all. Additionally, there was a QDC module failure between Runsets B and C, resulting in an abrupt change in calibration for the two scintillators.

"The observant reader may find it curious that the listed runsets start at "B" and continue alphabetically. There was initially a "Runset A" collected as well, however it was determined later that this data could not be salvaged for use in the final analysis because one of the scintillators had its hardware threshold set above the compton peak, and without that reference point an accurate calibration could not be performed.'

	Electron Runs	Recoil Runs	OP Delay
Runset A	314, 362, 363, 383, 384, 385, 386, 393, 420.	303, 308-313, 318, 326, 327, 328, 340, 342, 343, 376, 377, 378, 394, 395, 396, 398-402, 409-419.	$300\ \mu s$
Runset B	428-437, 440-445.	421-426, 446, 447, 449.	$300\ \mu s$
Runset C	476, 477.	450, 454, 455, 460-466, 473, 474.	$700\ \mu s$
Runset D	478-489, 502, 503, 504, 505, 510, 513.	491, 497, 498, 499, 509.	$400\ \mu s$

MUST check to make sure I didn't use Run 420 in "good runs" in the end!!!

Ugh. My categorization system is slightly different than Ben's on the later recoils. That's annoying.

Other things I could list here: Electric field strengths, total runtime.

Table 3.2: A list of 2014 online runs with potentially usable data. Runset A was discarded completely due to problems with hardware threshold settings. There was a QDC module failure before Run 450, so it and all subsequent runs were performed using a different module, and as a result the scintillator calibrations changed slightly at this time. Anyway, the point of this thing is to show which electron runs and recoil runs go together, for the purposes of evaluating polarization and cloud attributes.

	OP Delay	Electric Field	Usable Events
Runset A	$300\ \mu s$	66.67 V/cm	0
Runset B	$300\ \mu s$	150.0 V/cm	173,640
Runset C	$700\ \mu s$	150.0 V/cm	18,129
Runset D	$400\ \mu s$	150.0 V/cm	207,596

Table 3.3: Electron Runs and Parameters.

This table might eventually go away. Mostly I just want a record of the total 'good' counts. In total, $N = 399,365$.

Before proceeding further, several basic cuts are performed on the data. For the

Electron Runs which are to be processed directly into a physical measurement, we consider only events in which there was a recorded hit *both* on the eMCP *and* on (at least) one of the scintillators. The required scintillator hit, of course, is potentially a beta, and so it is obvious why this must be present. The eMCP hit requirement – particularly with the timing of the eMCP hit occurring within a certain time range relative to the scintillator hit – is used to tag beta decay events originating from the cloud, as opposed to those originating from some other surface within the chamber. The precise time interval to be used, and how its results should be evaluated, is discussed in Section 3.4, but for the first pass through the data it is good enough to simply require that an eMCP hit occurred. Although not every beta decay event from the cloud will produce a hit on the eMCP, this requirement eliminates a great deal of background that would otherwise be challenging to evaluate.

also discussed: how we decide what counts as an eMCP hit at all

Awkward stupid phrasing.

Also, we claim that it doesn't bias the data. Much. Didn't I try to evaluate how much it biased the data at one point?

Because the eMCP hit is required as a ‘tag’ of good events, it is also necessary to remove from direct consideration any event which is coincident with a pulse of the photoionization laser. When photoionization occurs within the atom cloud, an orbital electron is removed from the atom and will be accelerated by the electric field into the eMCP, just as a shake-off electron from a decay might be. If, by chance, this photoelectron arrives in coincidence with a scintillator hit, it would be interpreted as a decay event from the trap – unless we preemptively discard it.

Over the course of the runtime, there were several instances where we noted an apparent electrical discharge within the experimental chamber, producing enormous backgrounds for a short time. The detectors typically recovered quickly afterward, so it was neither necessary nor useful to stop an entire run to wait for the system to recover. Instead, the time when the discharge occurred was recorded, and events within approximately one minute of the spark time were discarded.

We use only the “fully polarized” events for which we have a detailed understanding of the nuclear polarization (described in more detail in [1]). This means we must use *only* events from the “optical pumping” portion of the duty cycle (see Fig. 2.4), and discard events when the DC- or AC-MOT is active. After the AC-MOT is shut off, there is a short delay before optical pumping begins (see Table 3.2) to allow the magnetic field to decay, and it is only after $100\ \mu s$ of optical pumping that we consider the atoms to be fully polarized. Furthermore, because the magnetic field from the DC-MOT is slow to decay (relative to the field from the AC-MOT), all events from the first five AC/OP cycles after every atom transfer are discarded. A secondary

benefit of our insistence on considering only polarized data is that the scintillators' gains are more stable in the presence of only the (small, stable) magnetic field used for optical pumping than they are in the presence of a larger oscillating magnetic field used for trapping.

change by 0.2% of its value vs change by 0.5% of its value, according to Ben's thesis pg 143.

Finally, because this analysis depends heavily on energy measurements from the two scintillators as a proxy for beta energy, it is necessary to remove events in which the pulser LED fired. Although the pulser LED is useful for evaluating the stability of the scintillators, in the case where an LED pulse occurs together with a true beta hit in the scintillator, it may change the measured energy. Therefore, we discard all events that include an LED pulse.

3.3 Further Cuts Using the DSSD

Pretty sure I'm repeating myself from Chapter ??

JB says: To repeat a comment, since the Appendix on analysis changes is being dispersed throughout, when you state somewhere (I think it's in Ch. 6)((5?)) make sure you state clearly that the only change for BB1 cuts is the radius cut, e.g. that you took the same T and E from the waveforms (I'm not even sure whether the waveforms are recorded anyway). You ask 'how can I state this' but there's no reason to be subtle. Just say upfront that Ben and Spencer's theses did all the groundwork on the BB1, and here you include selected details needed to understand the present analysis. If you need to include some redundant material, don't worry too much about that.

...

MJA: In fact, I think the BB1 radius may have been the same. The uniform energy threshold was different though. But I get the point.

...

Also, yes, the waveforms are absolutely recorded in the MIDAS files but they haven't been saved to modern ntuples, because they made the files huge. I think it's probably pretty easy to switch that on/off in the Analyzer though to generate a set of ntuples that has that info included.

Although it was not possible to use the DSSD in real-time analysis or event triggering, the DSSDs may be used, after the data has been collected, to distinguish between different types of particles incident on the detector, as more energy will be deposited by heavier particles. When a scintillator hit is triggered by a particle originating within the experimental chamber, that particle will typically have passed

through the DSSD before arriving at the scintillator.

In the present experiment, the two primary particles that will concern us are β^+ particles originating from the decay of ^{37}K , and γ rays, which may be produced through a variety of processes, e.g. directly from the 2% decay branch, through annihilation of β^+ particles upon their interaction with regular-matter electrons, or bremsstrahlung radiation from emitted β s.

We would like to look specifically at events involving β^+ particles arriving direct from a decay within the atom cloud, and the DSSD may be used to eliminate events in which the scintillator is triggered by a γ . An incident β will typically deposit some portion of its energy in the DSSD as it passes through, however an incident γ will deposit significantly less energy; for this setup the energy deposited by a γ is generally indistinguishable from background on the DSSDs. Therefore, we require that a ‘good’ event must include a ‘good’ hit to the DSSD as well as a hit to the associated scintillator.

In order to proceed at this point, and because the DSSD readout records so much information, it is necessary to develop some criteria to determine whether or not we will accept any given DSSD readout as a β hit.

How do I *say* that Ben was the one who did most of the DSSD calibration stuff? I maybe don't need to describe all of it here, but I *could*, and maybe it's needed in order to understand like 4 rows in my error budget.

JB: “You can describe anything you did differently or improved, but you can and should otherwise defer all details of the scintillator calibration and DSSD calibration to Ben’s paper and his thesis and Spencer’s. E.g. Section 5.2 “statistical agreement between BB1 X and Y detectors’ energies only makes a small effect on results” does not need the technical details beyond that statement.”

JB: “If you have some way of documenting the coding you used, that would be great.” ... yeah, it would, wouldn’t it?

We read out the full waveform for every strip at each event with a scintillator hit, but in post-processing take *only* the ‘time’ and ‘energy’ from the peak waveform height and the time in the waveform at which that occurs. Each strip will have its own noise spectrum and energy calibration. To classify an event as a good DSSD hit, we require at least one ‘x’ strip and one ‘y’ strip record an energy above the noise threshold. We require that the x strip and the y strip agree (to within some number of standard deviations) in amount of energy deposited, and in the time at which that hit occurred. In order to avoid problems resulting from the strips’ non-uniform

noise thresholds, we further require that the energy deposited be greater than some lower-end cutoff which is selected so as to be higher than every individual strip's noise threshold. In this case, the DSSD's lower energy uniform threshold was set at 50 keV.

I think Ben might have selected 60 keV? That's maybe something for the appendix.

We also elect to use only events where a beta hit the DSSD within a 15.5 mm radius of the center of the detector, so as to avoid scattering effects from the collimator walls.

Also-also (did I mention it already?) look for events with only **one** DSSD hit (two could indicate the beta scattered back out of the detector in another pixel, or alternately an accidental coincidence of two beta decay events. either way, no good for analysis.) Also, only one scint hit, and it has to be the on the same detector with the DSSD. (...A scintillator hit as indicated by a TDC readout, as well as a max. recorded scint energy for the "extra" scintillator at something stupidly tiny, like 10 keV. Probably **actually** 10 keV.)

Did I even mention the collimator? Like, in the previous chapter or something..?

After all other cuts – not before!! – we eventually use only events with scint energy between 400 - 4800 keV. High cutoff is because of the low number of events, which makes the observable—the superratio asymmetry—poorly defined and poorly behaved. Low cutoff is because it's really hard to model what's going on down there to the required level of precision. The observable depends most heavily on low beta energy events, so it is imperative that the lower energy portion of the spectra be thoroughly understood if they are to be used for analysis.

Somewhere I should list what the energy cutoff is for this spectrum. Or semi-equivalently, the Q-value.

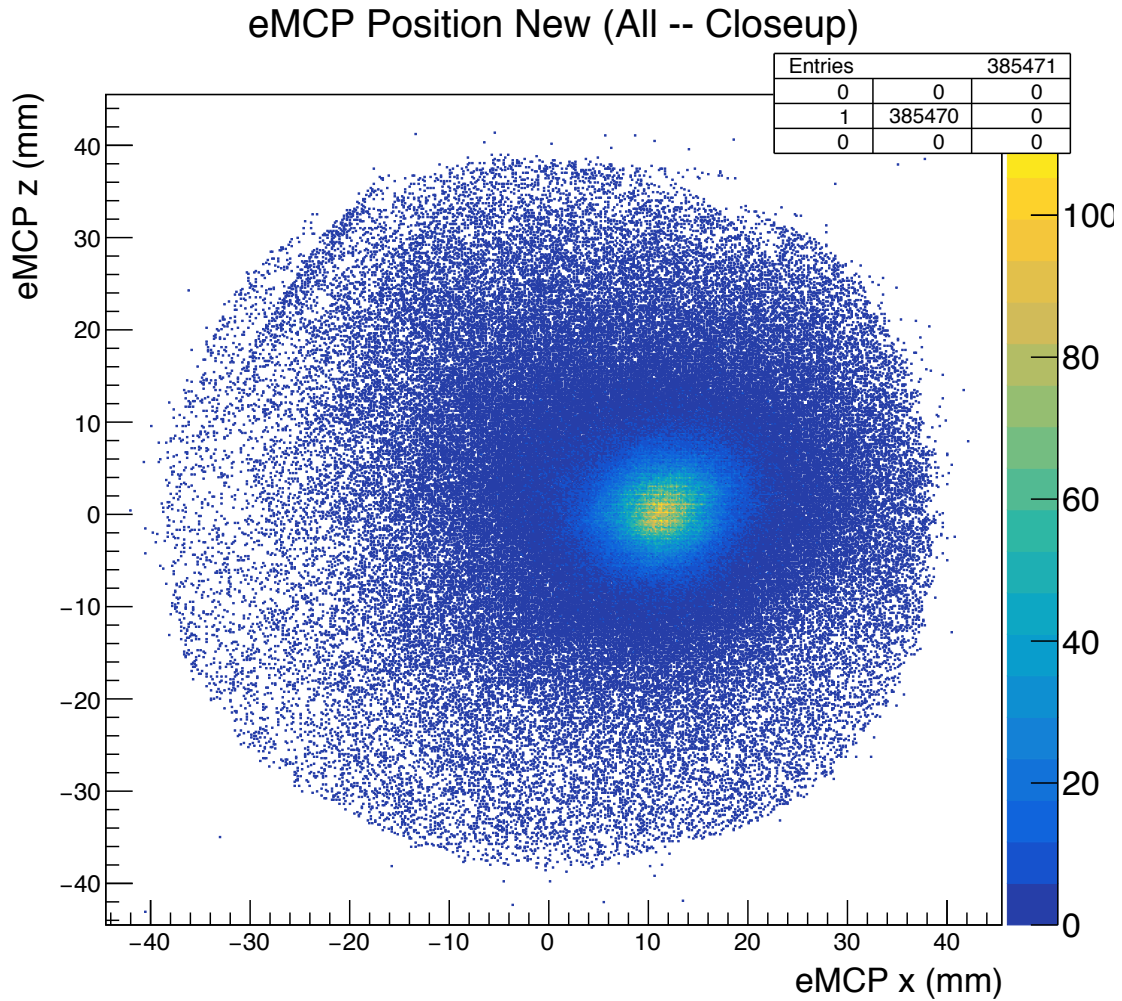
3.4 Further Cuts Using the eMCP

I described the HEX-75 somewhere in a previous chapter, right??

The eMCP features a set of three delay lines, intended to be used to record the position of a hit, as in Fig. 3.9. Though only two delay lines is sufficient to determine the position within the plane of the MCP if they are both hit, the presence of a third delay line allows for some redundancy. In practice, however, a large fraction of otherwise 'good' events include a hit on the eMCP, but have insufficient information recorded on the delay line channels to reconstruct a position.

Do I need to describe MCPs and delay lines somewhere? Maybe not...

Because a SOE from the trap is most likely to land in the centre of the plate, while the background from other sources is roughly constant across the plate, it might make sense to accept only events where the eMCP hit is within some radius of the central peak. This methodology was seriously considered because the remaining data has

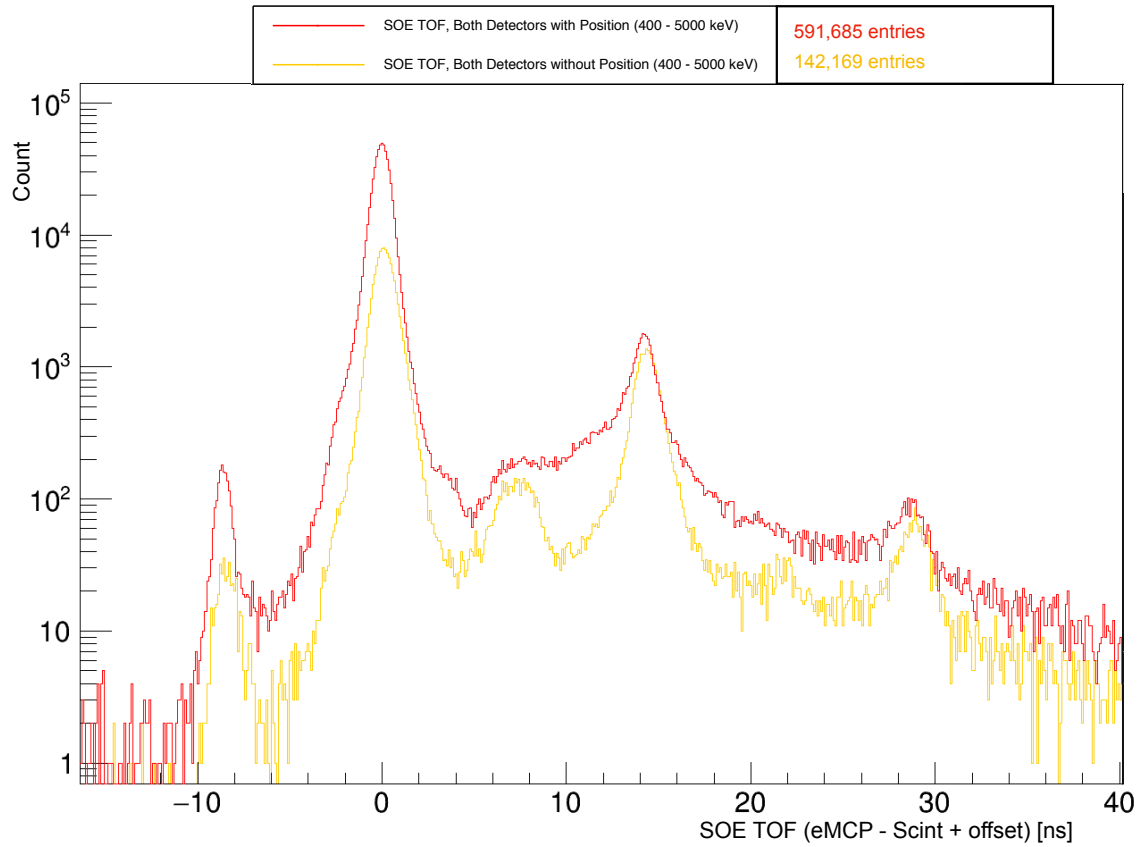


This picture is ‘slow’. Need to re-save it as a png.

Figure 3.9: Position as measured on the eMCP, after some data cleaning.

a much lower fraction of background events polluting it – however this results in a loss of around half of the events even for the most generous eMCP radius cuts (see Fig. 3.10). Therefore, it was decided that no position cuts on the eMCP would be made in the final analysis.

Several years after the data was initially collected, a problem was discovered with our low-level analyzer software, which we had been using to convert large and unwieldy MIDAS data sets into somewhat smaller and more manageable ROOT data sets. In particular, for every timestamp recorded, our raw MIDAS data actually included both



Um. Did I for sure get the labels correct on this??? It seems really wrong.

Figure 3.10: Beta-electron TOF, for events with and without eMCP hit position information. A cut will eventually be taken to accept only events sufficiently near the largest peak – in this case the number of events is ‘only’ decreased by a factor of 2.

a timestamp for the leading edge (LE) of the pulse, and a timestamp for the trailing edge (TE). The analyzer had—for years—been reporting the timestamp associated with the trailing edge of the pulse. Initially it was unclear if there might have been a reason behind this choice, but a closer examination of the data showed that the LE data included less timing jitter and noise, as well as a sharper peak for timing pulses across the board (as in Fig. 3.11), with some channels showing a larger effect than others. This was corrected, and the entirety of this analysis has been performed now using the cleaner LE spectra.

The LE spectra allows for us to use a more precise model of the SOE TOFs, so that’s nice.

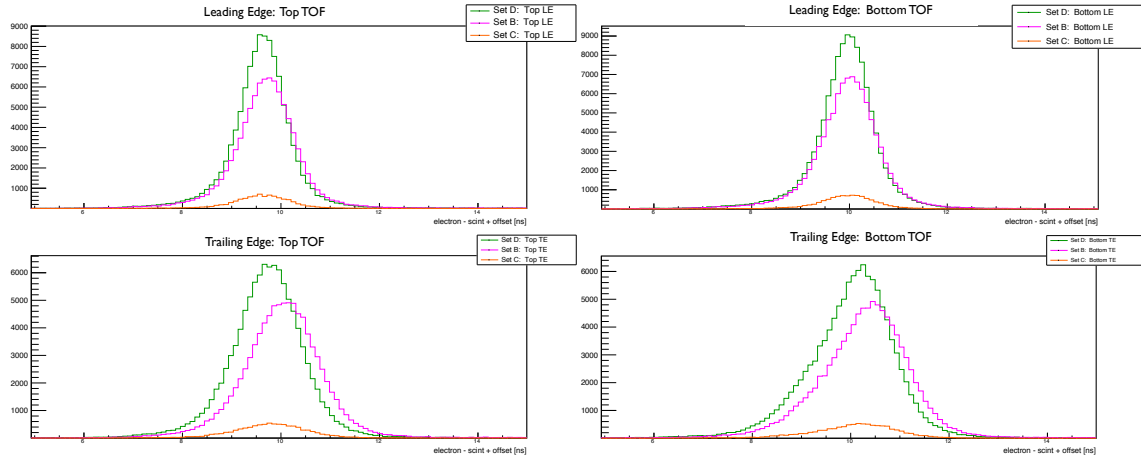


Figure 3.11: SOE TOF peaks (eMPC - Scintillator), using the leading edge (LE) and using the trailing edge (TE). Data is sorted according to runset. For each individual runset, the TE peak is broader than the LE peak. The centroid of each runset is also more variable in the TE plots.

The place where this change between the TE and LE timestamps had the biggest impact on the analysis is in the shake-off electron time-of-flight spectra, on which a cut must eventually be taken. Although this problem was not discovered in time to be used in the previous measurement of A_β using this same data [22], it likely would have had a negligible effect on the final result, because the SOE TOF cut that was used there was comparatively loose, and the evaluation of the background that remained was not a dominant systematic effect.

With the data reprocessed using the leading edge for timestamps, I wanted to eliminate as much background as possible from the SOE TOF spectrum. With this goal in mind, the next step was to correct the scintillator timing for its low energy ‘walk’ (see Fig. 3.12). A quartic polynomial was fit to each of the 2D timing vs energy spectra (the top and bottom detectors were treated separately), and the result was used to produce a ‘straightened’ SOE TOF spectrum with respect to measured scintillator energy, and as expected, the resulting SOE TOF spectrum was a bit more sharply peaked.

With the SOE TOF spectra cleaned up, a cut can be taken to reduce the fraction of background events. Informed by the model of background spectra described in Section 4.3, a was made to include only a 2.344 ns window around the primary peak in further analysis . (see Fig. 3.13).

This goes in that one appendix, if I haven't already put it there.

“...removing X fraction of the remaining events.”

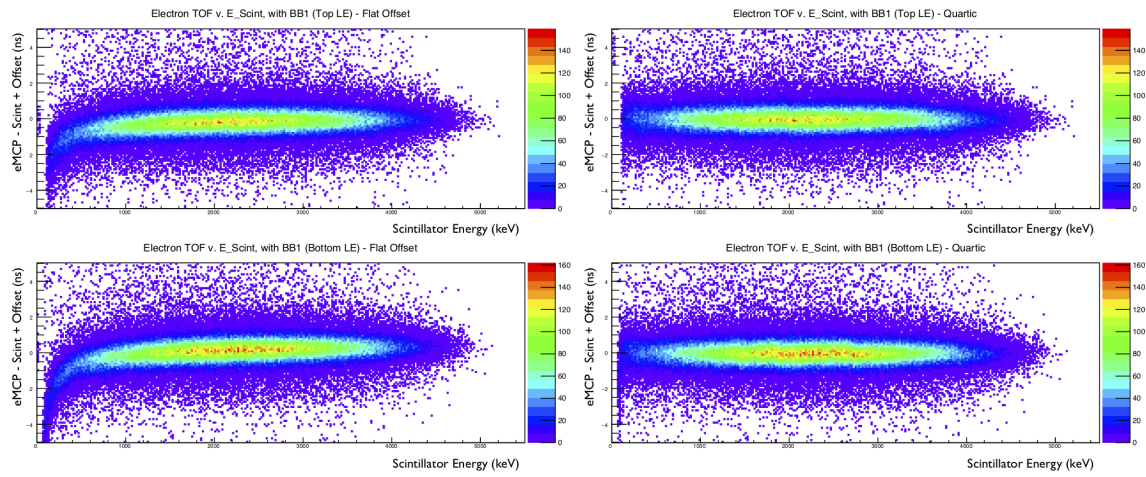


Figure 3.12: SOE TOF walk, before (left) and after (right) applying a quartic adjustment to straighten out the effective TOF.

Probably need to put that figure somewhere else.

"To check the agreement of the model with reality, we compare the averaged superratio asymmetries from both, as in Fig. 3.15." probably goes in the other section.

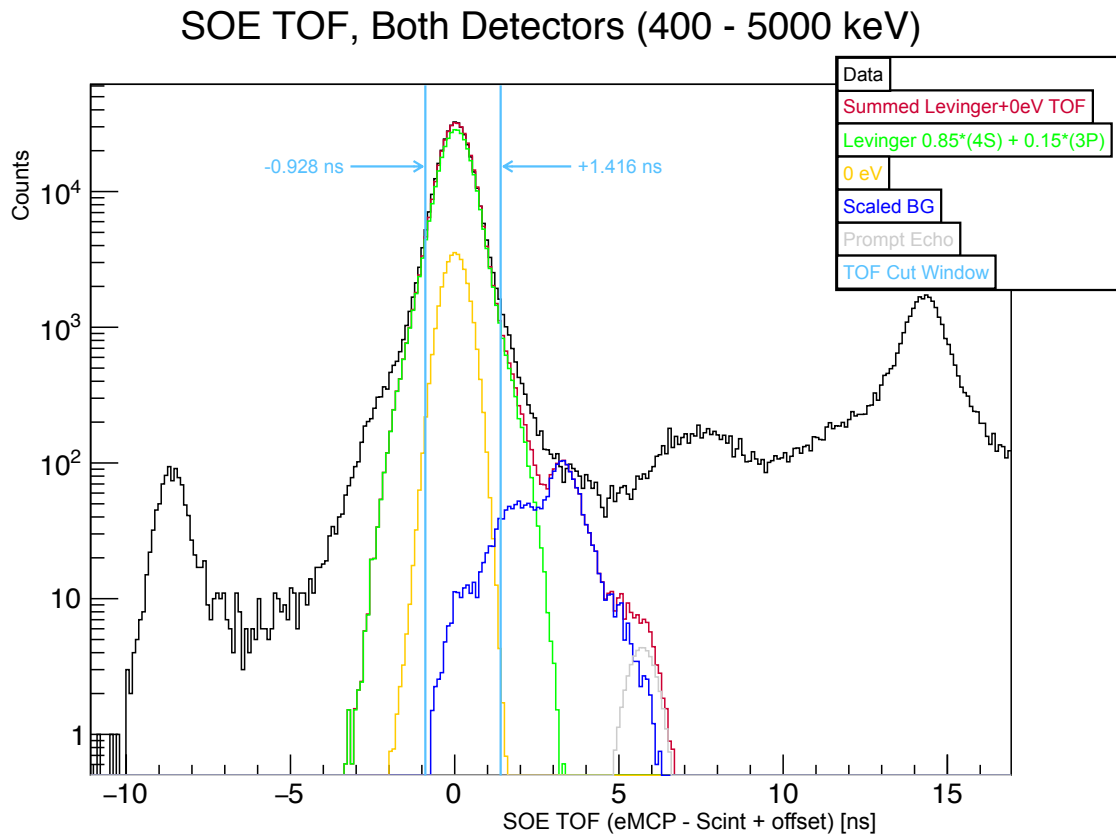


Figure 3.13: SOE TOF, model and data. In the end, I cut the data to use only events with a TOF between -0.928 ns and +1.416 ns. Max. possible background is like a factor of two too big. Similar quality results no matter how you distribute the Levinger spectra between 4S and 3P, however adding the 0 eV electrons makes a big improvement to the agreement.

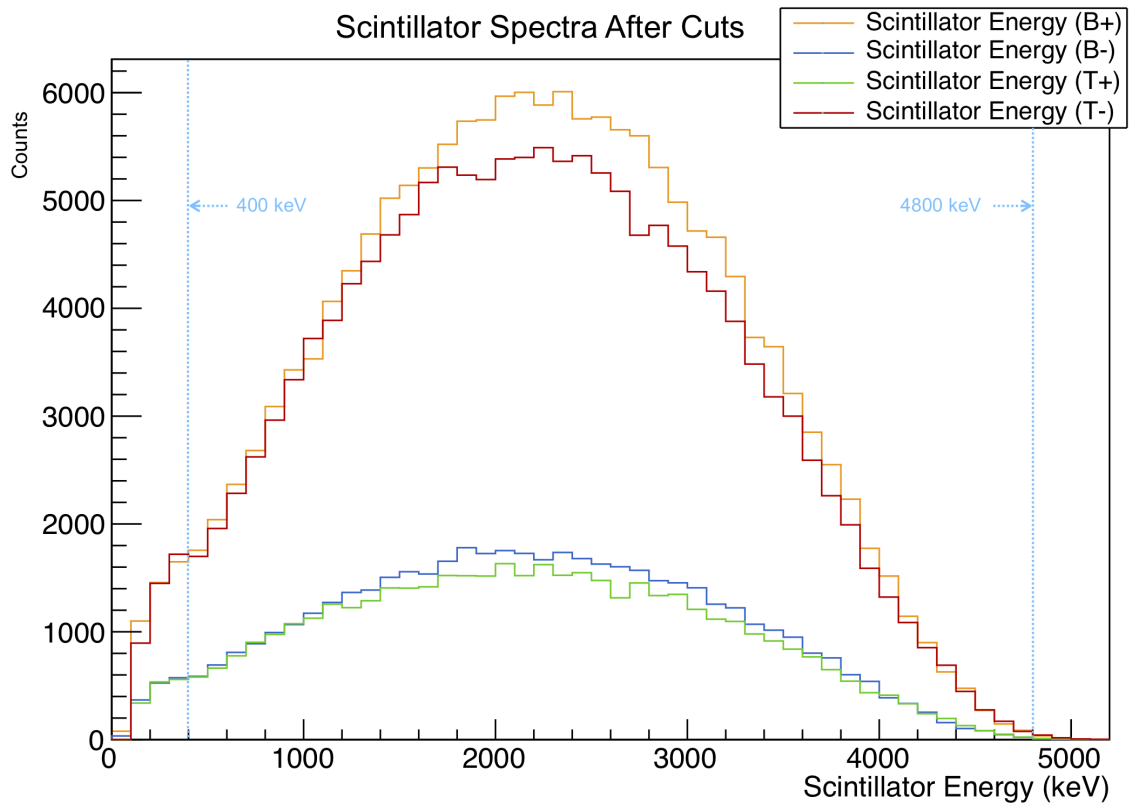
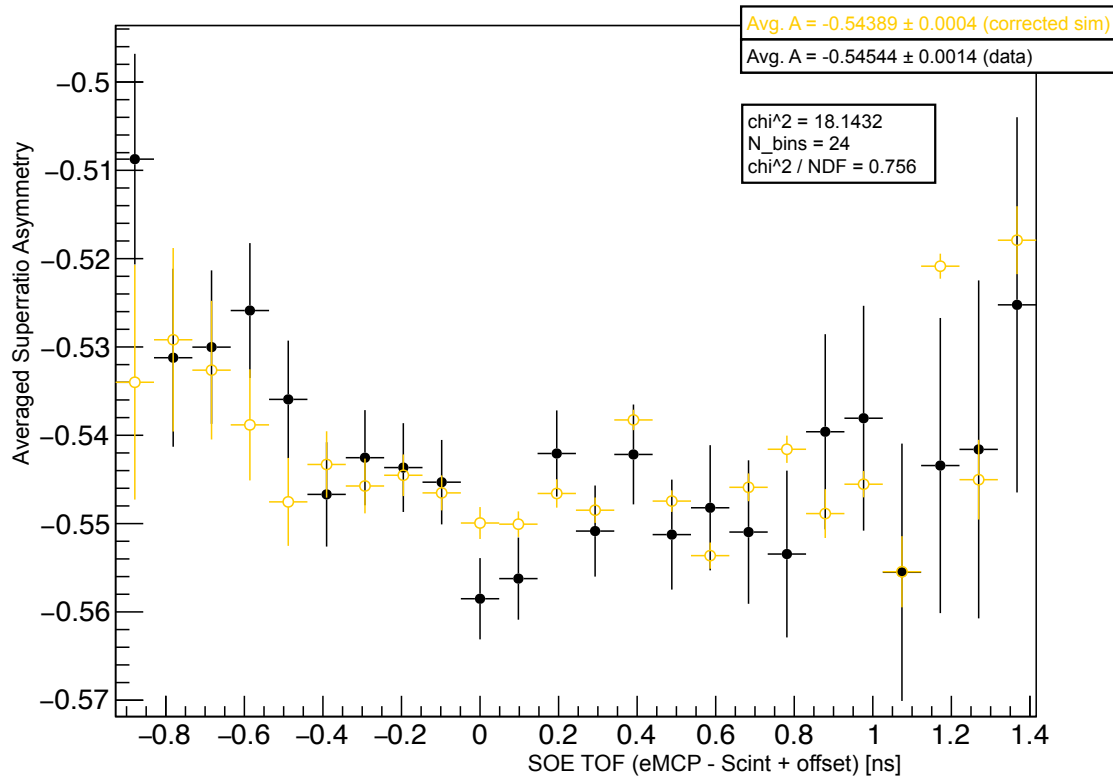


Figure 3.14: Experimental Scintillator Spectra, for both detectors in both polarization states. These spectra are what remain after all cuts have been taken. All runsets are included.

Superratio Asymmetry



I think I want this picture to go in some other section.

Figure 3.15: The superratio asymmetry, averaged over all scintillator energies between 400-4800 keV, is used to compare the experimental data and simulated TOF model as a proxy for the quality of the model to estimate the background. All other cuts have been applied.

Chapter 4

Simulations

I really need an excuse to include more pictures of data. Also, more pictures of simulations.

Missing figure

Show simulated spectra separated by scattering category.

Missing figure

Show SimpleMC spectra, show the supersum, show the superratio, show the superratio asymmetry. Maybe do some simple fits to show how much better the superratio asymmetry is than *not* the superratio asymmetry.

John says: “I doubt I will have further useful comments on the Ch. ((this chapter)) as they are now.” – Yeah, but *now* he will.

The TRINAT collaboration has created a Geant4 (G4) simulation which models the geometry and materials within the experimental chamber, and uses a monte carlo algorithm to describe generalized physical processes such as particle scattering and energy loss, within the geometry specific to the experiment. This software library has been maintained and updated over several generations of graduate students.

4.1 Considerations for Software Upgrade Implementation

Prior to the simulations required for this particular experiment, two different sets of changes to the G4 code were needed – the first to enable multithreading, and the second to introduce certain BSM interactions to the decay distribution.

Enabling multithreading allows for a single instance of the Geant4 simulation to run on several processors at once, effectively speeding up the overall simulation by a factor of the number of processors used. In the years since the simulation was originally created, the Geant4 collaboration had created libraries intended specifically to support multithread usage, and since the running G4 simulations had historically been very time consuming for the TRINAT collaboration, the decision was made to implement multithreading within our own monte carlo software, on the hopes that this would enable faster progress in analysis.

Enabling multithreading support turned out to be quite time consuming, and in the end it might have been faster to have spent those months running simulations one processor at a time. Perhaps the improvement will prove valuable for use in future TRINAT experiments.

The TRINAT G4 monte carlo package had never been used to directly model interactions beyond the standard model within the decay physics. It had previously been set up by the collaboration to use a probability density function (PDF) including most of the terms from Holstein's Eq. (51) [17], which describes both electron and neutrino momenta from polarized beta decay. This treatment is quite robust, and includes corrections at recoil-order, as well as certain other corrections of similar size.

Unfortunately, terms arising from interactions beyond the standard model are not included in Holstein's description of the decay process. To understand the kinematic results of the exotic interactions of interest to us here, we turn to the classic JTW treatment of beta decay [5] [16]. In addition to the (expected) vector and axial interactions, JTW also describes the interaction in terms of (exotic) scalar and tensor interactions, should such be present.

because for A_β even a BSM interaction will *basically* look like a SM interaction, and I think something somewhere isn't precise enough to distinguish it.

which other corrections? coulomb and/or radiative corrections, but somehow when I say that, I'm apparently talking about a different thing than everyone else who uses those terms. also, weak magnetism. also ... ???

Is this true? Does it not include *any* BSM interactions?

Furthermore, although it is currently understood that the weak interaction is predominantly or perhaps entirely ‘left-handed’, the JTW treatment leaves certain phase angles unfixed, and is therefore able to accurately describe a decay which is, for example, partially ‘right-handed’ – however the latter feature is not directly relevant to the project at hand. [It’s several phase angles in JTW, but maybe it’s fundamentally only like one angle on some level? Also I think it’s not actually a “gauge freedom,” per se. No, I’m pretty sure this ‘phase angle’ description is all wrong.] Also, consider time reversal! Anyway, most of this paragraph probably goes better in Section 1.3.

Despite JTW’s broad ability to describe beta decay under a variety of physical models, this treatment includes only the leading-order terms, and smaller terms, such as recoil-order corrections, are neglected entirely.

Surely I describe what recoil-order corrections even *are* in some appendix somewhere, right?
Or, possibly, in Section 1.3. Possibly the paragraphs above need to be moved...

Because the present project is a precision measurement of the Fierz interference, a term which arises from scalar and tensor couplings, it was imperative to create an event generator for our G4 simulations that could account for these exotic interactions while also including in its PDF the higher-order effects which, in some cases, can mimic the effects of a scalar or tensor current.

While it might have been possible to directly combine JTW’s result with Holstein’s Eq. (51), it should be noted that JTW’s expression is not compatible in general with the principle of conservation of momentum; as recoil momentum is neglected entirely, the description is only of two leptons emerging from a nucleus in directions that do not directly oppose one another. Therefore, the prospect of combining these two slightly incompatible expressions directly might be enough to give one pause. On an experimental level, the mathematical description of an emerging neutrino is only of interest to us to the extent we can reconstruct it based on detecting both a beta and the recoiling nucleus from a single decay event, and within the present experiment we do not have simultaneous access to both a beta detector and a recoil detector.

In light of the above considerations, it was decided that an entirely new event generator must be created, based instead on Holstein’s Eq. (52), in which neutrino momentum has been integrated over and is therefore no longer an explicit part of the PDF [17]. As one might guess, Holstein’s Eq. (52) is greatly simplified in comparison to Holstein’s Eq. (51). A similar integration over all possible neutrino momenta can also be performed on the JTW PDF, causing several terms to vanish. The result in both the Holstein and JTW cases is a PDF over only beta energy and direction

as measured with respect to nuclear polarization, and the two expressions can be combined in a straightforward manner by comparing similar terms.

It is this combined Holstein+JTW expression that forms the basis of the new G4 event generator. It must be noted that although the largest effect from any present scalar or tensor interactions would likely (depending on certain phase angles) be in a non-zero value of b_{Fierz} , these interactions can also introduce a perturbation to A_β at a higher order. In order for any precision experimental measurement of b_{Fierz} to be generalized to limits on the parameter space of scalar and tensor currents, it is important to incorporate an accurate representation of the results of such exotic interactions on *all* available observables, and the new G4 event generator does this.

Things that the G4 simulation did that I kept include: an accurate representation of the complex details of our experimental geometry. Also, the noise spectra on the DSSDs.

4.2 The Simple Monte Carlo and Response Function

Because of the large number of systematic effects to be examined, and because of the processor time required to run a high statistics Geant4 simulation even after enabling multithreading support, it was desirable to develop a procedure by which it would be possible to evaluate certain systematic effects while avoiding the computationally intensive simulations that might traditionally be used. To this end, a fast-running Simple Monte Carlo (SMC) was developed together with an empirical “response function” similar to the one described by Clifford et al [10] to describe probabilistic beta energy loss before its detection in a scintillator. In the end, the lineshape description became quite involved, and it is unclear whether, in the end, any time was saved this way.

The purpose of the SMC was to *quickly* generate initial particle kinematics probabilistically for beta decay events, and it uses the very same event generator based on Holstein’s Eq. (52) [17] that was developed for use with the more sophisticated Geant4 simulations. However, unlike in a G4 simulation, the SMC makes no attempt to track particles through the chamber, and instead simply calculates detector hits based on initial particle momentum. This procedure obviously neglects scattering effects, which can (in differing regimes) both *increase* and *decrease* the number of beta particles incident on a detector. Furthermore, this procedure also neglects any energy absorption in materials through which the beta passes before hitting a scintillator –

Reference previous section where I discuss this, maybe?

and the beta *must* pass through several such materials (see Fig. 2.6).

To make the best use of the SMC for evaluating systematic errors, the energy lost before a beta hits a scintillator must be accounted for somehow in order to ensure all relevant physical effects are propagated through. In particular, before hitting a scintillator, a beta must pass through a $275\ \mu m$ thick silicon carbide mirror, a $229\ \mu m$ thick beryllium foil, and finally a set of $300\ \mu m$ thick double-sided silicon strip detectors (DSSDs), before finally having its remaining energy absorbed within a scintillator. Although the DSSDs are themselves detectors with the ability to record the amount of energy deposited by an incident particle, there are some known problems in achieving a uniform level of precision across the full surface of the DSSDs, so adding the DSSD energy back to the scintillator energy to produce a better estimate of the original beta energy has the potential to create some problems for the analysis. Furthermore, given the presence of the mirror, an object with a similar thickness and scattering properties to the DSSDs, re-adding the energy lost in the DSSDs would not eliminate the need to estimate probabilistic energy loss in similar materials.

See: Some other section? Maybe?

In order to create a quantitative description of the effective response function, which varies with initial beta energy, we have created an analytic function of 14 parameters for each of four detector and polarization combinations (56 parameters in total), to represent the final beta energy spectra in the scintillators. The values of these parameters must be determined empirically, by a fit to simulated spectra. Since the final response function is expected to be a function of initial beta energy, we must allow for these parameters to also vary as a function of initial beta energy. To effect this result, the TRINAT Geant4 simulation is used to generate a series of ‘mono-energetic’ spectra. That is, for each energy value under consideration (selected to span the energy range of betas in our decay), events are generated in which every outgoing beta initially has the same amount of kinetic energy, and the angular distribution of these betas is physically appropriate for the polarization and beta energy under consideration. Both polarization states must be considered separately. These mono-energetic betas are propagated through the experimental geometry via Geant4, and the resulting scintillator spectra are recorded. Cuts identical to those imposed on the experimental data are implemented (see Chapter 3). Several such spectra are shown for the Bottom Detector in the ‘-’ polarization state, with their best fits and the residuals thereof in Figs. 4.1, 4.2, 4.3, 4.4, and 4.5.

somewhere I have to talk about the empirical noise spectrum etc. on the BB1s. Or maybe I've already mentioned it somewhere.

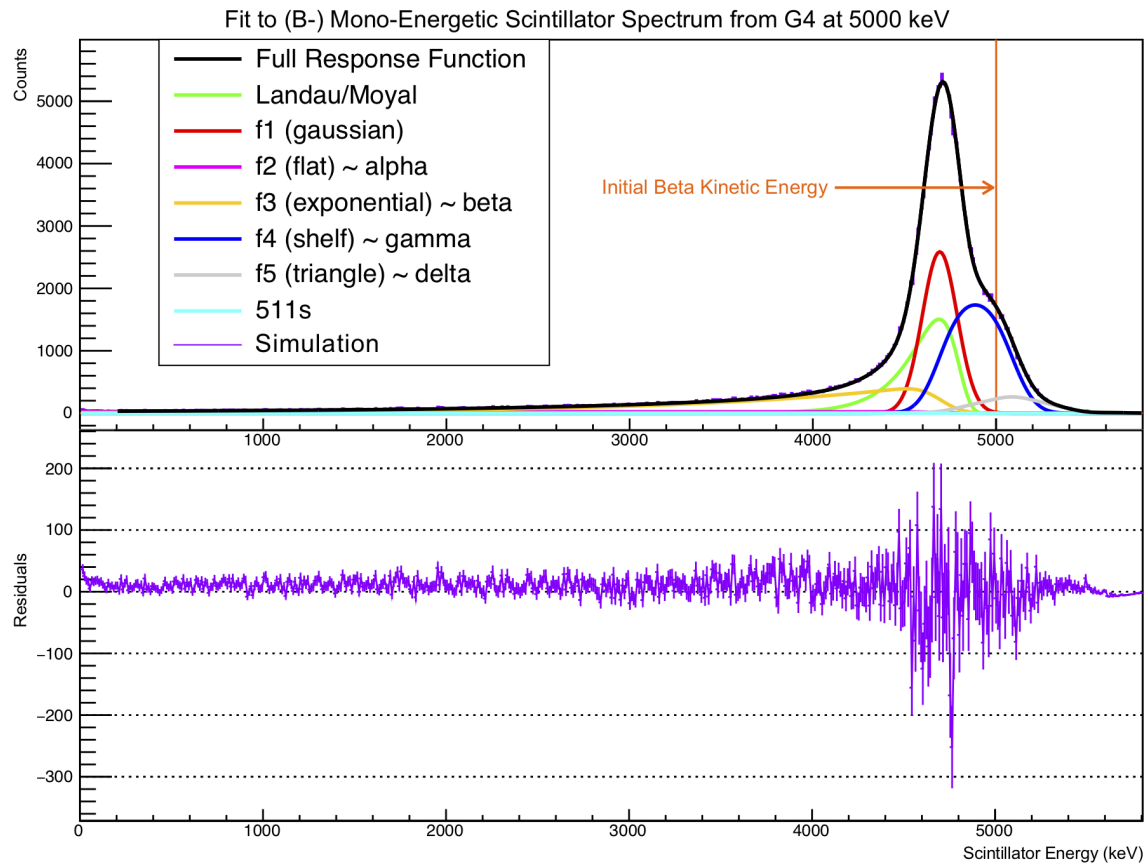


Figure 4.1: Fit to Mono-Energetic Spectrum, 5000 keV (B-)

It's clear that the model goes to shit at low energies. I don't really get it. Anyway, we'll never even *look* at events with scintillator energy below 400 keV, so at the very lowest energies it doesn't matter. Though, it gets bad before we get that low in the spectrum. Sadly.

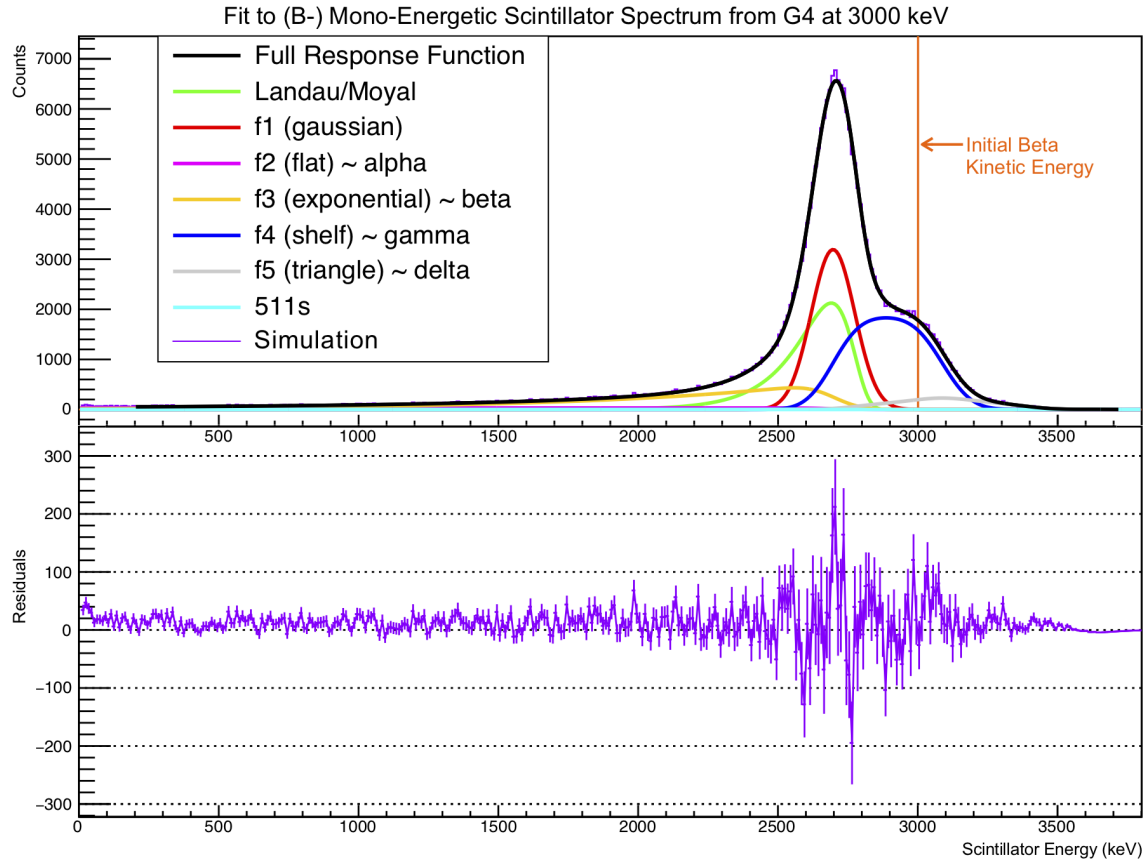


Figure 4.2: Fit to Mono-Energetic Spectrum, 3000 keV (B-)

Parameters alpha, beta, gamma, delta, W, k, and functions $f_1()$, $f_2()$, $f_3()$, $f_4()$, $f_5()$ are named that way because we're following Clifford. Exact definitions of the functions aren't really identical though, and my parameters don't necessarily have the same normalization. Qualitatively, all the same features are there though. Also, the moyal function isn't from Clifford, because ... reasons.

...

In particular, Clifford's treatment describes the measured energy (which in their case is a sum of scintillator energy and DeltaE energy) for beta particles interacting with a detector with a collimator, much like ours, however in our case, some energy is lost to the intervening SiC mirror and beryllium foil, and as we don't measure that directly, it can't be directly added back in. Although we might add back in the energy from the BB1 detectors, we have to model other energy losses in similar materials anyway, and as previously mentioned, re-introducing the energy from the BB1s invites problems with maintaining a uniform energy threshold over the entire detector.

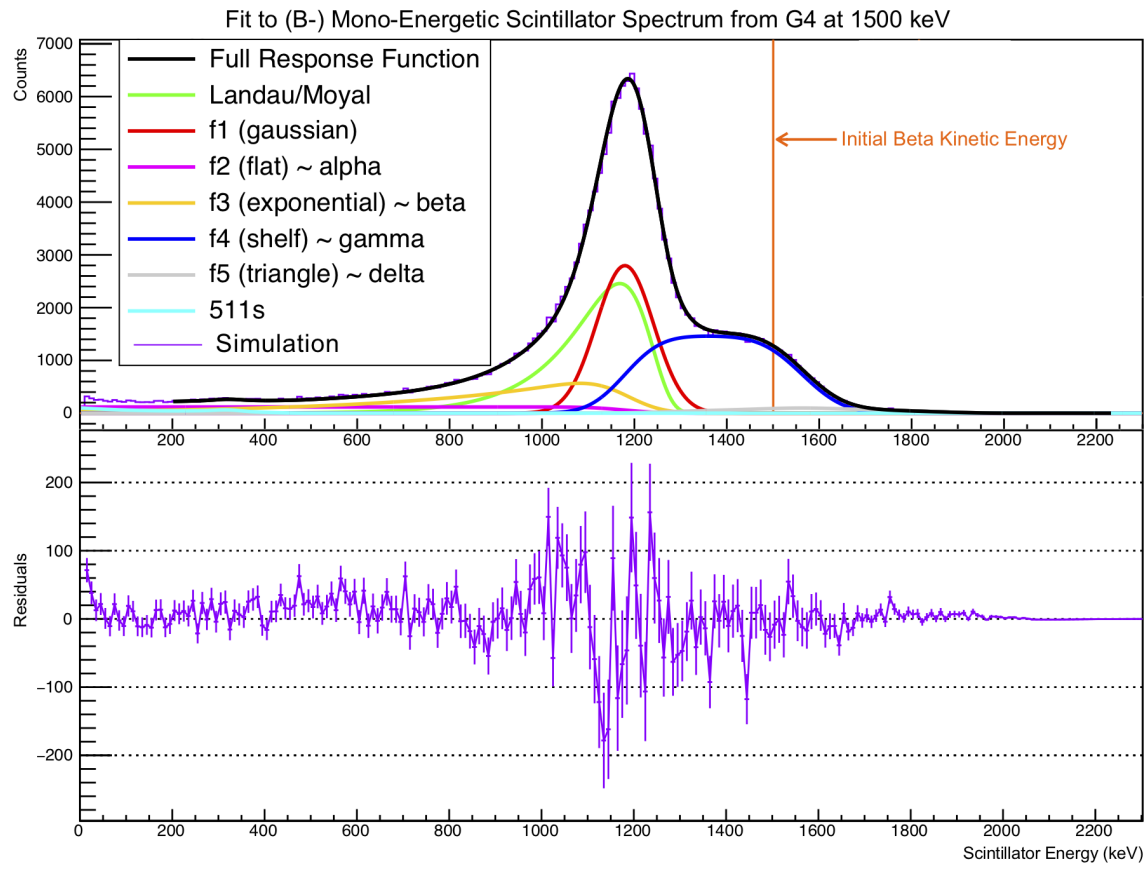


Figure 4.3: Fit to Mono-Energetic Spectrum, 1500 keV (B-)

$$R(E_0, \text{Detector}, \text{Polarization}) = p_{\text{norm}} (f_{\text{moyal}} + f_1 + f_2 + f_3 + f_4 + f_5) + f_{511} \quad (4.1)$$

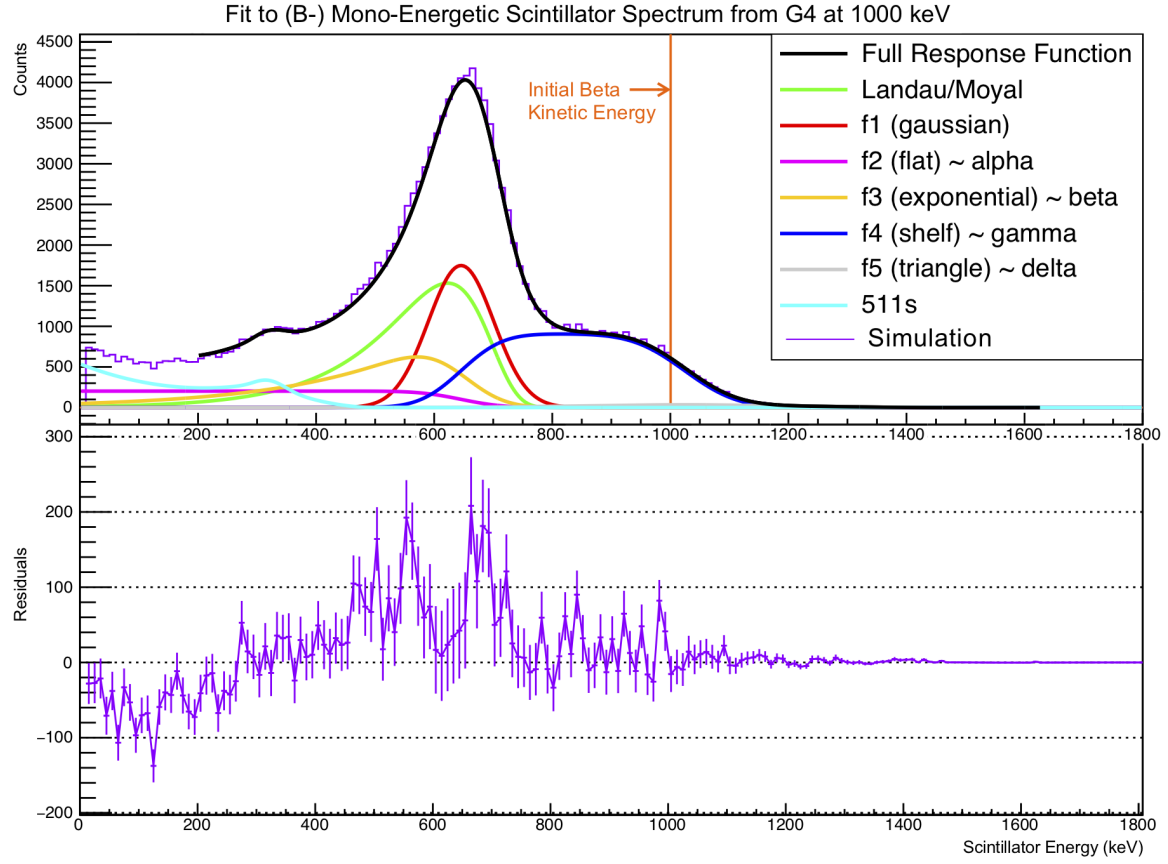


Figure 4.4: Fit to Mono-Energetic Spectrum, 1000 keV (B-)

where

$$\begin{aligned}
 f_{\text{moyal}}() &= (1 - p_{\text{gfrac}}) \left(1 + \frac{-p_\alpha - p_\beta}{|E_0|} - \frac{p_\Delta}{p_\gamma p_W} - p_\gamma p_W \right) \\
 &\times \left(\frac{e^{\left(\frac{x - (E_0 - \frac{1}{2}p_{dE0})}{2p_{lres}|E_0 - \frac{1}{2}p_{dE0}|} \right)} e^{\left(-\frac{1}{2}e^{\left(\frac{x - (E_0 - \frac{1}{2}p_{dE0})}{p_{lres}|E_0 - \frac{1}{2}p_{dE0}|} \right)} \right)}}{\sqrt{2\pi p_{lres} |E_0 - \frac{1}{2}p_{dE0}|}} \right) \quad (4.2)
 \end{aligned}$$

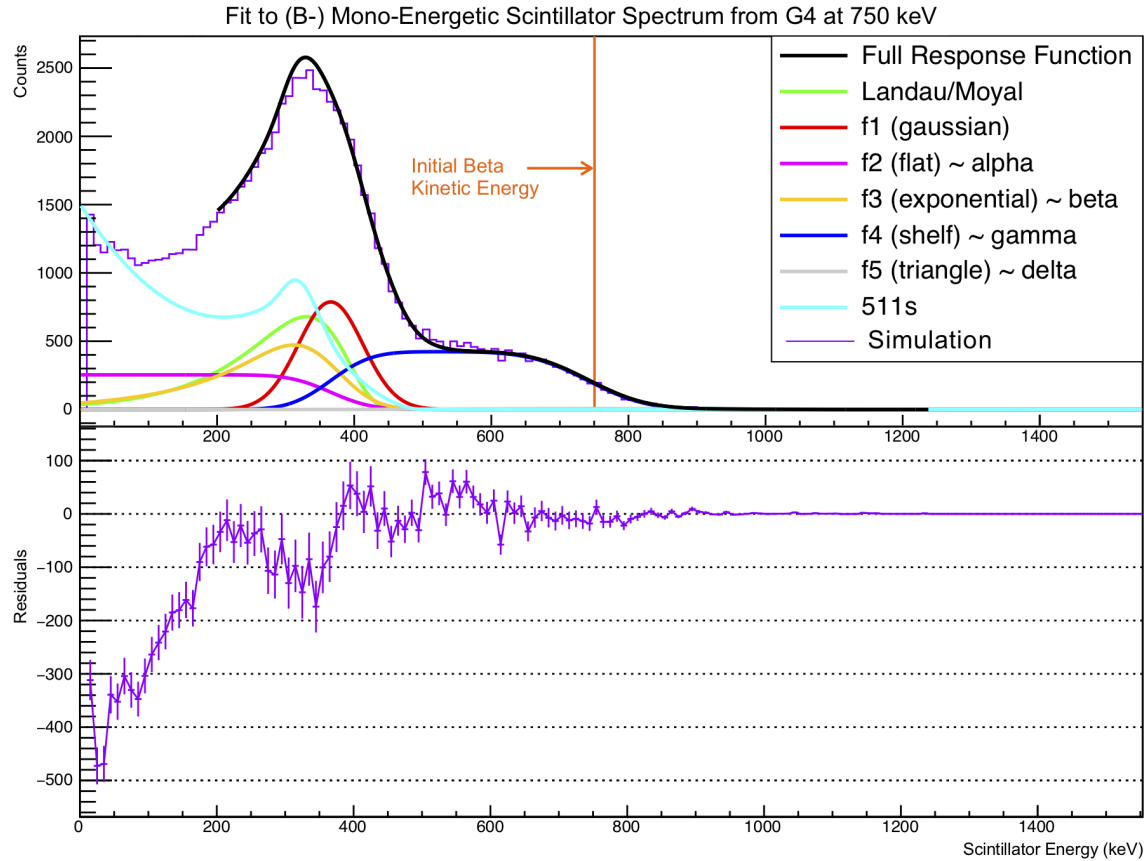


Figure 4.5: Fit to Mono-Energetic Spectrum, 750 keV (B-)

$$\begin{aligned}
 f_1() &= p_{\text{gfrac}} \left(1 + \frac{-p_\alpha - p_\beta}{|E_0|} - \frac{p_\Delta}{p_\gamma p_W} - p_\gamma p_W \right) \left(\frac{e^{\left(-\frac{(x - (E_0 + \frac{1}{2} p_{dE0}))^2}{2 p_{\text{toeres}} |E_0 + \frac{1}{2} p_{dE0}|} \right)}}{\sqrt{2\pi p_{\text{toeres}} |E_0 + \frac{1}{2} p_{dE0}|}} \right) \\
 f_2() &= \frac{p_\alpha}{|E_0|} \left(\frac{1 - \text{Erf} \left[\frac{(x - |E_0|)}{\sqrt{2 p_{\text{toeres}} |E_0|}} \right]}{2 |E_0|} \right)
 \end{aligned} \tag{4.3}$$

$$f_3() = \frac{p_\beta}{|E_0|} \left(\frac{e^{\frac{p_k^*(x-E_0)}{|E_0|}} * e^{\frac{p_{\text{toeres}} p_k^2}{2|E_0|}}}{2(1 - e^{-p_k})} \right) \left(1 - \text{Erf} \left[\frac{(x - E_0 + p_{\text{toeres}} p_k)}{\sqrt{2 p_{\text{toeres}} |E_0|}} \right] \right) \quad (4.4)$$

$$f_4() = \frac{p_\gamma}{2} \left(\text{Erf} \left[\frac{x - E_0}{\sqrt{2 p_{\text{toeres}} |E_0|}} \right] - \text{Erf} \left[\frac{x - E_0 - p_W}{\sqrt{2 p_{\text{toeres}} |E_0 + p_W|}} \right] \right) \quad (4.5)$$

$$\begin{aligned} f_5 &= \frac{p_\Delta}{2 p_\gamma p_W^3} \left[(x - E_0) \left(\text{Erf} \left[\frac{(x - E_0)}{\sqrt{2 p_{\text{toeres}} |E_0|}} \right] - 2 \text{Erf} \left[\frac{(x - E_0 - p_W)}{\sqrt{2 p_{\text{toeres}} |E_0 + p_W|}} \right] \right. \right. \\ &\quad \left. \left. + \text{Erf} \left[\frac{(x - E_0 - 2p_W)}{\sqrt{2 p_{\text{toeres}} |E_0 + 2p_W|}} \right] \right) + (2 p_W) \left(\text{Erf} \left[\frac{(x - E_0 - p_W)}{\sqrt{2 p_{\text{toeres}} |E_0 + p_W|}} \right] \right. \right. \\ &\quad \left. \left. - \text{Erf} \left[\frac{(x - E_0 - 2p_W)}{\sqrt{2 p_{\text{toeres}} |E_0 + 2p_W|}} \right] \right) + (2 p_{\text{toeres}} |E_0|) \left(\left(\frac{e^{\left(\frac{-(x-E_0)^2}{(4 p_{\text{toeres}} |E_0|)} \right)}}{\sqrt{2\pi p_{\text{toeres}} |E_0|}} \right) \right. \right. \\ &\quad \left. \left. + \left(\frac{-2e^{\left(\frac{-(x-E_0-p_W)^2}{(4 p_{\text{toeres}} |E_0 + p_W|)} \right)}}{(\sqrt{2\pi p_{\text{toeres}} |E_0 + p_W|})} \right) + \left(\frac{e^{\left(\frac{-(x-E_0-2p_W)^2}{(4 p_{\text{toeres}} |E_0 + 2p_W|)} \right)}}{\sqrt{2\pi p_{\text{toeres}} |E_0 + 2p_W|}} \right) \right) \right] \end{aligned} \quad (4.6)$$

$$\begin{aligned} f_{511} &= |p_{\text{scale}}| \left[\left(\frac{195}{17} \sqrt{\frac{2}{\pi}} e^{\left(\frac{-(x-308)^2}{578} \right)} \right) + \left(40 + \frac{(x-210)^2}{900} \right) \left(1 - \text{Erf} \left[\frac{x-334}{30} \right] \right) \right. \\ &\quad \left. + \left(\frac{(x-505)^2}{1440} \right) \left(1 - \text{Erf} \left[\frac{x-505}{30} \right] \right) \left(1 + \text{Erf} \left[\frac{x-334}{30} \right] \right) \right] \end{aligned} \quad (4.7)$$

Obviously, from a physical standpoint, the initial beta energy E_0 must be positive, but the response function still includes several expressions of the form, $|E_0|$. This is not done by accident, but rather is an intentional adjustment used to encourage the parameters to behave well within a fit.

... Similarly, Clifford doesn't include a compton edge. I think. But I want to.

Needs a picture of the *full* beta energy distributions that come out of the lineshape thing. To compare with (a) data and (b) G4. Probably a superratio in there somewhere too.

Um. Which of the scattering things did I actually put in at the end? And when did I do it?
Like, how did I account for (back-)scattering? I tried with/without scattering, I think? and
eventually decided not to do it. for some reason. I think it breaks normalization in some way
that's more subtle than you would think.

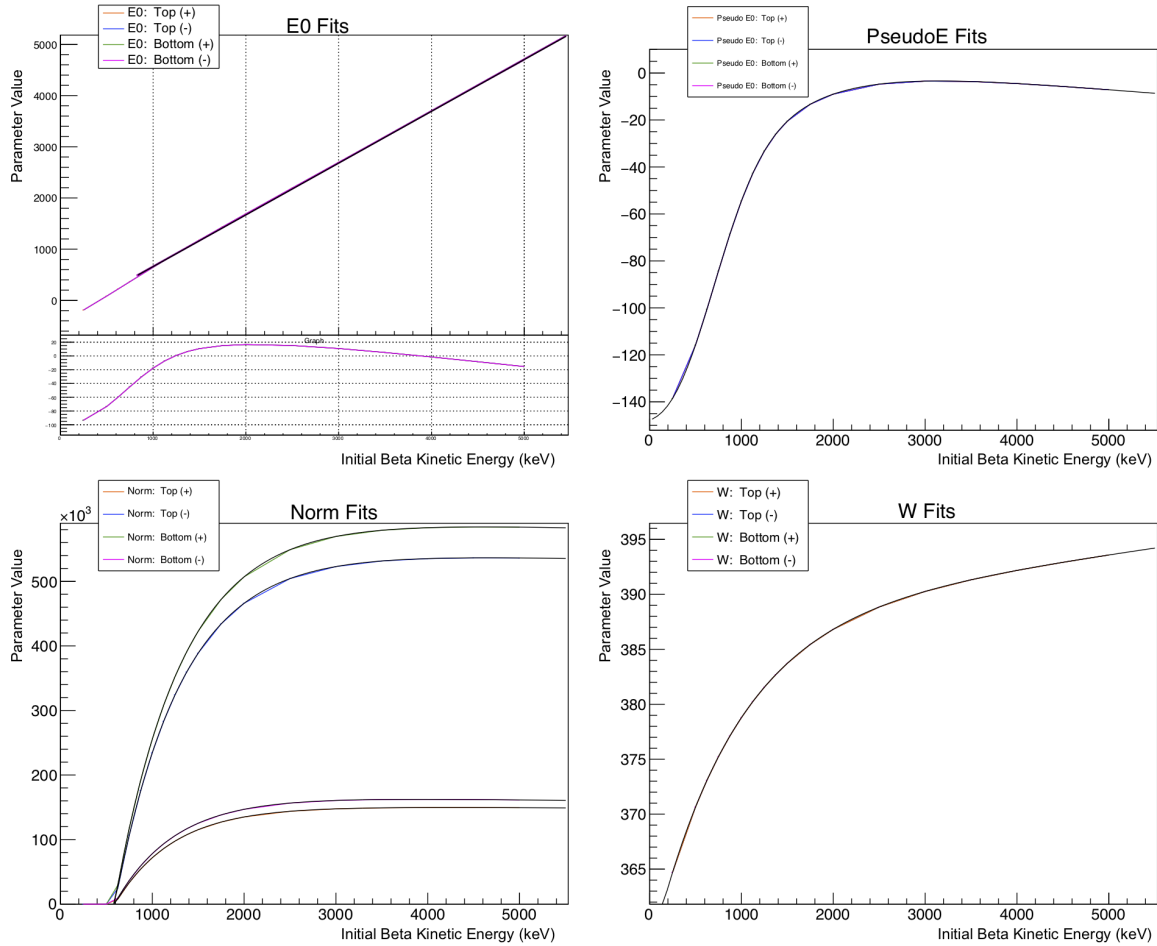
- ... And then, you have values of all the parameters, as measured at a bunch of input energies. Make sure all the fits converge and don't do something crazy.
- Fit all the parameters as a function of energy to empirical functions. Doesn't even matter what the form of the functions are, as long as it fits well.
- the parameters extracted from the mono-energetic beta spectrum fits, and empirical functions to model how these parameters vary with beta energy, are shown in Figs. 4.6, 4.7, 4.8, and 4.9.
- How good are these fits, you ask? See Fig. 4.10

4.3 Simulating the Background

Our experiment has some background. It's annoying and stupid, but as long as we can estimate how much of it there is and what it does, it's basically fine.

Reference Section 3.4

- TOF cut requires a whole extra model of background in the TOF spectrum..
- Suppose background in the TOF spectrum is coming from decays of atoms that have gotten themselves stuck to surfaces within the chamber...
- Run G4 to get a beta TOF spectrum (w.r.t. the decay)
- Run COMSOL (credit to Alexandre) to track low-energy SOEs through the electric field from wherever they started, into the detectors. Energy spectra from Levinger.
- Combine G4 and COMSOL spectra, event-by-event, while requiring that both the beta detector and the eMCP are hit according to the set of random numbers generated by each monte carlo separately. Then, the beta and SOE will each



What even *is* the thing plotted below E0 in the ‘residuals’ spot, you ask? It’s ‘PseudoE’, which is describes the difference between the original input energy, E_0 , and the energy where the output spectrum is maximal. Or something. To ‘pretty good’ order, it’s a straight line. the ‘PseudoE’ plot shows what’s left after you fit it to a straight line. It’s fucking weird that it’s negative everywhere. Like, what?

Figure 4.6: Lineshape Parameter Fits (Part 1)

have a TOF from decay to detector, and subtracting one from the other gives a timing spectrum that can be observed experimentally. See Fig. 3.13.

- Upper limit for the fraction of events generated this way can be estimated by assuming that all losses from the trap not due to radioactive decay emerge isotropically from the trap and then stick to whatever chamber wall is in its path. This upper limit is too big by a factor of 2.

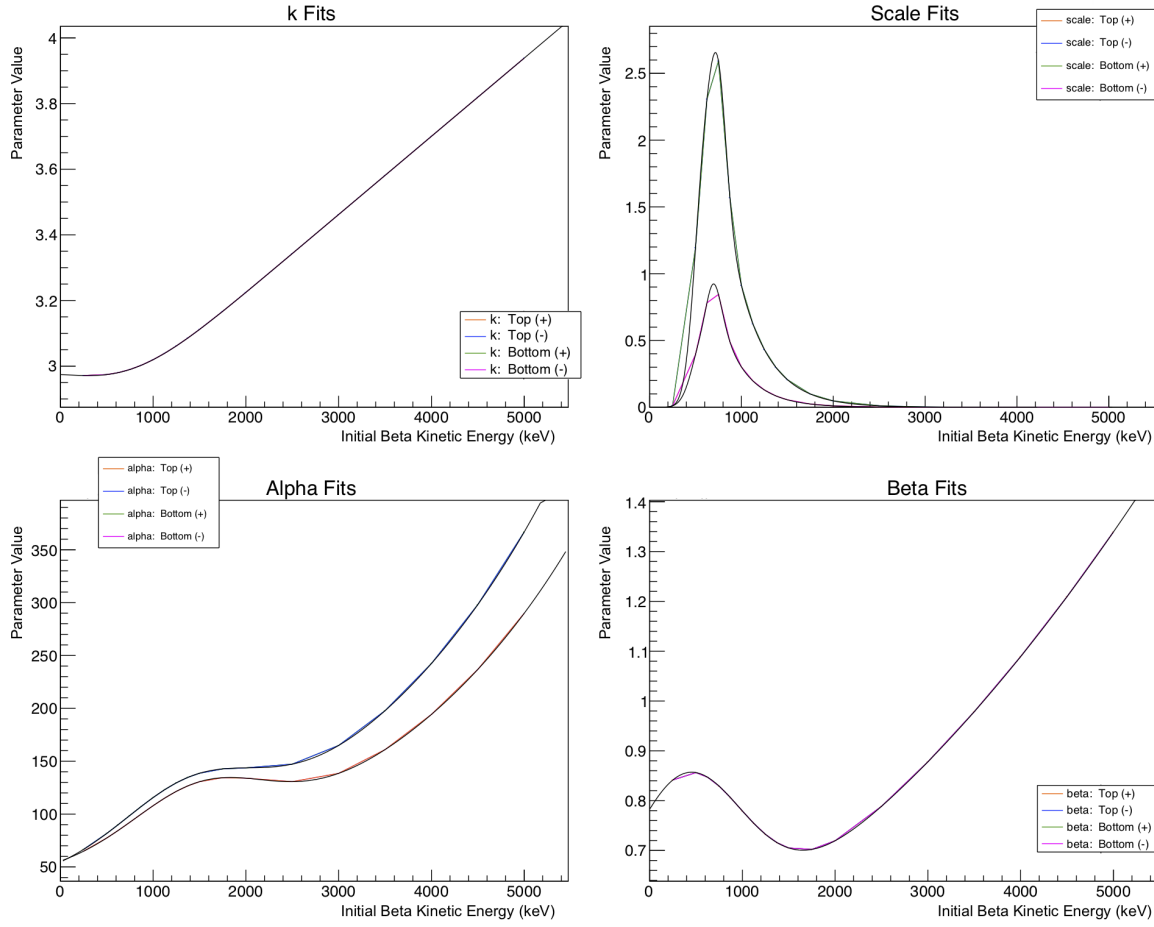


Figure 4.7: Lineshape Parameter Fits (Part 2)

- For each of those 3 simulations, sort the “good” data according to emission angle relative to the detector. Do each detector individually. For both polarizations.
- Assemble the (simulated) superratio asymmetry. We’ll compare it to data, and the χ^2 from that comparison will be our figure of merit.
- We can make a whole 2D parameter space for different values of A_β and b_{Fierz} , and compare them all (via their superratio asymmetries) to the experimental data. We get the “best” values of A_β and b_{Fierz} , where χ^2 is minimized.
- We can do this whole thing again for simulated data sets with different values of parameters that we vary as systematics. Note how the best values of A_β and b_{Fierz} change when each of the systematics are varied.

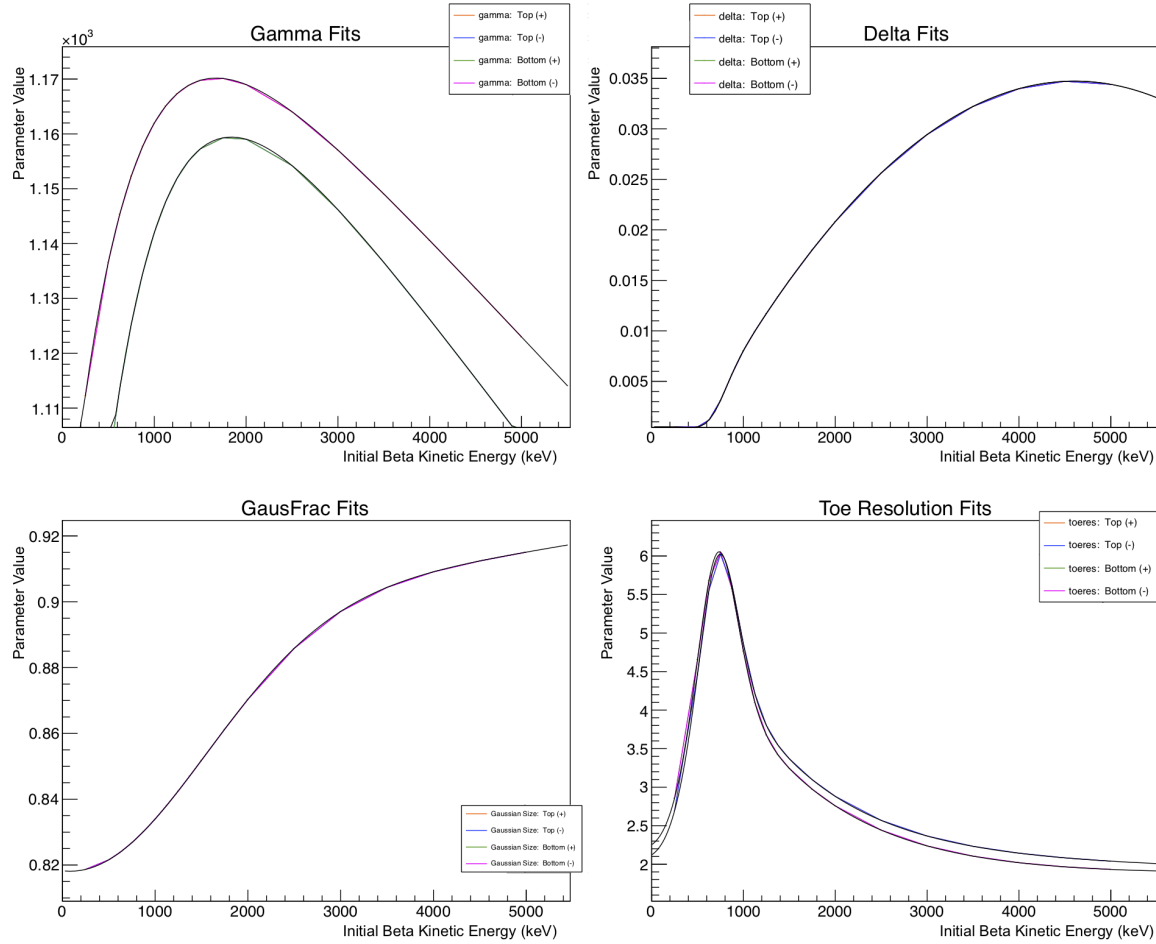


Figure 4.8: Lineshape Parameter Fits (Part 3)

4.4 Comparing Simulations with Experimental Data

- Run 3 sets of G4 simulations with a bunch of statistics (N events, for data with like $N/10$ events). Each one has the same nominal value of A_β , but with 3 different values of the scalar coupling C_S : zero, and $+/-$ (whatever). Keep $C_T = 0$. Because reasons, we're not really able to distinguish between C_S and C_T in this experiment anyway, so might as well keep the analysis simple.

Total good events after all the cuts:

Set B: 173,640

Set C: 18,129

Set D: 207,596

– All Runsets: 399,365

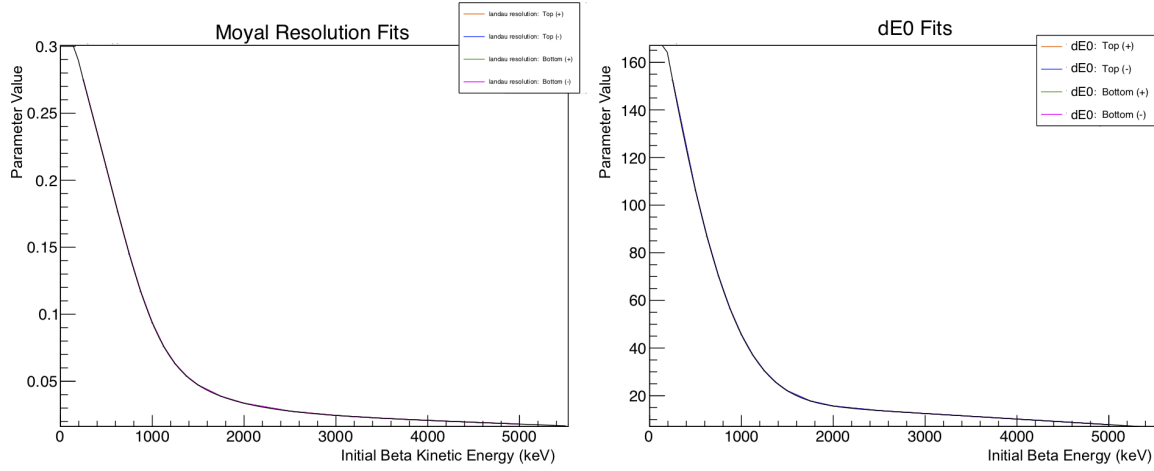
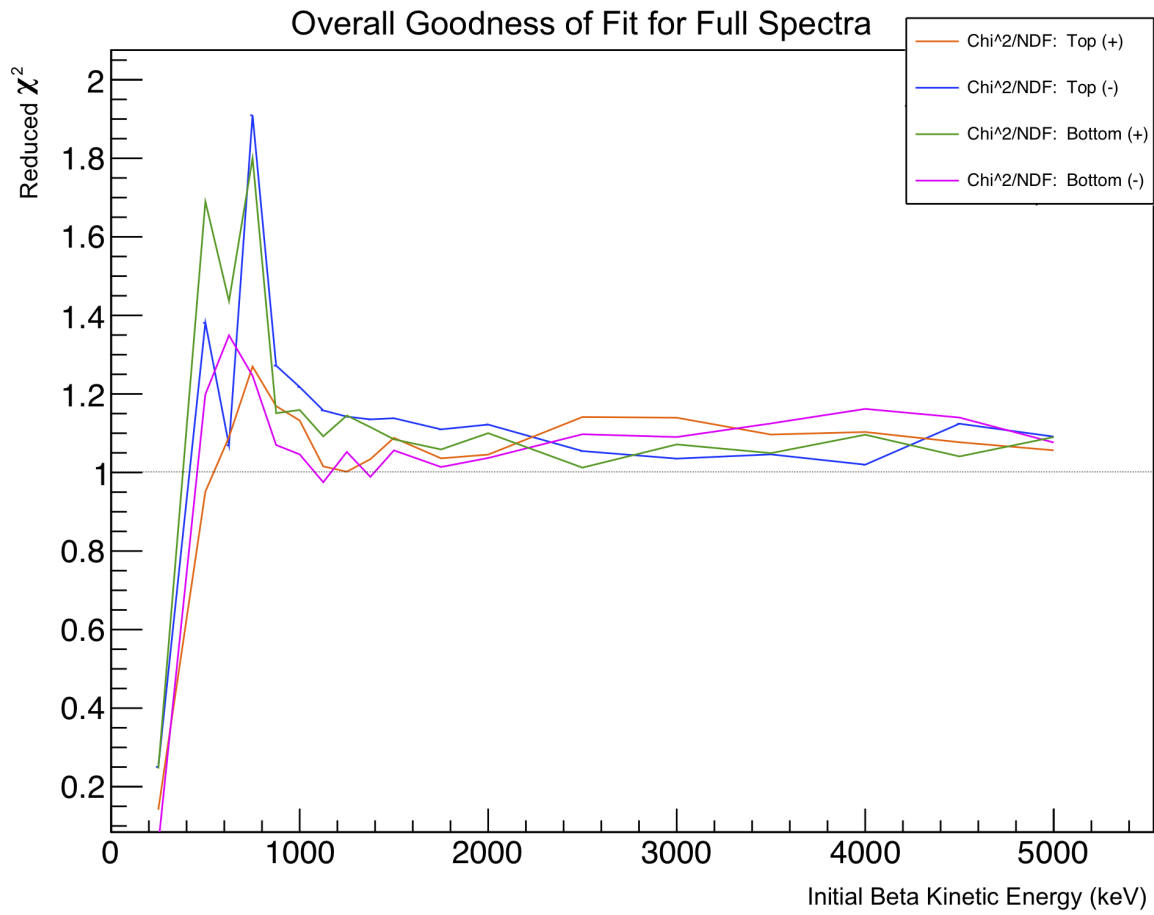


Figure 4.9: Lineshape Parameter Fits (Part 4)

- Just run one set of 0.02^*N events for the two percent branch. We can't neglect it, but it isn't going to change much when we adjust BSM couplings. Just use the old event generator from Holstein Eq. (51).
- Match cuts in simulated data up to the cuts on experimental data. Obviously. DSSD cut, DSSD energy, one hit DSSD, one hit scint. TOF cut, which requires a whole extra model of background in the TOF spectrum (see Section 4.3).



How many DOF for these things? I should put it on the picture.

Figure 4.10: Goodness of Fit for Modeled Lineshapes

Chapter 5

Analysis and Estimates of Systematic Effects

I really need an excuse to include more pictures of data. Also, more pictures of simulations.

Missing figure

Show simulated spectra separated by scattering category.

Missing figure

Show SimpleMC spectra, show the supersum, show the superratio, show the superratio asymmetry. Maybe do some simple fits to show how much better the superratio asymmetry is than *not* the superratio asymmetry.

John proposes an intro statement for this chapter (by which I really mean that other chapter, but I'm pretty sure it goes here now). But anyway, the following two paragraphs are a direct quote from him:

Analysis is critical to a precision measurement, as most of the research is in determining systematic uncertainties by self-consistent analysis and simulations. Each detector in this experiment is critical and has independent calibrations and cuts. Full

explanation is here (and in two following chapters) justifying choice of the deterministic cuts, because in the analysis in this thesis the data was not blinded. The main goal of blinding was nevertheless achieved— to make sure all analysis is done completely with full redundancy of checks wherever possible— so the discipline entailed must be described in full detail. Here there are details of detectors: eMCP rMCP beta DSSD scintillator.

The collaboration has done an independent analysis fixing bFierz to zero. Differences with that analysis are interleaved in this section. Critical physics improvements concern an emcp-beta timing walk correction which enabled an improved cut against background, also incorporating a more complete modelling of decay backgrounds from untrapped atoms. Technical corrections include a correct treatment of the polarization cycle. An arbitrary change in the deltaE radius cut is kept self-consistent.

JB: "I doubt I will have further useful comments on the Ch. (((this chapter))) as they are now.

JB:

I've tried to email you the paragraphs on "collaboration determination of uncertainties" for (((Ch. 5)))

My intent of all that other advice was to keep your time spent on Chs 1-4 ((Now Ch. 1-2)) concise, so you could concentrate on these real jobs. (n.b.: the advice he's already sent was almost all about chapters 1-4, which are the various intros/background info and experimental setup stuff)

...

I can only say that if you have an equal choice between including a detail or not, pick "not."

JB: I will try to schedule meeting with Dan for you to show us the final version of (((Ch. 5)))
Estimating systematic effects soon.

JB says:

A simple estimate from the collaboration that builds intuition for this result: Scatter in the SiC mirrors and DSSD actually produces an efficiency change at low beta energy. Energy loss is not minimally ionizing in these structures, and instead will have a long Landau tail that can take events below energy threshold in the scintillator. The collaboration has modelled explicitly the false asymmetry as a function of Kbeta between 600 and 1300 keV, producing roughly $(K-0.6 \text{ MeV})/(0.7 \text{ MeV})$, i.e. 50% at $K\beta=0.95 \text{ MeV}$. This efficiency degradation would be distributed roughly equally between the SiC and DSSD. If completely ignored, this would introduce by inspection a false bFierz of approximately 0.5. Scattering effects will vary between linear and sqrt of thickness, so assuming worst case of linear, the mechanical thickness uncertainty of 5 micron/300 micron and 6 micron /275 micron, an average of 2%, making a random contribution of order 0.01 each. The Be window has larger mechanical thickness uncertainty of 23micron/229 micron, but energy loss and scattering in this material is 5x smaller, so the net effect would be similar.

...

To minimize this systematic for future experiments, the collaboration has implemented pellicle mirrors of negligible thickness, 100 nm Au on 4 micron kapton. The collaboration is also implementing Be-windowed wire chambers in place of the DSSD.

...

MJA:huh?

5.1 Overview

A summary of systematics goes here. In words, yes, but also in table form.

Choice of low-energy scintillator threshold has a large systematic effect...

from John: "I used Ben's threshold when determining the uncertainty from the lineshape tail (UFTLT). If you're saying the UFTLT depends on the threshold used, ok, of course it does. But if you're claiming that UFTLT depends on the **uncertainty** of the threshold, that's manifestly smaller than the UFTLT itself, and I'm going to assert it isn't worth evaluating."

It's actually not nearly as big as I'd originally expected. It's huge in the line-shape thing, but pretty tiny in everything else.

5.2 BB1 Radius, Energy Threshold, Agreement

BB1 radius cut can help to eliminate scattered events. Energy threshold selection and statistical agreement between BB1 detectors' energies only makes a small effect on results. BB1 radius itself has a pretty big effect on the result, but we can at least just G4 it away. The remaining systematic effect is pretty small.

Source	b_{Fierz}		A_β	
	Uncertainty	Correction	Uncertainty	Correction
Scintillator Calibration	0.003	-	0.0003	-
Scintillator Threshold	0.004	-	0.0004	-
DSSD Individual Strip SNR	0.006	-	0.0007	-
DSSD Energy Agreement	0.005	-	0.0006	-
DSSD Detection Radius	0.006	-	0.0017	-
DSSD Energy Threshold	0.005	-	0.0005	-
Atomic Cloud	0.002	(...)	0.0002	(...)
Background	0.004	(...)	0.0003	(...)
Beta Scattering	0.031	(...)	0.0025	(...)
Low Energy Tail	0.008	-	0.0007	-
Mirror Thickness	0.026	-	0.0025	-
DSSD Thickness	0.026	-	0.0025	-
Be Foil Thickness	0.026	-	0.0025	-
Total Systematics	0.056	-	0.0055	-
Statistics	0.084	-	0.0082	-

Table 5.1: Error Budget goes here.

JB: I hope the discussion is clear in your head. Any effect that relies on scattering computation in G4 should have an uncertainty on order 10% of the correction – hopefully you are keeping a distinction here between the finite geometry acceptance (which I guess is exact) scattering off the collimator.

As per JB's comment in section 3.3: "statistical agreement between BB1 X and Y detectors' energies only makes a small effect on results" does not need the technical details beyond that statement."

Missing figure

Surely this requires at *least* one image of the pixelated BB1 data. Maybe some of a few waveforms and energy distributions too.Feels like cheating to include some of that stuff, since Ben was the one who actually used it mostly.

JB on missing figure: "if you used such an image as part of your uncertainty estimate, yes [include it]"

Remember: There's noise applied to simulated BB1s, matching some spectrum.

In the end, we get our results from the scintillator energy only, without summing

the BB1 energy back in. Energy absorbed in DSSDs is only used as (a) a tag for events, and (b) contributing to the total beta energy loss before the beta arrives at the scintillator.

JB: The simulations of course include it event-by-event, not just a minimally ionizing average loss.

5.3 Background Modeling – Decay from Surfaces within the Chamber

So many surfaces, all of which can get stray 37K atoms stuck to them. Then they decay from a place that isn't the actual trap center, and it contaminates our stuff.

JB on figures that might go here: Figure 6.4 (currently that picture of the TOF spectrum) could either be here, or you could reference it from here. The TOF histogram is a great start. Adding the asymmetry[TOF] indeed would be vital.

Missing figure

Show the "average asymmetry" (all energies) as a function of TOF, with real data, best model normalization, and extrema of model normalizations. Show our cut. Turns out, it's a lot of work for a really tiny correction. Oh well.

JB on the *actual* figure I had been planning to put here, and my remarks about it: Indeed it will be critical to show a clear compelling version of this figure in thesis and in a paper. It was vital to minimize and determine this background to avoid fitting a polynomial to it from the wings, even more so for the energy dependence of A than for its average – you should say so.

...

The reason the correction is small is because of all your hard work.

We model the beta TOF from the surfaces in G4, event by event. This is necessary because scattered events will have their TOF changed to account for a longer beta pathlength, and we're preferentially cutting away the events that don't have a TOF in the appropriate range.And then have COMSOL generate electron TOFs for SOEs starting from the start points picked by G4. Ran COMSOL for 0 eV SOEs, and again for Levinger spectrum SOEs. Used 9% 0eV SOEs in the end. I forgot which Levinger distribution I used in the end. The point is, for each event, you've simulated a beta TOF that may or may not be scattered off of something before

JB: "I wouldn't call these "scattered" events... that's very misleading."

...
Yeah, I should really stop doing that.

...
Wait no, scattered is what I mean! But fine, my phrasing is really unclear.

JB: Please comment on whether or not it was important to have this energy distribution.

it hits a detector, and you have a SOE TOF for an event originating at that same point, so you subtract them to model the TOF you'd measure in an experiment. Also, because you've done the scattering with G4, you get the beta energy corrected for any scattering that happened. This way, one can estimate how many "bad" events are eliminated with the TOF cut, as well as the fraction of "bad" events left in what remains.

5.4 Quantifying the Effects of Backscatter with Geant4

Beta decay (back-)scatter from surfaces within the experimental chamber is a significant systematic, and it must be evaluated, quantified, and corrected for. This is done via a series of GEANT4 simulations. While only a small fraction of events are affected, the process results in an energy loss in the beta that can, if not understood, be misinterpreted as the exact signal we're searching for. It is therefore imperative that this be well understood.

JB says: I would say you have a well-determined TOF cut to minimize this error– a cut that could not have been done blind without an unreasonably perfect simulation. Thus the exact spot of the cut should not be considered to introduce a systematic.

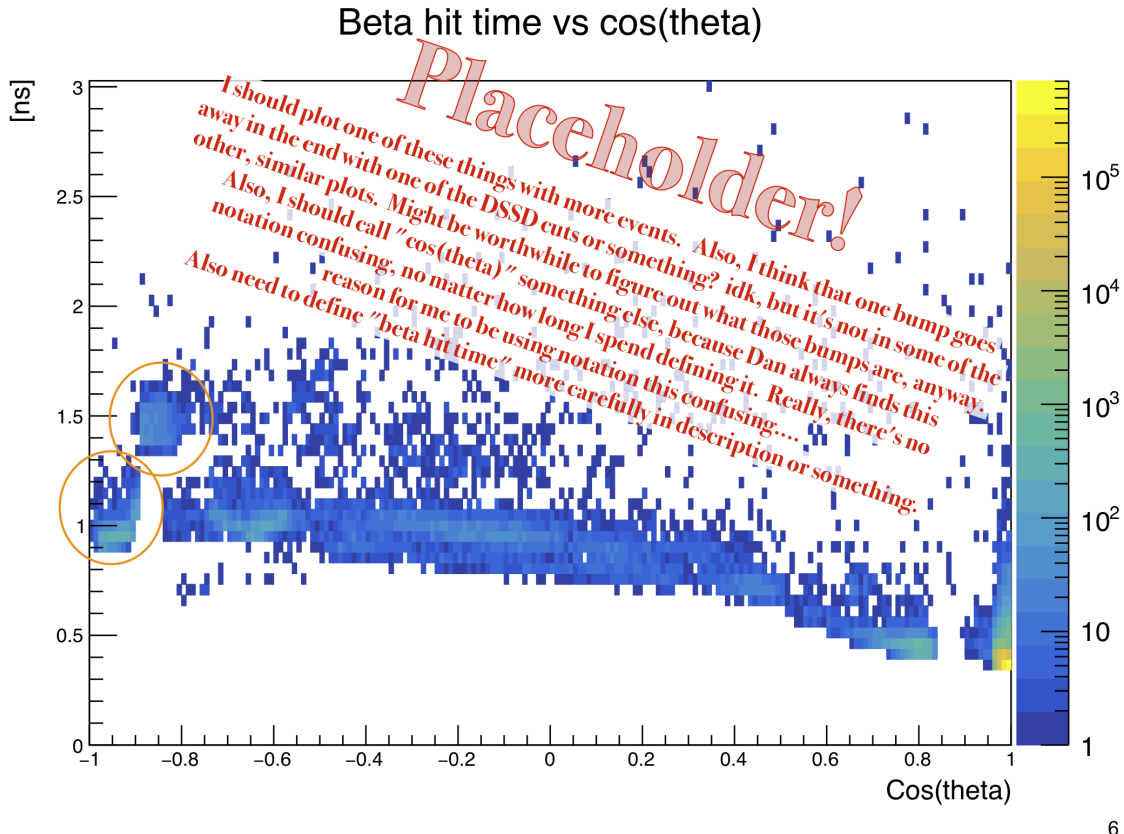
5.5 Lineshape Reconstruction

I think I'm going to put most of the content in this section into the 'Simulations' chapter (Section 4.2) instead. I really need to just mention it here (Sec. 5.5) and give an indication of how good the result is. Then evaluate stuff.

Clifford tells us what to do. [10].

5.5.1 Motivation

This process is used because the (back-)scatter, which it itself an important systematic, is largely independent of a wide variety of other experimental effects. These other effects must all be evaluated, but it is computationally prohibitive to re-evaluate the scattering with every other effect under consideration.



6

Figure 5.1: Simulated Beta TOA vs emission angle w.r.t. detector orientation

5.5.2 What is it and how does it work?

Mono-energetic beta decay events are generated in GEANT4, which outputs an energy spectrum for unscattered and forward-scattered beta events in the detector. These spectra are fit to a function to model the scintillator resolution, as well as energy loss in materials that the beta passed through before arriving at the scintillator. These spectrum fits are performed for a set of beta energies, and parameters are extrapolated to be applied to betas emitted at intermediate energies. Thus, the whole spectrum can be modeled. Pictures will make this clearer.

5.5.3 The Math-Specifics

I'll write down the specific functions I'm using, and the parameter values I'm using. (Maybe this should go in an appendix instead?) I'll describe the adjustments I

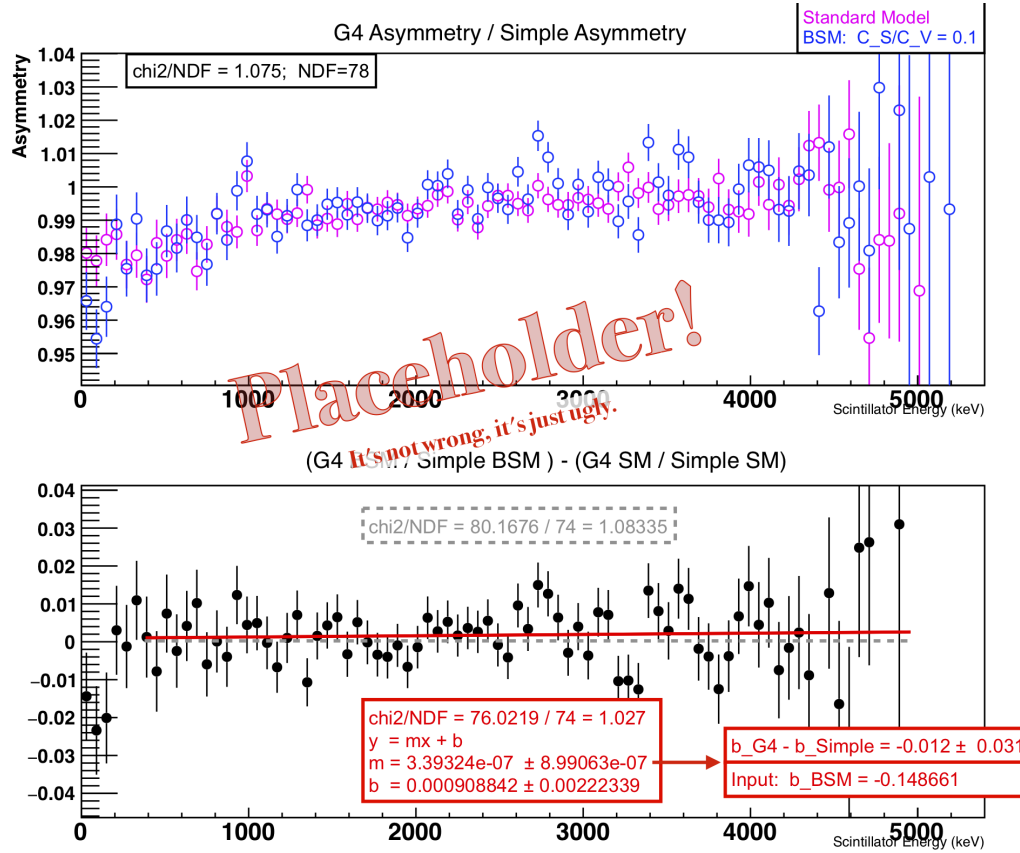


Figure 5.2: I'm not actually sure if this picture shows what I want it to. The point is, if I apply this rough lineshape to stuff that I SimpleMC-ed, then I can evaluate that way various systematic effects that would be time-consuming to actually simulate with G4. This picture is *supposed* to be a demonstration that this approach actually works...

make to the spectrum so that it can work even for the dataset where the scintillators' resolutions have changed.

5.5.4 The Results – Things That Got Evaluated This Way

As it turns out, only cloud parameters were evaluated this way. Trap position, size, sail velocity, temperature. But then we varied the lineshape anyhow, to account for G4 doing a bad job of modelling the bremsstrahlung (sp?).

JB: yes, brems strahlung is 'braking radiation' so gets 2 ss's. the lineshape tail in any scintillator also includes backscattered events – we are not claiming the 2-pixel cut is complete

JB: so it's still critical to write down more of the lineshape work.

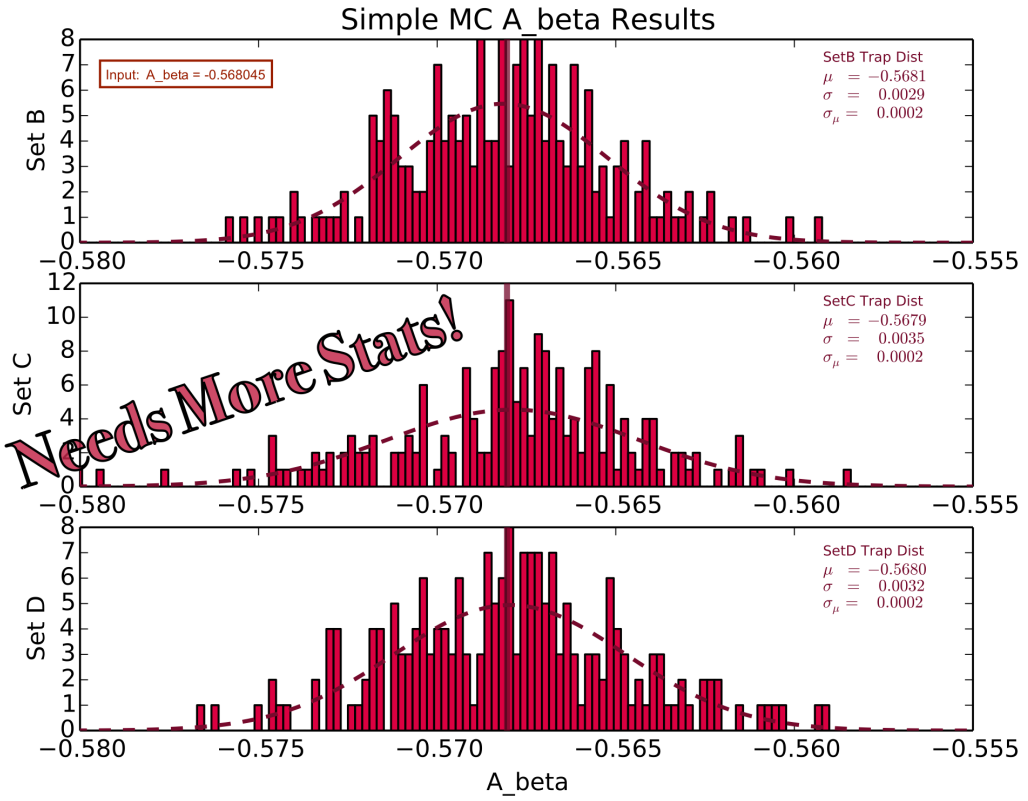


Figure 5.3: Estimated uncertainty in A_{β} resulting from uncertainty and variation in the cloud parameters. Evaluated by the lineshape reconstruction method.

5.5.5 The low-energy tail uncertainty, and what it does

Bremsstrahlung. It does Bremsstrahlung.

Here is Subsection 9.5.5 “The low-energy tail uncertainty, and what it does” complete. There should be no figure.

Direct quote from John follows in the next two paragraphs. Maybe I should paraphrase, but it’s so nicely written!

This subsection has the collaboration’s evaluation of the uncertainty from the scintillator detector’s lineshape tail. The energy from a monoenergetic beta is not always fully absorbed in a plastic scintillator. Although most backscattered betas are vetoed by the DSSD, some produce bremsstrahlung photons, and these frequently escape low-Z plastic scintillator— all cross-sections are known to high accuracy, but there is always uncertainty entailed in the MC implementation. This lineshape tail

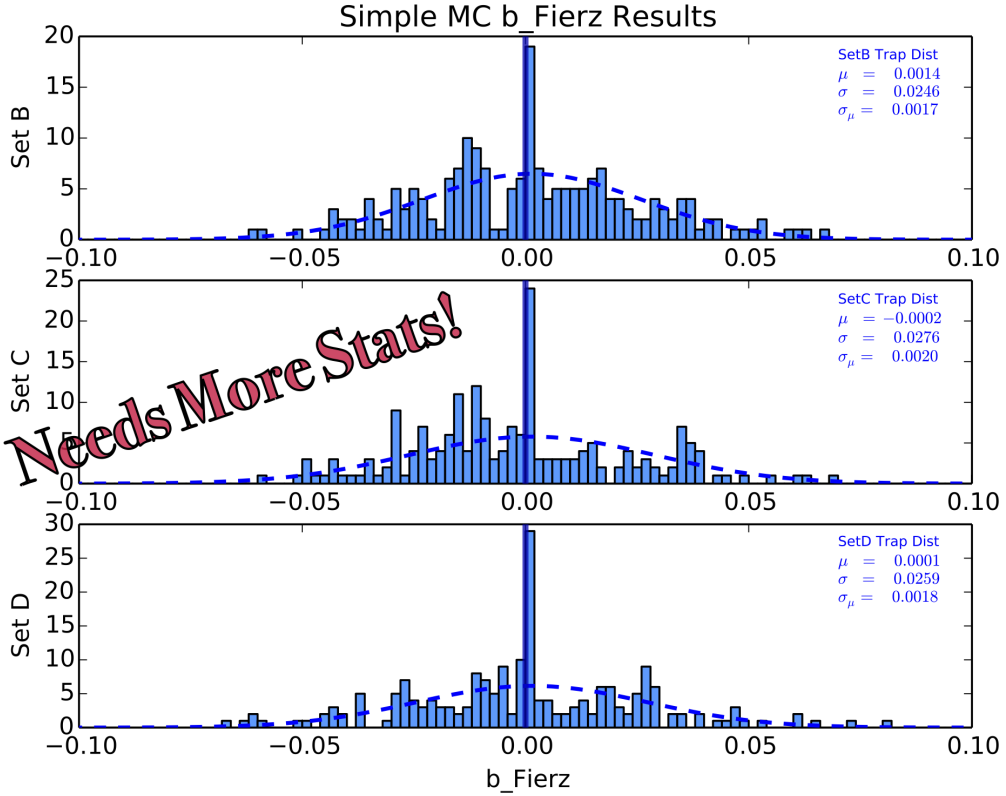


Figure 5.4: Estimated uncertainty in b_{Fierz} resulting from uncertainty and variation in the cloud parameters. Evaluated by the lineshape reconstruction method.

will then effectively move events from higher to lower measured energy, artificially altering the lower-energy asymmetries and mimicking the effects of a Fierz term.

Since this detector effect is difficult to disentangle from the other scattering effects off volumes, the collaboration adds a linear function down to zero for the tail to a Gaussian for the peak, with linewidth varying by photon statistics [10]. The convolution of this simple detector response function with v/c then scales the centroid MC, with the lineshape tail varied by $\pm 10\%$ of its value, a generic uncertainty accepted by the community for MC electromagnetic simulations. The fit b_{Fierz} centroid changes by ± 0.0076 , summarized as the 0.008 “Low Energy Tail” in the systematics table at the start of this chapter. Compared to other uncertainties of the present data set, this is small enough that the accuracy of this estimate is adequate.

Chapter 6

Results and Conclusions

JB: Dan and I independently discussed (((Ch. 6))) yesterday, and he has suggestions to help. So I will also schedule a meeting with Dan and you to discuss (((Ch. 6))) Results and whether the S,T part must be deleted and left to a paper. You don't have enough time, and although this should be quite straightforward, it is not your critical result and it's the only thing that can go.

6.1 Measured Limits on b_{Fierz}

Results go here, with measured limits described and quantified in all formats anyone could ever care about.

John says to just skip doing the C_S and C_T stuff, for now. No time. Really, C_S is already basically done, but then that'll lead to awkward questions about C_T .

6.2 Discussion of Corrections and Uncertainties

Just write a blurb to qualitatively summarize a bunch of the stuff in Ch. 5. Do I want to put my error budget table here? If not, here it is! (5.1).

Other things to discuss here: which things are dominant error sources, and how viable it would be to improve those for future experiments.

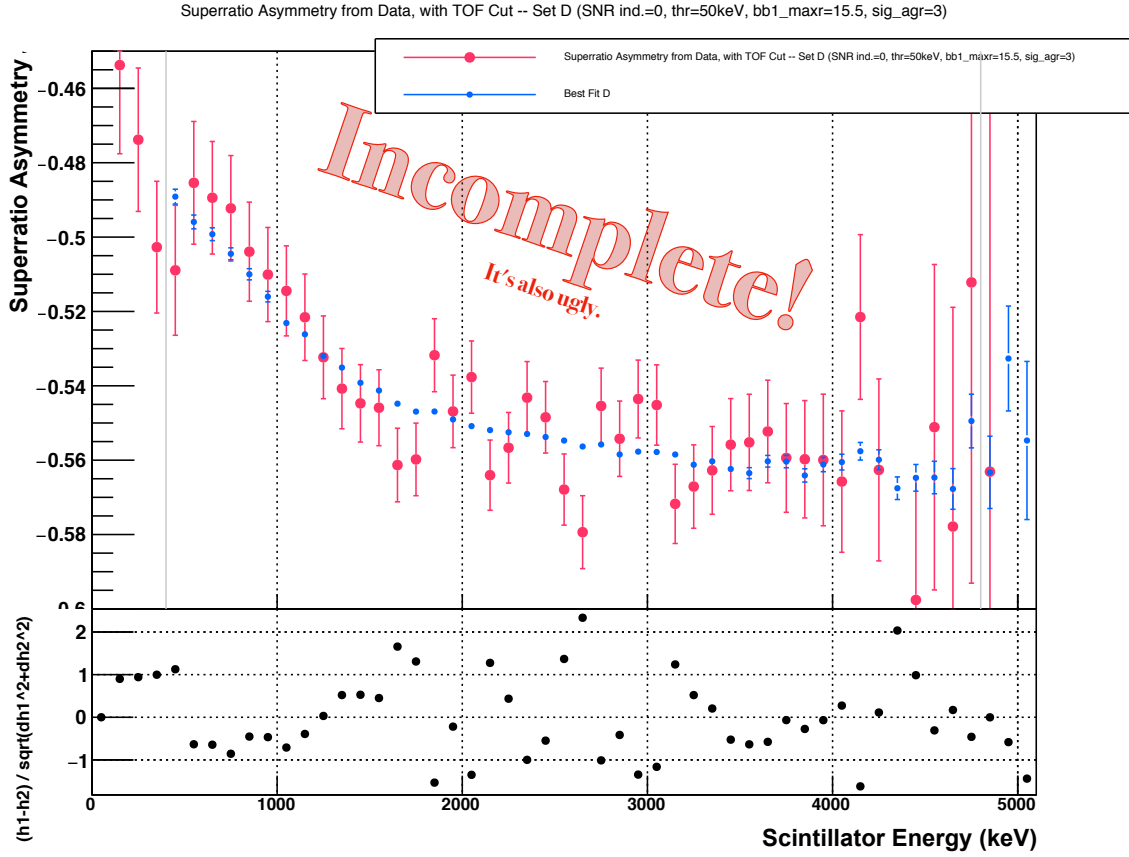


Figure 6.1: A superratio asymmetry from the data, and the best fit from simulations.

6.3 Relation to Other Measurements and New Overall Limits

In which I'll show exclusion plots and write down new limits, combining my result with results from the literature. Or, y'know, maybe I'll just talk about doing that.

JB says: To put your work in context, please add at the end of that minimal S,T section, or at the end of "Our Decay" section

...

The best existing measurement of b_{Fierz} is in the decay of the neutron [11], $b_{\text{Fierz}} = 0.017 \pm 0.021$, consistent with the Standard Model prediction of zero. Our measurement is strongly related, yet complementary. In terms on non-Standard Model Lorentz current structures, to lowest order in the non-SM currents the same equation applies:

$$b_{\text{Fierz}} = \pm (C_S + C'_S + (C_T - C'_T)\lambda^2)/(1 + \lambda^2)$$

(the plus is for β^- decay and the - for β^+ decay) [5]. [to be continued...]

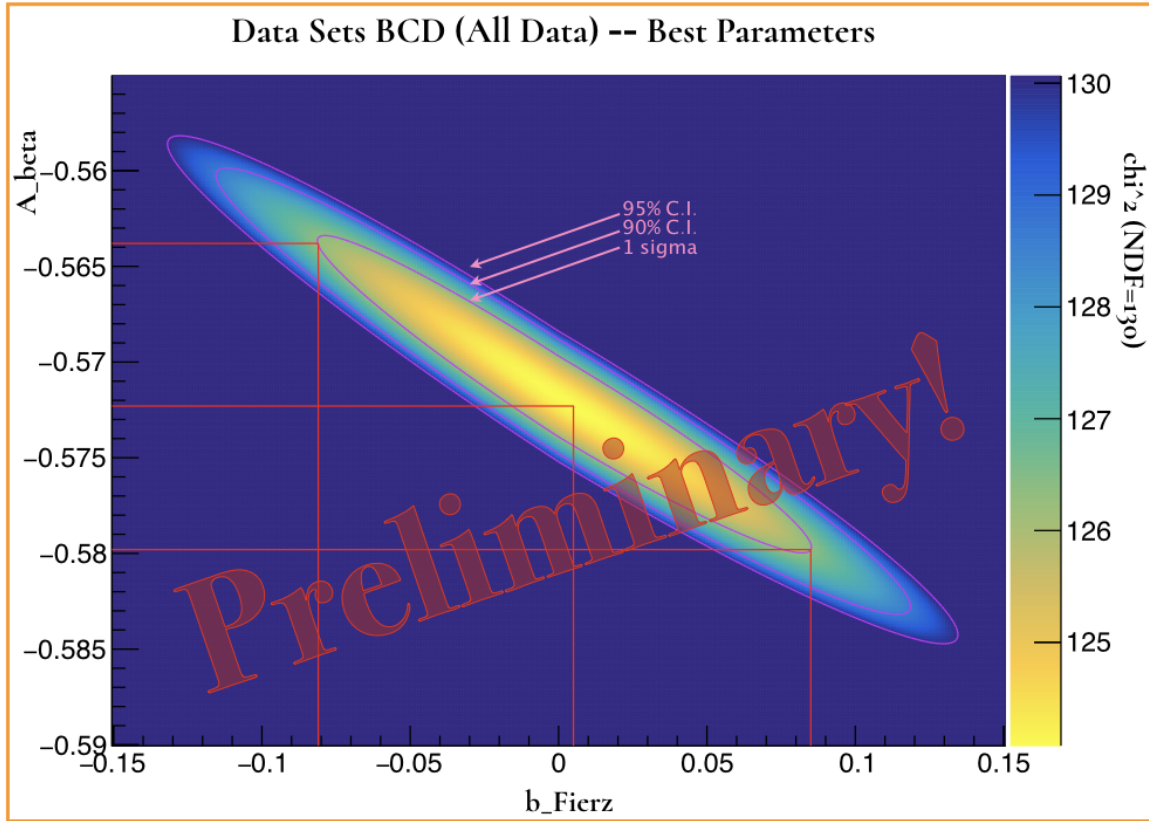


Figure 6.2: Some results. I'll want to show at least one of these things. Probably show a separate one for each runset, actually.

[...continued from prev.]

In our ^{37}K case, $\lambda^2 = |M_{\text{GT}}|^2/|M_F|^2$ is close to $3/5$ (the expected value $j/(j+1)$ for a single $j=3/2$ d $3/2$ nucleon) [12], while for the neutron λ^2 is close to 3 (the expected value for an $(j+1)/j$ $j=1/2$ s $1/2$ nucleon). $|M_F|$, the Fermi matrix element, is nearly the same for both of these isospin = $1/2$ decays (the largest correction is the larger isospin mixing of ~ 0.01 in ^{37}K). So our observable is relatively less sensitive to Lorentz tensor currents, and will predominantly constrain or discover Lorentz scalar currents.

...

Full considerations would require a weighted fit of b_{Fierz} experiments and similar observables [?], and are beyond the scope of this thesis. The info from this thesis, values of A_β and b_{Fierz} with their uncertainties, can together with the known fT value (lifetime and branching ratio) allow the community and/or the collaboration to include the results in a future constraint or discovery of scalar and tensor Lorentz currents contributing to β decay.

6.4 R_{slow} and Other Possible Future Work for the Collaboration

John says the whole R_{slow} thing should go in here somewhere.

Appendix I keep, it's excellent. It should be moved as is to Conclusions under "Future Experiment for the collaboration"! so people know you worked so hard on it!!

The nuclear weak force is known to be a predominantly left-handed vector and axial-vector (V-A) interaction. An experiment is proposed to further test that observation, constraining the strength of right-handed (V+A) currents by exploiting the principle of conservation of angular momentum within a spin-polarized beta decay process. Here, we focus on the decay $^{37}\text{K} \rightarrow ^{37}\text{Ar} + \beta^+ + \nu_e$. The angular correlations between the emerging daughter particles provide a rich source of information about the type of interaction that produced the decay.

6.4.1 Motivation

The nuclear weak force has long been known to be a predominantly left-handed chiral interaction, meaning that immediately following an interaction (such as a beta decay) with a weak force carrying boson (W^+ , W^- , Z), normal-matter leptons (such as the electron and electron neutrino) emerge with left-handed chirality while the anti-leptons (e.g. the positron and electron anti-neutrino) emerge with right-handed chirality. In the limit of massless particles, the particle's chirality is the same as its helicity. Thus, in a left-handed model, the direction of an (ultrarelativistic) normal lepton's spin is antiparallel direction of its motion, and the direction of spin for an anti-lepton is parallel to its direction of motion. For a non-relativistic particle the property of chirality is fairly abstract, and describes the appropriate group representation and projection operators to be used in calculations. It should be noted that a fully chiral model is also one which is maximally parity violating.

This odd quirk of the nuclear weak force is not only *predominantly* true, but it is, to the best of our current scientific knowledge, *always* true – that is, attempts to measure any right-handed chiral components of the weak force have produced results consistent with zero [14][25]. This project proposes a further measurement to constrain the strength of the right-handed component of the weak interaction.

6.4.2 The Decay Process

The kinematics of nuclear β^+ decay are described by the following probability density function:

$$W(\langle I \rangle | E_\beta \hat{\Omega}_\beta \hat{\Omega}_\nu) = \left(\frac{1}{2\pi} \right)^5 F(-Z, E_\beta) p_\beta E_\beta (E_0 - E_\beta)^2 dE_\beta d\hat{\Omega}_\beta d\hat{\Omega}_\nu \xi \left[1 + a_{\beta\nu} \frac{\vec{p}_\beta \cdot \vec{p}_\nu}{E_\beta E_\nu} + b_{\text{Fierz}} \frac{m_e}{E_\beta} \right. \\ + c_{\text{align}} \left(\frac{\frac{1}{3} \vec{p}_\beta \cdot \vec{p}_\nu - (\vec{p}_\beta \cdot \hat{j})(\vec{p}_\nu \cdot \hat{j})}{E_\beta E_\nu} \right) \left(\frac{I(I+1) - 3\langle (\vec{I} \cdot \hat{i})^2 \rangle}{I(2I-1)} \right) \\ \left. + \frac{\langle \vec{I} \rangle}{I} \left(A_\beta \frac{\vec{p}_\beta}{E_\beta} + B_\nu \frac{\vec{p}_\nu}{E_\nu} + D_{\text{TR}} \frac{\vec{p}_\beta \times \vec{p}_\nu}{E_\beta E_\nu} \right) \right], \quad (6.1)$$

where \vec{I} is the nuclear spin-polarization, $F(-Z, E_\beta)$ is the Fermi function, and parameters ξ , $a_{\beta\nu}$, b_{Fierz} , c_{align} , A_β , B_ν , and D_{TR} are functions that vary with the strengths of the vector, axial, scalar, and tensor couplings (constant throughout nature), as well as the Fermi and Gamow-Teller nuclear matrix elements (specific to the individual decay) [5][16].

The decay may be treated as a three-body problem in which the available kinetic energy is divided up between the beta, the neutrino, and the recoiling ^{37}Ar nucleus, and (of course) the total linear and angular momentum are conserved. While the neutrino cannot be detected directly, its kinematics may be reconstructed from observations of the beta and the recoiling daughter nucleus. By placing detectors above and below the decaying atom along the axis of its polarization, we are able to obtain information about the outgoing beta's energy and momentum, in the cases of interest to us, where it is emitted along (or close to) the axis of polarization.

The recoiling ^{37}Ar nucleus is a bit trickier to work with, but the task is not impossible. One useful feature of the $^{37}\text{K} \rightarrow ^{37}\text{Ar}$ transition is that, in addition to the β^+ emitted in the decay itself, one or more *orbital* electrons from the parent atom are typically lost. In the majority of decay events only one orbital electron is ‘shaken off’ and so the daughter ^{37}Ar atom is electrically neutral [20][26]. In the remaining cases, two or more orbital electrons are lost this way, and the daughter atom is positively charged. If we apply an electric field perpendicular to the direction of polarization, these positively charged $^{37}\text{Ar}^{(+n)}$ ions may be collected into a detector, from which hit position and time of flight information may be extracted. These shake-off electrons

are emitted with an average energy of only ~ 2 eV so to a very good approximation the other decay products are not perturbed by the presence of shake-off electrons.

It should be noted that for the class of decays of greatest interest, where the beta and the neutrino emerge back-to-back along the polarization axis, the recoiling daughter nucleus will have zero momentum along the directions perpendicular to this axis, and on average less total energy than if the beta and neutrino were emitted in a parallel direction. Henceforth, daughter nuclei from a back-to-back decay as shown in Figure ?? will be described as ‘slow’ recoils. In terms of observables, this means that if the electric field is configured to point along one of the axes perpendicular to the polarization direction, then when the recoiling ion is swept away into a detector, the slow recoil’s hit position should be exactly along the projection of the polarization axis. Furthermore, the slow recoil’s time of flight should be in the middle of the time of flight spectrum, since other recoils will be emitted with momentum towards or away from the detector.

6.4.3 Current Status

In June 2014, after several years of preparatory work beforehand (the author has been continuously involved with this project since 2010), approximately 7 days of beam time at TRIUMF was dedicated to the TRINAT ^{37}K beta decay experiment. Approximately half of this data is suitable for use in this project. During this period, approximately 10,000 atoms were held within the trap at any given time. The cleaned spectra show around 50,000 polarized beta-recoil coincidence events in total, divided among measurements at three different electric field strengths (535 V/cm, 415 V/cm, 395 V/cm).

A fit to simulation has shown that the data that has already been collected has sufficient statistical power to measure the *fractional* contribution of any polarized ‘new physics’ beta decay parameter (ie right-handed, scalar, and tensor currents within the weak interaction) to a sensitivity of $\sim 2\%$ of its true value. Systematic limitations are still being assessed.

6.5 Conclusions

Conclusions go here.

Bibliography

- [1] Fenker, B., Behr, J. A., Melconian, D., Anderson, R. M. A., Anholm, M., Ashery, D., Behling, R. S., Cohen, I., Craicu, I., Donohue, J. M., Farfan, C., Friesen, D., Gorelov, A., McNeil, J., Mehlman, M., Norton, H., Olchanski, K., Smale, S., Thériault, O., Vantyghem, A. N. and Warner, C. L., *Precision measurement of the nuclear polarization in laser-cooled, optically pumped ^{37}K* , New Journal of Physics, Vol. 18, No. 7, pp. 073028, 2016.
- [2] Anholm, M., Characterizing the AC-MOT, Master's thesis, University of British Columbia, 2014.
- [3] Falkowski, A., González-Alonso, M. and Naviliat-Cuncic, O., *Comprehensive analysis of beta decays within and beyond the Standard Model*, Journal of High Energy Physics, Vol. 2021, No. 4, pp. 1–36, 2021.
- [4] Hong, R., Sternberg, M. G. and Garcia, A., *Helicity and nuclear β decay correlations*, American Journal of Physics, Vol. 85, No. 1, pp. 45–53, 2017.
- [5] Jackson, J. D., Treiman, S. B. and Wyld, H. W., *Possible Tests of Time Reversal Invariance in Beta Decay*, Phys. Rev., Vol. 106, pp. 517–521, May 1957.
- [6] Levinger, J. S., *Effects of Radioactive Disintegrations on Inner Electrons of the Atom*, Phys. Rev., Vol. 90, pp. 11–25, Apr 1953.
- [7] Harvey, M. and Murray, A. J., *Cold Atom Trap with Zero Residual Magnetic Field: The AC Magneto-Optical Trap*, Phys. Rev. Lett., Vol. 101, pp. 173201, Oct 2008.
- [8] Sun, X., Adamek, E., Allgeier, B., Bagdasarova, Y., Berguno, D. B., Blatnik, M., Bowles, T. J., Broussard, L. J., Brown, M. A.-P., Carr, R., Clayton, S.,

Cude-Woods, C., Currie, S., Dees, E. B., Ding, X., Filippone, B. W., García, A., Geltenbort, P., Hasan, S., Hickerson, K. P., Hoagland, J., Hong, R., Holley, A. T., Ito, T. M., Knecht, A., Liu, C.-Y., Liu, J., Makela, M., Mammei, R., Martin, J. W., Melconian, D., Mendenhall, M. P., Moore, S. D., Morris, C. L., Nepal, S., Nouri, N., Pattie, R. W., Pérez Gálvan, A., Phillips, D. G., Picker, R., Pitt, M. L., Plaster, B., Salvat, D. J., Saunders, A., Sharapov, E. I., Sjue, S., Slutsky, S., Sondheim, W., Swank, C., Tatar, E., Vogelaar, R. B., VornDick, B., Wang, Z., Wei, W., Wexler, J. W., Womack, T., Wrede, C., Young, A. R. and Zeck, B. A., *Improved limits on Fierz interference using asymmetry measurements from the Ultracold Neutron Asymmetry (UCNA) experiment*, Phys. Rev. C, Vol. 101, pp. 035503, Mar 2020.

- [9] Saul, H., Roick, C., Abele, H., Mest, H., Klopf, M., Petukhov, A. K., Soldner, T., Wang, X., Werder, D. and Märkisch, B., *Limit on the Fierz Interference Term b from a Measurement of the Beta Asymmetry in Neutron Decay*, Phys. Rev. Lett., Vol. 125, pp. 112501, Sep 2020.
- [10] Clifford, E., Hagberg, E., Koslowsy, V., Hardy, J., Schmeing, H. and Azuma, R., *Measurements of the response of a hybrid detector telescope to mono-energetic beams of positrons and electrons in the energy range 0.8–3.8 MeV*, Nuclear Instruments and Methods in Physics Research, Vol. 224, No. 3, pp. 440–447, 1984.
- [11] Saul, H., Roick, C., Abele, H., Mest, H., Klopf, M., Petukhov, A. K., Soldner, T., Wang, X., Werder, D. and Märkisch, B., *Limit on the Fierz Interference Term b from a Measurement of the Beta Asymmetry in Neutron Decay*, Phys. Rev. Lett., Vol. 125, pp. 112501, Sep 2020.
- [12] de Shalit, A. and Talmi, I., Nuclear Shell Theory.
- [13] Krane, K. S., Introductory Nuclear Physics, Wiley, New York, 1988.
- [14] Severijns, N., Beck, M. and Naviliat-Cuncic, O., *Tests of the standard electroweak model in nuclear beta decay*, Rev. Mod. Phys., Vol. 78, pp. 991–1040, September 2006.
- [15] Wong, S., Introductory Nuclear Physics, Prentice Hall Advanced Reference Series Prentice Hall Labora, Prentice Hall, 1990.

- [16] Jackson, J. D., Treiman, S. B. and Wyld, H. W., *Coulomb Corrections in Allowed Beta Transitions*, Nuclear Physics, Vol. 4, pp. 206–212, Nov. 1957.
- [17] Holstein, B. R., *Recoil effects in allowed beta decay: The elementary particle approach*, Reviews of Modern Physics, Vol. 46, No. 4, pp. 789–814, Oct. 1974.
- [18] Raab, E. L., Prentiss, M., Cable, A., Chu, S. and Pritchard, D. E., *Trapping of Neutral Sodium Atoms with Radiation Pressure*, Phys. Rev. Lett., Vol. 59, pp. 2631–2634, Dec 1987.
- [19] Corney, A., Atomic and Laser Spectroscopy, Oxford University Press, New York, 1977.
- [20] Gorelov, A., Behr, J., Melconian, D., Trinczek, M., Dubé, P., Häusser, O., Giesen, U., Jackson, K., Swanson, T., D'Auria, J., Dombsky, M., Ball, G., Buchmann, L., Jennings, B., Dilling, J., Schmid, J., Ashery, D., Deutsch, J., Alford, W., Asgeirsson, D., Wong, W. and Lee, B., *Beta-neutrino correlation experiments on laser trapped ^{38m}K , ^{37}K* , Hyperfine Interactions, Vol. 127, No. 1, pp. 373–380, 2000.
- [21] Swanson, T. B., Asgeirsson, D., Behr, J. A., Gorelov, A. and Melconian, D., *Efficient transfer in a double magneto-optical trap system*, J. Opt. Soc. Am. B, Vol. 15, No. 11, pp. 2641–2645, Nov 1998.
- [22] Fenker, B., Gorelov, A., Melconian, D., Behr, J. A., Anholm, M., Ashery, D., Behling, R. S., Cohen, I., Craiciu, I., Gwinner, G., McNeil, J., Mehlman, M., Olchanski, K., Shidling, P. D., Smale, S. and Warner, C. L., *Precision Measurement of the β Asymmetry in Spin-Polarized ^{37}K Decay*, Phys. Rev. Lett., Vol. 120, pp. 062502, Feb 2018.
- [23] Audi, G., Wapstra, A. and Thibault, C., *The AME2003 Atomic Mass Evaluation*, Nuclear Physics A, Vol. 729, No. 1, pp. 337 – 676, 2003.
- [24] Holstein, B. R., *Erratum: Recoil effects in allowed beta decay: The elementary particle approach*, Rev. Mod. Phys., Vol. 48, pp. 673–673, Oct 1976.
- [25] Severijns, N. and Naviliat-Cuncic, O., *Symmetry tests in nuclear beta decay*, Annual Review of Nuclear and Particle Science, Vol. 61, pp. 23–46, 2011.

- [26] Melconian, D. G., Measurement of the Neutrino Asymmetry in the Beta Decay of Laser-Cooled, Polarized ^{37}K , Ph.D. thesis, Simon Fraser University, 2005.

The citation format I'm using is really stupid. You **must** force yourself to ignore this right now,
Melissa!

Appendix A

Notable Differences in Data Selection between this and the Previous Result

Removed some appendices:

- Very Obvious Things (on lifetimes and half-lives)
- On Beta Endpoint Energies ("notationandprelimintegration")
- Wong Nuclear
- HowTo Lifetime

JB says Appendix A should all go in the analysis section, and not in an appendix at all.

JB says: Appendix A (ie, *this appendix*) is very important, and should at least be a subsection in the Analysis chapter.

...

You could condense the Appendix into a set of bullet points at the end of the intro to the Analysis section (which you still need, badly!), and then its content could be interleaved in the Analysis chapter. E.g. you already have redundancy in the LE and TE discussion vs. the Appendix, and the discussion is more complete in the Analysis chapter, which is good.

I really want this appendix to stay here. I'll make sure to mention everything in the body of the thesis though, since it **is** important. But at some point, somebody is going to really want to have this info written into a short summary.

A.1 Polarization Cycle Selection

Data used for our recent PRL article was slightly less polarized than we thought it was, due to an oversight in the data selection procedure.

A.2 Leading Edge / Trailing Edge and Walk Correction

Using the leading edge rather than the trailing edge to mark the timing of TDC pulses cleans up jitter, eliminates background, and changes the relative delays between different inputs. It is immediately relevant to the shape of the ‘walk correction’ on scintillator timing pulses, which give a different prediction for beta arrival time as a function of scintillator energy.

A.3 TOF Cut + Background Modelling

A SOE-beta time-of-flight cut is necessary to reduce background. The above mentioned walk correction directly results in an change in which specific events are selected in a given TOF cut. It further results in an adjustment to the expected fraction of background events in any such cut.

A.4 BB1 Radius

Possibly my default radius cut on the DSSDs is a bit different. The region of the parameter space that I’m taking for the systematic uncertainty on this is definitely a bit different.

Somebody will surely ask for a justification for why I did this differently, and I don’t have one beyond “this seemed more reasonable to me”, which is of course nobody will ever accept as a reason.

Appendix B

A PDF For The People

John says to keep this appendix, because it's great now.

B.1 JTW

Here's a master equation from JTW to describe beta decay kinematics [5], [16]:

$$\begin{aligned} d^5\Gamma_{\text{JTW}} \equiv & \frac{F_{\mp}(Z, E_\beta)}{(2\pi)^5} p_\beta E_\beta (E_0 - E_\beta)^2 dE_\beta d^3\hat{\Omega}_\beta d^3\hat{\Omega}_\nu \\ & \times \xi \left[1 + a_{\beta\nu} \frac{\vec{p}_\beta \cdot \vec{p}_\nu}{E_\beta E_\nu} + b_{\text{Fierz}} \frac{m_e c^2}{E_\beta} + c_{\text{align}} T_{\text{align}}(\vec{J}) \left(\frac{\vec{p}_\beta \cdot \vec{p}_\nu}{3E_\beta E_\nu} - \frac{(\vec{p}_\beta \cdot \hat{\vec{j}})(\vec{p}_\nu \cdot \hat{\vec{j}})}{E_\beta E_\nu} \right) \right. \\ & \left. + \frac{\vec{J}}{J} \cdot \left(A_\beta \frac{\vec{p}_\beta}{E_\beta} + B_\nu \frac{\vec{p}_\nu}{E_\nu} + D_{\text{TR}} \frac{\vec{p}_\beta \times \vec{p}_\nu}{E_\beta E_\nu} \right) \right] \end{aligned} \quad (\text{B.1})$$

where, for convenience, we have defined a nuclear alignment term,

$$T_{\text{align}}(\vec{J}) \equiv \frac{J(J+1) - 3\langle(\vec{J} \cdot \hat{\vec{j}})^2\rangle}{J(2J-1)}. \quad (\text{B.2})$$

Note that this master equation depends on neutrino momentum, which we cannot observe directly. Furthermore, we cannot reconstruct neutrino momenta in our decay events either, because it would be necessary to account for the momentum of the recoiling daughter nucleus, treating the decay as a three-body problem. From

We have already specialized to β^+ decay.

an experimental standpoint, we failed to measure the momenta of the daughters in conjunction with the “tagged” beta decay events with which we are primarily concerned in this thesis. From a theoretical standpoint, JTW has intentionally neglected recoil-order terms – meaning that the daughter nucleus is treated, for the purpose of kinetic energy calculations, as being infinitely massive, and as such it must have no change in kinetic energy from the decay. This approximation makes it a bit tricky to correctly re-formulate Eq. (B.1) in terms of the momentum of the daughter instead of the momentum of the neutrino.

Fortunately, it is possible to simplify Eq. (B.1) by integrating over all possible neutrino directions, such that the result no longer depends on parameters that we do not observe. The neutrino energy itself is not a free variable in this equation, because the energy release in the decay is fixed, and given the approximation that none of that energy is allocated to the recoiling daughter, it is very straightforward to calculate the neutrino energy for a decay event in which the beta energy is known.

The result of performing this integration over neutrino direction is:

$$\begin{aligned} d^3\Gamma dE_\beta d^3\hat{\Omega}_\beta &= \frac{2}{(2\pi)^4} F_{\mp}(Z, E_\beta) p_\beta E_\beta (E_0 - E_\beta)^2 dE_\beta d^3\hat{\Omega}_\beta \xi \\ &\times \left[1 + b_{\text{Fierz}} \frac{m_e c^2}{E_\beta} + A_\beta \left(\frac{\vec{J}}{J} \cdot \frac{\vec{p}_\beta}{E_\beta} \right) \right], \end{aligned} \quad (\text{B.3})$$

which is a great simplification on Eq. (B.1). We still must write the remaining parameters in terms of the relevant nuclear matrix elements and fundamental coupling constants. These coupling constants are, in general, complex-valued, and JTW does not choose a phase angle for us. We write them out in Eqs. (B.4-B.6).

$$\begin{aligned} \xi &= |M_F|^2 (|C_S|^2 + |C_V|^2 + |C'_S|^2 + |C'_V|^2) \\ &+ |M_{GT}|^2 (|C_T|^2 + |C_A|^2 + |C'_T|^2 + |C'_A|^2) \end{aligned} \quad (\text{B.4})$$

$$b_{\text{Fierz}} \xi = \pm 2\gamma \text{Re} [|M_F|^2 (C_S C_V^* + C'_S C_V'^*) + |M_{GT}|^2 (C_T C_A^* + C'_T C_A'^*)] \quad (\text{B.5})$$

$$\begin{aligned} A_\beta \xi &= |M_{GT}|^2 \lambda_{J'J} \left[\pm 2\text{Re}[C_T C_T'^* - C_A C_A'^*] + 2 \frac{\alpha Z m_e}{p_\beta} \text{Im}[C_T C_A'^* + C'_T C_A^*] \right] \\ &+ \delta_{J'J} M_F M_{GT} \left(\frac{J}{J+1} \right)^{1/2} \left[2 \text{Re}[C_S C_T'^* + C'_S C_T^* - C_V C_A'^* - C'_V C_A^*] \right. \\ &\left. \pm 2 \frac{\alpha Z m_e}{p_\beta} \text{Im}[C_S C_A'^* + C'_S C_A^* - C_V C_T'^* - C'_V C_T^*] \right] \end{aligned} \quad (\text{B.6})$$

Note that JTW presents slightly different expressions for the sign convention in components of A_β within [5] and [16]. Here, we adopt the convention from the latter publication. Furthermore, we do not require that either M_F or M_{GT} be positive (which would allow us to safely drop their absolute value indicators and make the conventions of these two papers equivalent). In order to obtain the correct, physically observed value for A_β , we require that the $M_F M_{GT}$ term in Eq. (B.6) have an overall positive value. Because we know that the scalar and tensor couplings must be small, and any imaginary contributions to the term must be small, we conclude that

$$M_F M_{GT} (C_V C_A'^* + C_V' C_A^*) < 0. \quad (\text{B.7})$$

Also, $\xi = G_v^2 \cos \theta_C f_1(E)$.

B.2 Holstein

Holstein [17] [24] generously provides explicit equations to match both Eq. (B.1) (i.e. Holstein's Eq. (51), where neutrino direction is a parameter of the probability distribution) and Eq. (B.3) (Holstein's Eq. (52), where neutrino direction has already been integrated over).

Here's Holstein's Eq. (52):

$$\begin{aligned} d^3\Gamma_{\text{Holstein}} &= 2G_v^2 \cos^2 \theta_c \frac{F_\mp(Z, E_\beta)}{(2\pi)^4} p_\beta E_\beta (E_0 - E_\beta)^2 dE_\beta d^3\hat{\Omega}_\beta \\ &\times \left\{ F_0(E_\beta) + \Lambda_1 F_1(E_\beta) \hat{\mathbf{n}} \cdot \frac{\vec{p}_\beta}{E_\beta} + \Lambda_2 F_2(E_\beta) \left[\left(\hat{\mathbf{n}} \cdot \frac{\vec{p}_\beta}{E_\beta} \right)^2 - \frac{1}{3} \frac{p_\beta^2}{E_\beta^2} \right] \right. \\ &\left. + \Lambda_3 F_3(E_\beta) \left[\left(\hat{\mathbf{n}} \cdot \frac{\vec{p}_\beta}{E_\beta} \right)^3 - \frac{3}{5} \frac{p_\beta^2}{E_\beta^2} \hat{\mathbf{n}} \cdot \frac{\vec{p}_\beta}{E_\beta} \right] \right\} \end{aligned} \quad (\text{B.8})$$

A careful reader will eventually note that Holstein's spectral functions $F_i(E_\beta)$ are not the same as the $F_i(E_\beta, u, v, s)$ in any limit, despite the notational similarities. Among other rules, Holstein's spectral functions obey these:

$$F_i(E_\beta) \neq F_i(E_\beta, u, v, s) \quad (\text{B.9})$$

$$F_i(E_\beta) = H_i(E_\beta, u, v, 0) \quad (\text{B.10})$$

$$f_i(E_\beta) = F_i(E_\beta, u, v, 0). \quad (\text{B.11})$$

For the $F_i(E_\beta)$ functions of interest to us here, we find the following relationships:

$$\begin{aligned}
F_0(E_\beta) &= H_0(E_\beta, J, J', 0) = F_1(E_\beta, J, J', 0) &= f_1(E_\beta) \\
F_1(E_\beta) &= H_1(E_\beta, J, J', 0) = F_4(E_\beta, J, J', 0) + \frac{1}{3}F_7(E_\beta, J, J', 0) &= f_4(E_\beta) + \frac{1}{3}f_7(E_\beta) \\
F_2(E_\beta) &= H_2(E_\beta, J, J', 0) = F_{10}(E_\beta, J, J', 0) + \frac{1}{2}F_{13}(E_\beta, J, J', 0) &= f_{10}(E_\beta) + \frac{1}{3}f_{13}(E_\beta) \\
F_3(E_\beta) &= H_3(E_\beta, J, J', 0) = F_{18}(E_\beta, J, J', 0) &= f_{18}(E_\beta). \quad (\text{B.12})
\end{aligned}$$

Note that the $f_i(E_\beta)$ in Eq. B.12 are the same spectral functions used to describe a polarized decay spectrum when the neutrino (ie, the recoil) is also observed – though of course such a spectrum must have other terms as well. For the spectrum of interest to us here, in which the neutrino direction has already been integrated over, we can simply look up the $H_i(E_\beta, J, J', 0) = H_i(E, u, v, s=0)$ spectral functions, and leave it at that. We find:

$$\begin{aligned}
F_0(E_\beta) &= |a_1|^2 + 2 \operatorname{Re}[a_1^* a_2] \frac{1}{3M^2} \left[m_e^2 + 4E_\beta E_0 + 2 \frac{m_e^2}{E_\beta} E_0 - 4E_\beta^2 \right] \\
&\quad + |c_1|^2 + 2 \operatorname{Re}[c_1^* c_2] \frac{1}{9M^2} \left[11m_e^2 + 20E_\beta E_0 - 2 \frac{m_e^2}{E_\beta} E_0 - 20E_\beta^2 \right] \\
&\quad - 2 \frac{E_0}{3M} \operatorname{Re}[c_1^*(c_1 + d \pm b)] + \frac{2E_\beta}{3M} (3|a_1|^2 + \operatorname{Re}[c_1^*(5c_1 \pm 2b)]) \\
&\quad - \frac{m_e^2}{3ME_\beta} \operatorname{Re} \left[-3a_1^* e + c_1^* \left(2c_1 + d \pm 2b - h \frac{E_0 - E_\beta}{2M} \right) \right] \quad (\text{B.13})
\end{aligned}$$

$$\begin{aligned}
F_1(E_\beta) &= \delta_{u,v} \left(\frac{u}{u+1} \right)^{1/2} \left\{ 2 \operatorname{Re} \left[a_1^* \left(c_1 - \frac{E_0}{3M} (c_1 + d \pm b) + \frac{E_\beta}{3M} (7c_1 \pm b + d) \right) \right] \right. \\
&\quad + 2 \operatorname{Re}[a_1^* c_2 + c_1^* a_2] \left(\frac{4E_\beta(E_0 - E_\beta) + 3m_e^2}{3M^2} \right) \Big\} \\
&\quad \mp \frac{(-1)^s \gamma_{u,v}}{u+1} \operatorname{Re} \left\{ c_1^* \left(c_1 + 2c_2 \left(\frac{8E_\beta(E_0 - E_\beta) + 3m_e^2}{3M^2} \right) - \frac{2E_0}{3M} (c_1 + d \pm b) \right. \right. \\
&\quad \left. \left. + \frac{E_\beta}{3M} (11c_1 - d \pm 5b) \right) \right\} + \frac{\lambda_{u,v}}{u+1} \operatorname{Re} \left\{ c_1^* \left[-f \left(\frac{5E_\beta}{M} \right) \right. \right. \\
&\quad \left. \left. + g \left(\frac{3}{2} \right)^{1/2} \left(\frac{E_0^2 - 11E_0E_\beta + 6m_e^2 + 4E_\beta^2}{6M^2} \right) \pm 3j_2 \left(\frac{8E_\beta^2 - 5E_0E_\beta - 3m_e^2}{6M^2} \right) \right] \right\} \quad (\text{B.14})
\end{aligned}$$

$$\begin{aligned}
F_2(E_\beta) = & \theta_{u,v} \frac{E_\beta}{2M} \operatorname{Re} \left[c_1^* \left(c_1 + c_2 \frac{8(E_0 - E_\beta)}{3M} - d \pm b \right) \right] \\
& - \delta_{u,v} \frac{E_\beta}{M} \left[\frac{u(u+1)}{(2u-1)(2u+3)} \right]^{1/2} \operatorname{Re} \left\{ a_1^* \left(\left(\frac{3}{2}\right)^{1/2} f + g \frac{E_\beta + 2E_0}{4M} \right. \right. \\
& \left. \left. \pm \left(\frac{3}{2}\right)^{1/2} j_2 \frac{E_0 - E_\beta}{2M} \right) \right\} + (-1)^s \kappa_{u,v} \frac{E_\beta}{2M} \operatorname{Re} \left[c_1^* \left(\pm 3f \pm \left(\frac{3}{2}\right)^{1/2} g \frac{E_0 - E_\beta}{M} \right. \right. \\
& \left. \left. + 3j_2 \frac{E_0 - 2E_\beta}{2M} \right) \right] + \epsilon_{u,v} \operatorname{Re}[c_1^* j_3] \left(\frac{21E_\beta^2}{8M^2} \right)
\end{aligned} \tag{B.15}$$

$$\begin{aligned}
F_3(E_\beta) = & -\delta_{u,v} (3u^2 + 3u - 1) \left[\frac{u}{(u-1)(u+1)(u+2)(2u-1)(2u+3)} \right]^{1/2} \\
& \times \operatorname{Re}[a_1^* j_3] \left(\frac{E_\beta^2 \sqrt{15}}{4M^2} \right) + \frac{\rho_{u,v}}{u+1} \operatorname{Re} \left[c_1^* (g\sqrt{3} + j_2\sqrt{2}) \left(\frac{5E_\beta^2}{4M^2} \right) \right] \\
& \pm \frac{(-1)^s \sigma_{u,v}}{u+1} \operatorname{Re}[c_1^* j_3] \left(\frac{5E_\beta^2}{2M^2} \right)
\end{aligned} \tag{B.16}$$

and we might really appreciate if these things could be simplified a bit.

The terms $a_1, a_2, b, c_1, c_2, d, e, f, g, h, j_2, j_3$ are “structure functions”. Holstein gives some predictions for their form, assuming the impulse approximation holds, in his Eq. (67). For the most part, the values and form of these structure functions are beyond the scope of this thesis, so I will not re-write them all here. It should be noted that the numerical values used for these parameters came from a private communication from Ian Towner to the collaboration. However, it is important to note the expressions for a_i and c_i , because these will directly come into play when we try to reconcile Holstein’s expression with JTW’s. Therefore,

$$a(q^2) \approx \frac{g_V(q^2)}{\left(1 + \frac{\Delta}{2M}\right)} \left[M_F + \frac{1}{6}(q^2 - \Delta^2)M_{r^2} + \frac{1}{3}\Delta M_{\mathbf{r} \cdot \mathbf{p}} \right] \tag{B.17}$$

$$\begin{aligned}
c(q^2) \approx & \frac{g_A(q^2)}{\left(1 + \frac{\Delta}{2M}\right)} \left[M_{GT} + \frac{1}{6}(q^2 - \Delta^2)M_{\sigma r^2} + \frac{1}{6\sqrt{10}}(2\Delta^2 + q^2)M_{1y} \right. \\
& \left. + A \frac{\Delta}{2M} M_{\sigma L} + \frac{1}{2}\Delta M_{\sigma rp} \right]
\end{aligned} \tag{B.18}$$

There was something wrong with this assumption. Something circular. I forgot. Blah.

Somewhere I have to define q^2 and Δ are.

...where the M_{xxx} 's are certain nuclear matrix elements. However, Eqs. (B.13-B.16) are not written in terms of $a(q^2)$ and $c(q^2)$, but rather in terms of a_1 , a_2 , c_1 , and c_2 . In fact, Holstein is implicitly using series expansions to remove the dependence on recoil momentum, so that

$$a(q^2) = a_1 + \left(\frac{q^2}{M^2}\right) a_2 + \dots \quad (\text{B.19})$$

$$c(q^2) = c_1 + \left(\frac{q^2}{M^2}\right) c_2 + \dots \quad (\text{B.20})$$

Should I just list the values of things that I inherited from Ian Towner's personal communication that one time?

Next, Holstein goes and tweaks those $F_i(E_\beta)$ terms that we've already written out, by adding in an adjustment for Coulomb corrections. Those corrections have this form:

$$F_i(E_\beta) \rightarrow \tilde{F}_i(E_\beta) := F_i(Z, E_\beta) [F_i(E_\beta) + \Delta F_i(E_\beta)] \quad (\text{B.21})$$

To obtain expressions for the $\Delta F_i(E_\beta)$, Holstein invokes some Feynman diagrams and provides expressions for several integrals, all of which are both complex and complicated. The modified spectral functions are provided in terms of functions of these integrals. Since nobody wants to have to evaluate those integrals, Holstein makes a further approximation by taking only the first term in an expansion of the $\Delta F_i(E_\beta)$ in terms of $Z\alpha$, where $Z\alpha \ll 1$. Then, the resulting expressions for $\Delta F_i(E_\beta)$ can be written in terms of much more straightforward integrals over form factors for electric charge and weak charge.

If we make the further assumption that these form factors are identical, and that both types of charge are spread over a ball of uniform density with radius R , then we find:

$$X = Y = \frac{9\pi R}{140} \quad (\text{B.22})$$

and also, I think something like that the weak charge is the same distribution as the electric charge

in the Eqs. (B.23 - B.25) that follow.

Because Holstein doesn't actually write this stuff out in terms of $F_i(E_\beta)$, but rather in terms of $F_i(E_\beta, u, v, s)$, this correction presents yet another opportunity for the reader to interpret his notation incorrectly. We note that one must remember to make use of the relations in Eq. (B.12). Furthermore, Holstein notes that some of the terms $F_i(E_\beta, u, v, s)$ are suppressed already, and he does not consider those terms further. We will take this approximation to be adequate for our purposes here.

What is less clear, given the context in the paper, is whether or not when Holstein writes out his simplified expressions for $\Delta F_x(E_\beta, u, v, s)$ he actually means $F_\mp(Z, E_\beta)\Delta F_i(E_\beta, u, v, s)$. These terms are pretty small, so it probably doesn't *really* matter, but it would still be really nice to *know*, damn it.

So, we'll write out the functions for these corrections.

$$\begin{aligned}\Delta F_1(E_\beta, u, v, s) = & \mp \left(\frac{8\alpha Z}{3\pi} \right) X \left[E_\beta \left(8|a|^2 + \frac{28}{3}|c|^2 \right) + E_0 \left(|a|^2 - \frac{1}{3}|c|^2 \right) \right. \\ & \left. + 3 \left(\frac{m_e c^2}{E_\beta} \right) (|a|^2 + |c|^2) \right]\end{aligned}\quad (\text{B.23})$$

$$\Delta F_4(E_\beta, u, v, s) = \mp \left(\frac{8\alpha Z}{3\pi} \right) 9X E_\beta \left[2\delta_{u,v} \left(\frac{u}{u+1} \right)^{1/2} \text{Re}[a^*c] \mp (-1)^s \left(\frac{\gamma_{u,v}}{u+1} \right) |c|^2 \right]\quad (\text{B.24})$$

$$\begin{aligned}\Delta F_7(E_\beta, u, v, s) = & \mp \left(\frac{8\alpha Z}{3\pi} \right) X (E_0 - E_\beta) \left[2\delta_{u,v} \left(\frac{u}{u+1} \right)^{1/2} \text{Re}[a^*c] \right. \\ & \left. \mp (-1)^s \left(\frac{\gamma_{u,v}}{u+1} \right) |c|^2 \right]\end{aligned}\quad (\text{B.25})$$

We note that the above corrections have been written in terms of $a(q^2)$ and $c(q^2)$, and we must use Eqs. (B.19, B.20) to put the results in terms of a_1 , a_2 , c_1 , and c_2 so that they can be correctly combined with Eqs. (B.13-B.16).

If we evaluate Holstein's Eqs. (B8), which I will absolutely not type out here, for the case $u = v = J = J' = 3/2$, we find the following values:

$$\begin{aligned}\delta_{u,v} &= 1 & \theta_{u,v} &= 1 & \rho_{u,v} &= \frac{-41}{40} \\ \gamma_{u,v} &= 1 & \kappa_{u,v} &= \frac{1}{2\sqrt{2}} & \sigma_{u,v} &= \frac{-41}{4\sqrt{35}} \\ \lambda_{u,v} &= \frac{-\sqrt{2}}{5} & \epsilon_{u,v} &= \frac{-1}{2\sqrt{5}} & \phi_{u,v} &= 0\end{aligned}\quad (\text{B.26})$$

Furthermore, in our calculations here, we will be considering only the β^+ decay modes,

and therefore we take the *lower* sign when the option arises. We also will use $s = 0$, so that $(-1)^s = +1$.

Also, pretty sure one of those never gets used. Which one was it? idk.

- - - - -

Let's define some of that notation! Firstly,

$$\text{Holstein's } \hat{n} = \text{JTW's } \mathbf{j}, \quad (\text{B.27})$$

and the Λ_i are given by Holstein's Eq. (48):

$$\Lambda_1 := \frac{\langle M \rangle}{J} \quad (\text{B.28})$$

$$\Lambda_2 := 1 - \frac{3\langle M^2 \rangle}{J(J+1)} \quad (\text{B.29})$$

$$\Lambda_3 := \frac{\langle M \rangle}{J} - \frac{5\langle M^3 \rangle}{J(3J^2 + 3J - 1)}. \quad (\text{B.30})$$

We immediately see that Holstein's Λ_1 is closely related to JTW's $\frac{\vec{J}}{J}$, and a bit later after John points it out to us, we see that Holstein's Λ_2 is closely related to JTW's T_{align} . JTW doesn't have any equivalent to Λ_3 . In particular, we find:

$$\Lambda_1 \hat{\mathbf{j}} = \frac{\langle M \rangle}{J} \hat{\mathbf{j}} = \frac{\vec{\mathbf{J}}}{J} \quad (\text{B.31})$$

$$\Lambda_2 = T_{\text{align}} \frac{(2J-1)}{(J+1)}. \quad (\text{B.32})$$

Note: It's not the case that $|\vec{\mathbf{J}}| == J$. It's actually super fucking infuriating notation.

Appendix C

Comparing Notation between Holstein and JTW

I see some stuff in my old Appendix D that needs to be moved (in here? Or maybe in Old Appendix E) before it goes away forever.

JB: Appendix C has some redundancies with B. You will have to sort that out. (n.b.: from context, it's less clear which appendices he's actually talking about, but whatever, there's certainly redundancies all around.)

C.1 Comparison Guide

This is a short guide to differences in notation, sign convention, and normalization. There are several tables here, chosen to aid in conversion between the two conventions. This section also includes handwritten notes.

C.2 Imported from Another Appendix

Here are some equations. I want to keep these somewhere in this chapter. For the equations below, I am intentionally not including the ROC terms. We take only

Holstein	JTW	Thesis	Comments
k			Neutrino momentum 4-vector
	E_ν		Neutrino energy
\hat{k}	$\frac{\mathbf{p}_\nu}{E_\nu}$		3D Neutrino emission direction unit vector. Neutrinos are always treated as massless.
p			Beta momentum 4-vector, or sometimes the magnitude of the beta momentum 3-vector. Never the magnitude of the 4-vector.
E	E_e	E_β	Beta energy
\mathbf{p}	\mathbf{p}_e	\vec{p}_β	Beta momentum 3-vector
q			Recoil momentum 4-vector, or sometimes a magnitude.

Table C.1: A comparison of some kinematic terms in JTW [5] [16] and Holstein [17]. Yes, the bolding/italicization carries meaning.

Holstein	JTW	Comments
u	J	Initial state total nuclear angular momentum.
v	J'	Final state total nuclear angular momentum.
s	No equivalent?	Umm... I should check on this.

Table C.2: A comparison of some angular momenta in JTW [5] [16] and Holstein [17].

enough Holstein terms to construct the expressions JTW gives us.

$$\xi = G_v^2 \cos \theta_C f_1(E) \quad (\text{C.1})$$

$$a_{\beta\nu} = f_2(E) / f_1(E) \quad (\text{C.2})$$

$$\frac{\langle \vec{J} \rangle}{J} \cdot \frac{\vec{p}}{E} A_\beta = \Lambda_1 \hat{n} \cdot \frac{\vec{p}}{E} f_4(E) / f_1(E) \quad (\text{C.3})$$

$$\frac{\langle \vec{J} \rangle}{J} \cdot \frac{\vec{p}_\nu}{E_\nu} B_\nu = \Lambda_1 \hat{n} \cdot \vec{k} f_6(E) / f_1(E) \quad (\text{C.4})$$

$$\frac{\langle \vec{J} \rangle}{J} \cdot \frac{(\vec{p} \times \vec{p}_\nu)}{EE_\nu} D_{\text{TR}} = \Lambda_1 \hat{n} \cdot \left(\frac{\vec{p}}{E} \times \hat{k} \right) f_8(E) / f_1(E) \quad (\text{C.5})$$

Holstein	JTW	Thesis	Comments
$G_v^2 \cos \theta_C f_1(E)$	ξ	$\xi(E_\beta)$	Normalization. Proportional to the fractional decay rate.
\hat{n}	\mathbf{j}	$\hat{\mathbf{j}}$	Nuclear polarization unit vector. Also the axis of quantization.
J	J		Total nuclear angular momentum quantum number
$\langle M \rangle$	$ \langle \mathbf{J} \rangle $		Angular momentum projection along the axis of quantization
$\Lambda^{(1)} \hat{n} = \frac{\langle M \rangle}{J} \hat{n}$	$\frac{\langle \mathbf{J} \rangle}{J}$	$\Lambda_1 \hat{n}$	Dipole element vector. Proportional to nuclear polarization. <i>(Rephrase this.)</i>
$\Lambda^{(1)} = \frac{\langle M \rangle}{J}$...	Λ_1	...
$\Lambda^{(2)}$	$\frac{J(J+1)-3\langle(\vec{J}\cdot\hat{j})^2\rangle}{J(2J-1)} \frac{(2J-1)}{(J+1)}$	$T_{\text{align}}(\vec{J}) \frac{(2J-1)}{(J+1)}$	Quadrupole element
$\Lambda^{(3)}$	No equivalent	Λ_3	Octopole element
$\Lambda^{(4)}$	No equivalent	Λ_4	Hexadecapole element

Table C.3: A comparison of the multipole elements and their normalizations (and some other stuff) in JTW [5] [16] and Holstein [17].

$$\begin{aligned}
& \left[\frac{J(J+1)-3\langle(\vec{J}\cdot\hat{j})^2\rangle}{J(2J-1)} \right] \left[\frac{1}{3} \frac{\vec{p}\cdot\vec{p}_\nu}{EE_\nu} - \frac{(\vec{p}\cdot\hat{j})(\vec{p}_\nu\cdot\hat{j})}{EE_\nu} \right] c_{\text{align}} \\
&= \Lambda_2 \left[(\hat{n}\cdot\frac{\vec{p}}{E})(\hat{n}\cdot\hat{k}) - \frac{1}{3} (\frac{\vec{p}}{E}\cdot\hat{k}) \right] f_{12}(E) / f_1(E) \quad (C.6)
\end{aligned}$$

Term	Integral
$f_1(E_\beta)$	$\int 1 \, d\hat{\Omega}_k = 4\pi$
$f_2(E_\beta)$	$\int \left(\frac{\vec{p}_\beta \cdot \hat{k}}{E_\beta} \right) d\hat{\Omega}_k = 0$
$f_3(E_\beta)$	$\int \left(\left(\frac{\vec{p}_\beta \cdot \hat{k}}{E_\beta} \right)^2 - \frac{1}{3} \frac{p_\beta^2}{E_\beta^2} \right) d\hat{\Omega}_k = 0$
$f_4(E_\beta)$	$\int \left(\hat{n} \cdot \frac{\vec{p}_\beta}{E_\beta} \right) d\hat{\Omega}_k = 4\pi \left(\hat{n} \cdot \frac{\vec{p}_\beta}{E_\beta} \right)$
$f_5(E_\beta)$	$\int \left(\hat{n} \cdot \frac{\vec{p}_\beta}{E_\beta} \right) \left(\frac{\vec{p}_\beta \cdot \hat{k}}{E_\beta} \right) d\hat{\Omega}_k = 0$
$f_6(E_\beta)$	$\int \left(\hat{n} \cdot \hat{k} \right) d\hat{\Omega}_k = 0$
$f_7(E_\beta)$	$\int \left(\hat{n} \cdot \hat{k} \right) \left(\frac{\vec{p}_\beta \cdot \hat{k}}{E_\beta} \right) d\hat{\Omega}_k = \frac{1}{3} 4\pi \left(\hat{n} \cdot \frac{\vec{p}_\beta}{E_\beta} \right)$
$f_8(E_\beta)$	$\int \hat{n} \cdot \left(\frac{\vec{p}_\beta \times \hat{k}}{E_\beta} \right) d\hat{\Omega}_k = 0$
$f_9(E_\beta)$	$\int \hat{n} \cdot \left(\frac{\vec{p}_\beta \times \hat{k}}{E_\beta} \right) \left(\frac{\vec{p}_\beta \cdot \hat{k}}{E_\beta} \right) d\hat{\Omega}_k = 0$
$f_{10}(E_\beta)$	$\int T_2(\hat{n}) : \left[\frac{\vec{p}_\beta}{E}, \frac{\vec{p}_\beta}{E} \right] d\hat{\Omega}_k = 4\pi T_2(\hat{n}) : \left[\frac{\vec{p}_\beta}{E}, \frac{\vec{p}_\beta}{E} \right]$
$f_{11}(E_\beta)$	$\int T_2(\hat{n}) : \left[\frac{\vec{p}_\beta}{E}, \frac{\vec{p}_\beta}{E} \right] \left(\frac{\vec{p}_\beta \cdot \hat{k}}{E} \right) d\hat{\Omega}_k = 0$
$f_{12}(E_\beta)$	$\int T_2(\hat{n}) : \left[\frac{\vec{p}_\beta}{E}, \hat{k} \right] d\hat{\Omega}_k = 0$
$f_{13}(E_\beta)$	$\int T_2(\hat{n}) : \left[\frac{\vec{p}_\beta}{E}, \hat{k} \right] \left(\frac{\vec{p}_\beta \cdot \hat{k}}{E} \right) d\hat{\Omega}_k = \frac{1}{3} 4\pi T_2(\hat{n}) : \left[\frac{\vec{p}_\beta}{E}, \frac{\vec{p}_\beta}{E} \right]$
$f_{14}(E_\beta)$	$\int T_2(\hat{n}) : \left[\hat{k}, \hat{k} \right] d\hat{\Omega}_k = 0$
$f_{15}(E_\beta)$	$\int T_2(\hat{n}) : \left[\hat{k}, \hat{k} \right] \left(\frac{\vec{p}_\beta \cdot \hat{k}}{E} \right) d\hat{\Omega}_k = 0$
$f_{16}(E_\beta)$	$\int T_2(\hat{n}) : \left[\frac{\vec{p}_\beta}{E}, \frac{\vec{p}_\beta}{E} \times \hat{k} \right] d\hat{\Omega}_k = 0$
$f_{17}(E_\beta)$	$\int T_2(\hat{n}) : \left[\hat{k}, \frac{\vec{p}_\beta}{E} \times \hat{k} \right] d\hat{\Omega}_k = 0$
$f_{18}(E_\beta)$	$\int T_3(\hat{n}) : \left[\frac{\vec{p}_\beta}{E}, \frac{\vec{p}_\beta}{E}, \frac{\vec{p}_\beta}{E} \right] d\hat{\Omega}_k = 4\pi T_3(\hat{n}) : \left[\frac{\vec{p}_\beta}{E}, \frac{\vec{p}_\beta}{E}, \frac{\vec{p}_\beta}{E} \right]$

Table C.4: Integrals of terms from Holstein's Eq. (51) [17].

$C_A = C'_A ; \quad g = \pm \frac{1}{\sqrt{2}} M_{GT} (C_A + C'_A)$ ← prefer \oplus
 $C_V = C'_V ; \quad a_1 = \pm \frac{1}{\sqrt{2}} M_F (C_V + C'_V)$ ← depends on above sign.

In our code:
 $M_F = 1.0$
 $M_{GT} = -0.62376$

Also in our Code:
 $g_V = 1.00$
 $g_A = 0.91210$

* in Holstein itself, sometimes g_A and g_V show up without their associated M_{GT} and M_F .

* Really, the conversion above doesn't include the extra terms in a_1 and g that couple to nuclear elements other than M_F and M_{GT} .

I think the point is that I should actually interpret:

$g_V = \pm \frac{1}{\sqrt{2}} (C_V + C'_V) = 1.0 \rightarrow a_1 = g_V M_F \Rightarrow C_V = C'_V = \frac{1}{\sqrt{2}}$
 $g_A = \pm \frac{1}{\sqrt{2}} (C_A + C'_A) \approx 0.91210 \rightarrow C_1 = g_A M_{GT} \Rightarrow C_A = C'_A = \frac{-0.91210}{\sqrt{2}} \approx -0.644952$

* Check: with $C_A = C'_A$ and $C_V = C'_V$, does JTW give the right A_β ?
 ~~$A_\beta = 0.323683 ; A_\beta = 0.496903 \rightarrow A_\beta = \underline{\underline{0.375394}}$ (bad!)~~

$A_\beta = 0.763671 \leftarrow$ Allow M_{GT} and M_F to have opposite signs. (Bad!)
 $A_\beta = -0.568045 \leftarrow$ enforce $\oplus M_{GT}$. Or earlier JTW "convention".
 * Because Holstein insists on his own sign convention, we get $M_{GT-Holstein} = -M_{GT-JTW}$

Figure C.1: "Notes 0"

In our code:

$$\boxed{\begin{array}{lll} M_F = 1.0 & ; g_V = 1.0 & \rightarrow g_V M_F = 1.0 \\ M_{GT} = -0.62376 & ; g_A = 0.91210 & \rightarrow g_A M_{GT} = -0.568931 \end{array}} \Rightarrow \rho \equiv \frac{g_A M_{GT}}{g_V M_F} \approx -0.568931$$

Holstein

* If we require that $C_A, C_A', C_V, C_V', M_F, M_{GT}$ are all real, and enforce that these can all take values which allow for Holstein and JTWW to be equivalent in some limits, we require:

$$\begin{array}{lll} \text{JTWW} & \text{Holstein} & \text{Holstein} \quad \text{JTWW} \\ \left\{ \begin{array}{l} f_1(E) \\ f_4(E) \end{array} \right. & \rightarrow \begin{array}{l} |a_1|^2 = |M_F|^2 (|C_V|^2 + |C_V'|^2) \\ |C_1|^2 = |M_{GT}|^2 (|C_A|^2 + |C_A'|^2) \end{array} \\ \downarrow & \downarrow & \downarrow \\ \rightarrow |g_1|^2 = 2|M_{GT}|^2 \cdot \text{Re}[C_A C_A'^*] \end{array}$$

$$\begin{aligned} \text{Re}[a_1^* C_1] &= -\text{Re}[M_F M_{GT} (C_V C_A'^* + C_V' C_A^*)] \leftarrow \text{later} \\ \text{Re}[a_1^* C_1] &= -\text{Re}[|M_F| |M_{GT}| (C_V C_A'^* + C_V' C_A^*)] \leftarrow \text{earlier.} \end{aligned}$$

The Results:

$$\begin{array}{lll} C_V = C_V' & \text{Holstein} & \text{JTWW} \\ C_A = C_A' & a_1 = \pm \frac{1}{\sqrt{2}} M_F (C_V + C_V') = \pm M_F (\pm \sqrt{2}) (C_V) \\ & C_1 = \pm \frac{1}{\sqrt{2}} M_{GT} (C_A + C_A') = \pm M_{GT} (\pm \sqrt{2}) (C_A) \end{array}$$

$$a_1 \approx g_V M_{F,H};$$

$$C_1 \approx g_A M_{GT,H};$$

~~Holstein~~

$$\boxed{M_{GT, \text{Holstein}} = -M_{GT, \text{JTWW}}}$$

which sign?!

$$a_1 \approx g_V M_F; \quad g_V = \pm \frac{1}{\sqrt{2}} (C_V + C_V') = 1.0; \quad M_F = 1.0; \quad ; \quad C_V = C_V'$$

$$C_1 \approx g_A M_{GT}; \quad g_A = \pm \frac{1}{\sqrt{2}} (C_A + C_A') \approx 0.91210; \quad M_{GT} = -0.62376; \quad C_A = C_A'$$

$\uparrow \uparrow$
JTWW terms!

Figure C.2: "Notes 1"

$$\begin{aligned}
b \cdot \bar{z} &= \pm 2\gamma \operatorname{Re} \left[|M_F|^2 (C_S C_V^* + C'_S C_V'^*) + |M_{GT}|^2 (C_T C_A^* + C'_T C_A'^*) \right] \\
&= -2\gamma \left[|M_F|^2 (C_S C_V^* + C'_S C_V'^*) + |M_{GT}|^2 (C_T C_A^* + C'_T C_A'^*) \right] \\
&= -2\gamma |M_F|^2 (C_S + C'_S) C_V^* + -2\gamma |M_{GT}|^2 (C_T + C'_T) C_A^* \\
&= -2\gamma |M_F|^2 \cdot \frac{1}{\sqrt{2}} g_V \underbrace{(C_S + C'_S)}_{+\sqrt{2} g_S} + -2\gamma |M_{GT}|^2 \frac{(-1)}{\sqrt{2}} g_A \underbrace{(C_T + C'_T)}_{-\sqrt{2} g_T} \\
&= -2\gamma |M_F|^2 \cdot g_V \cdot g_S - 2\gamma |M_{GT}|^2 \cdot g_A \cdot g_T \\
\boxed{b \cdot \bar{z} = -2\gamma [|M_F|^2 g_V g_S + |M_{GT}|^2 g_A g_T]}
\end{aligned}$$

~~BYE~~ $\gamma = (1 - \alpha^2 z^2)^{1/2}$

Figure C.3: "Notes 2"

To Match Up Holstein and JT W:

$$g_V = \frac{1}{\sqrt{2}}(C_V + C_V') ; \quad C_V = C_V' = \frac{1}{\sqrt{2}}g_V = \frac{1}{\sqrt{2}}$$

$$a_1 \approx g_V M_F$$

$$g_A = \frac{-1}{\sqrt{2}}(C_A + C_A') ; \quad C_A = C_A' = \frac{-1}{\sqrt{2}}g_A \approx \frac{-1}{\sqrt{2}}(0.91210) \quad c_1 \approx g_A M_{GT}$$

Also define:

$$g_S \equiv \frac{1}{\sqrt{2}}(C_S + C_S') ; \quad C_S = C_S' = \frac{1}{\sqrt{2}}g_S \approx 0$$

$$g_T \equiv \frac{-1}{\sqrt{2}}(C_T + C_T') ; \quad C_T = C_T' = \frac{-1}{\sqrt{2}}g_T \approx 0$$

Then, we find:

$$\ddot{\xi} = |M_F|^2(g_V^2 + g_S^2) + |M_{GT}|^2(g_A^2 + g_T^2)$$

$$A_p \ddot{\xi} = \frac{2}{5}|M_{GT}|^2(g_A^2 + g_T^2) + 2(\frac{3}{5})^{\frac{1}{2}}M_F M_{GT}(g_V g_A - g_S g_T)$$

$$b \cdot \ddot{\xi} = -2\gamma [|M_F|^2 g_V g_S + |M_{GT}|^2 g_A g_T] ; \quad \gamma \equiv (1 - \alpha^2 \zeta^2)^{\frac{1}{2}}$$

$$(E) \rightarrow F_o(E) + |M_F|^2 g_S^2 + |M_{GT}|^2 g_T^2$$

$$F_i(E) \rightarrow F_i(E) + \delta_{uv} \left(\frac{u}{u+1} \right) (-2) \cdot M_F M_{GT} \cdot g_S g_T + \alpha_{uv} \left(\frac{1}{u+1} \right) |M_{GT}|^2 g_T^2$$

Figure C.4: "Notes 3"

- * In some limits, Holstein and JT_W are equivalent. For simplicity, we will require that JT_W's terms $C_A, C_A', C_V, C_V', M_F$, and M_{GT} are entirely real.
- * The physical interpretation of this is that we ~~do not~~ require time-reversal symmetry to be obeyed.
- * We use the following relationships:

$$\begin{aligned} \zeta &= f(E) \rightarrow |C_V|^2 = |M_F|^2 \cdot (|C_V|^2 + |C_V'|^2) \\ A_B \zeta &= f'(E) \rightarrow |C_V'|^2 = |M_{GT}|^2 \cdot (|C_A|^2 + |C_A'|^2) \\ \end{aligned}$$

use the later JT_W sign convention.

$$\begin{aligned} |C_V|^2 &= 2 \cdot |M_{GT}|^2 \cdot \operatorname{Re}[C_A C_A'^*] \\ \operatorname{Re}[a_i^* C_V] &= -M_F M_{GT} \cdot \operatorname{Re}[C_V C_A'^* + C_V' C_A] \end{aligned}$$

- * Then, via trial and error, we find that the following set of relationships gives consistent results:

$$\begin{aligned} C_V &= C_V'; & a_i &= \left(\pm \frac{1}{\sqrt{2}} M_F (C_V + C_V') \right) \\ C_A &= C_A'; & g_i &= \left(\mp \frac{1}{\sqrt{2}} M_{GT} (C_A + C_A') \right) \end{aligned} \quad \text{Thus far, either set of signs is consistent. But they must be opposite.}$$

- * In our code, which evaluates Holstein, we use these:

$a_i \approx g_V M_F$	$M_F = 1.0$	$g_V = 1.0$	Note that we believe we know M_F better than we know g_A . So, to measure " A_B ", we vary g_A and leave M_{GT} fixed.
$g_A \approx g_A M_{GT}$	$M_{GT} = -0.62376$	$g_A \approx 0.91210$	

- * We'll define some quantities, ρ :

$$\rho_{JT\bar{W}} = \frac{C_A \cdot M_{GT}}{C_V \cdot M_F}; \quad \rho_{\text{Holstein}} = \frac{g_A \cdot M_{GT}}{g_V \cdot M_F} \approx -0.568931$$

* This $\rho_{JT\bar{W}}$ uses our own definition from PRL.

* Note that A_B comes out physically wrong unless $\rho_{JT\bar{W}}$ is \oplus , ie, in A_B , there's a term $\sim [C_V C_A'^* + C_V' C_A]$ and we need the whole thing to come out \oplus . $\therefore C_V$'s and C_A 's must have opposite signs.

- * We'll take the convention that every body has the same matrix elements:

$$\begin{aligned} M_{GT, JT\bar{W}} &= M_{GT, \text{Holstein}} \\ M_{F, JT\bar{W}} &= M_{F, \text{Holstein}} \end{aligned}$$

- * Then:

$$\begin{aligned} C_V &= C_V' \Rightarrow \oplus \\ C_A &= C_A' \Rightarrow \ominus \end{aligned} \quad \text{This because at the end of the day, we want Holstein's } a_i \text{ to be } \oplus, \text{ and } g_i \text{ to be } \ominus, \text{ or else we don't produce the right physics.}$$

$g_V = \frac{1}{\sqrt{2}} (C_V + C_V') = 1.0$	$C_V = C_V' = \frac{+1}{\sqrt{2}} g_V = \frac{1}{\sqrt{2}}$
$g_A = \frac{-1}{\sqrt{2}} (C_A + C_A') \approx +0.91210$	$C_A = C_A' = \frac{-1}{\sqrt{2}} g_A \approx \frac{-1}{\sqrt{2}} (0.91210)$

Figure C.5: "Notes 4"

- * In some limits, Holstein and JTW are equivalent. We require that JTW's terms $C_A, C_A', C_V, C_V', M_F$, and M_{GT} must all be entirely real. We can probably do this WLOG. (Or without very much loss of generality, at least.)
- * Use the following relationships:

$$\xi = f_x(E) \rightarrow |q_i|^2 = |M_F|^2 (|C_V|^2 + |C_V'|^2)$$

$$|q_i|^2 = |M_{GT}|^2 (|C_A|^2 + |C_A'|^2)$$

$$A \cdot \xi = f_x(E) \rightarrow |C_V|^2 = 2 \cdot |M_{GT}|^2 \cdot \text{Re}[C_V C_A'^*]$$

$$\text{Re}[q_i] = -\text{Re}[M_F M_{GT} (C_V C_A'^* + C_V' C_A)] \leftarrow \text{later JTW convention.}$$

we'll only use this.

- * Then, the following relationships give us internally consistent results:

$$\begin{aligned} C_V &= C_V' ; & a_i &= \pm \frac{1}{\sqrt{2}} M_F (C_V + C_V') \\ C_A &= C_A' ; & c_i &= \pm \frac{1}{\sqrt{2}} M_{GT} (C_A + C_A') \end{aligned} \quad \begin{array}{l} \text{either set of signs is consistent.} \\ \text{But they must be opposite.} \end{array}$$

Code has these signs for q_i and c_i .
Do I know why?

- * In our code (which evaluates Holstein), we use these values:

\oplus	$a_i \approx g_V M_F$	$M_F = 1.0$	$g_V = 1.0$
\ominus	$c_i \approx g_A M_{GT}$	$M_{GT} = -0.62376$	$g_A = 0.91210$

- * We can also define:

$\rho_{\text{Holstein}} \equiv \frac{g_A M_{GT}}{g_V M_F} \approx -0.568931$	$\rho_{\text{JTW}} \equiv \frac{C_A M_{GT}}{C_V M_F} \leftarrow \text{we use } \rho_{\text{JTW}} \text{ def. in PRL.}$
--	--

- * We do not get the correct JTW A_B unless we require that ρ_{JTW} is \oplus . Equivalently, we require that $\text{Re}[M_F M_{GT} (C_V C_A'^* + C_V' C_A)]$ must be \oplus . But M_{GT} is \ominus ! \rightarrow Option 1: Take $M_{GT, \text{JTW}} = -M_{GT, \text{Holstein}}$. \rightarrow Option 2: Take $C_A = C_A'$ to be \ominus , and $C_V = C_V'$ to be \oplus .

(really, there are other options.
But let's leave M_F and C_V alone.)

- * For Holstein to come out right, we need c_i to be \ominus , and q_i to be \oplus . I think.

\bullet $g_V = \frac{1}{\sqrt{2}} (C_V + C_V') = 1.0$
 $g_A = \frac{-1}{\sqrt{2}} (C_A + C_A') = 0.91210 \Rightarrow C_A \text{ must be } \ominus \text{ then, bc } g_A \text{ is } \oplus \text{ and } M_{GT, \text{Holstein}} \text{ is } \ominus, \text{ and we need } C_A \text{ to be } \ominus.$

- * OK. Now what do I do with C_S and G_T ? \rightarrow can't just stick them into M_F and M_{GT} . even in JTW it doesn't come out consistent.
- * Have to write JTW in Holstein notation so I can figure out where to put C_S, G_T in.

Figure C.6: "Notes 5"

Appendix D

Derivation of the b_{Fierz} Dependence of the Superratio Asymmetry

Appendix KLM you have to pick what you want— I hope that's Appendix K (that's this one!) – and remove the rest as you say they're "old". Appendix K could be moved to the end of Experimental Methods because it's absolutely critical and helpful!! but if you want to reference it there and leave it as an Appendix, it's up to you.

Recall the integrated JTW probability distribution for outgoing beta particles from Eq. (B.3):

$$\begin{aligned} d^3\Gamma(E_\beta, \hat{\Omega}_\beta) dE_\beta d^3\hat{\Omega}_\beta &= \frac{2}{(2\pi)^4} F_{\mp}(Z, E_\beta) p_\beta E_\beta (E_0 - E_\beta)^2 dE_\beta d^3\hat{\Omega}_\beta \xi \\ &\times \left[1 + b_{\text{Fierz}} \frac{m_e c^2}{E_\beta} + A_\beta \left(\frac{\vec{J}}{J} \cdot \frac{\vec{p}_\beta}{E_\beta} \right) \right]. \end{aligned} \quad (\text{D.1})$$

We note that the only angular dependence remaining in this equation is the dot product between the direction of beta emission and the direction of nuclear spin-polarization. This allows us to pull out a further factor of 2π by choosing the axis of polarization as defining our coordinate system, and integrating over the “ ϕ_β ” coordinate. The result is a bit more friendly to work with:

$$d^2\Gamma(E_\beta, \theta) dE_\beta d\theta = W(E_\beta) \left[1 + b_{\text{Fierz}} \frac{m_e c^2}{E_\beta} + A_\beta \frac{v_\beta}{c} |\vec{P}| \cos \theta \right] dE_\beta d\theta, \quad (\text{D.2})$$

where θ is the angle between the beta emission direction and the polarization direc-

tion, and is the only angular dependence that remains. Here, we have grouped the overall energy dependence into $W(E_\beta)$, so that

$$W(E_\beta) = \frac{2}{(2\pi)^3} F_\mp(Z, E_\beta) p_\beta E_\beta (E_0 - E_\beta)^2. \quad (\text{D.3})$$

We could also use this with the Holstein formulation, at least some of it. The point is, we can put *anything* that only depends on beta energy into $W(E_\beta)$. It doesn't matter, because it's already only integrable through numerical methods anyway – so we can't possibly make it worse.

In the TRINAT geometry with two polarization states (+/-) and two detectors (T/B) aligned along the axis of polarization, we are able to describe four different count rates, with different combinations of polarization states and detectors. Thus, neglecting beta scattering effects, we have:

$$r_{T+}(E_\beta) = \varepsilon_T(E_\beta) \Omega_T N_+ \left[1 + b_{\text{Fierz}} \frac{m_e c^2}{E_\beta} + A_\beta \frac{v}{c} |\vec{P}_+| \langle \cos \theta \rangle_{T+} \right] \quad (\text{D.4})$$

$$r_{B+}(E_\beta) = \varepsilon_B(E_\beta) \Omega_B N_+ \left[1 + b_{\text{Fierz}} \frac{m_e c^2}{E_\beta} + A_\beta \frac{v}{c} |\vec{P}_+| \langle \cos \theta \rangle_{B+} \right] \quad (\text{D.5})$$

$$r_{T-}(E_\beta) = \varepsilon_T(E_\beta) \Omega_T N_- \left[1 + b_{\text{Fierz}} \frac{m_e c^2}{E_\beta} + A_\beta \frac{v}{c} |\vec{P}_-| \langle \cos \theta \rangle_{T-} \right] \quad (\text{D.6})$$

$$r_{B-}(E_\beta) = \varepsilon_B(E_\beta) \Omega_B N_- \left[1 + b_{\text{Fierz}} \frac{m_e c^2}{E_\beta} + A_\beta \frac{v}{c} |\vec{P}_-| \langle \cos \theta \rangle_{B-} \right], \quad (\text{D.7})$$

where $\varepsilon_{T/B}(E_\beta)$ are the (top/bottom) detector efficiencies, $\Omega_{T/B}$ are the fractional solid angles for the (top/bottom) detector from the trap position, $N_{+/-}$ are the number of atoms trapped in each (+/-) polarization state, and $|\vec{P}_{+/-}|$ are the magnitudes of the polarization along the detector axis for each polarization state. $\langle \cos \theta \rangle_{T/B,+/-}$ is the average of $\cos \theta$ for *observed* outgoing betas, for each detector and polarization state combination. This latter term is approximately ± 1 as a result of our detector geometry, but contains important sign information. For a pointlike trap in the center of the chamber, 103.484 mm from either (DSSSD) detector, each of which is taken to be circular with a radius of 15.5 mm, we find that $\langle |\cos \theta| \rangle_{T/B,+/-} \approx 0.994484$, and is the same for all four cases. Note that a horizontally displaced trap will decrease the magnitude of $\langle |\cos \theta| \rangle$, but as it is an expectation value of an absolute value, all four will remain equal to one another. In the case of a vertically displaced trap,

Not quite true. Some strips are missing.

This is only true if we neglect (back-)scatter. This is not actually a good approximation. But we have pretty good simulations to give us the real numbers, anyway.

these four values will no longer all be equal, however it will still be the case that $\langle |\cos \theta| \rangle_{T+} = \langle |\cos \theta| \rangle_{T-}$, and $\langle |\cos \theta| \rangle_{B+} = \langle |\cos \theta| \rangle_{B-}$.

In the case of the present experiment, we note that $|\vec{P}_+| = |\vec{P}_-|$ is correct to a high degree of precision.

Is that definitely true,
or is it only true to
lowest order?

Appendix E

Derivation of the b_{Fierz} Dependence of the Superratio Asymmetry (Old)

See content at Appendix (D). After reading that stuff, continue here.

For simplicity, we will henceforth assume that the trap is vertically centered, and take $|\vec{P}_+| = |\vec{P}_-|$.

The trap is *not* centered, but the polarizations in the two states are equal, to a very high level of precision. More than we need for b_{Fierz} anyway, and probably more than we'd need for A_β .

We also define the following:

$$A' = A'(E_\beta) \equiv A_\beta \frac{v}{c} |\vec{P}| \langle |\cos \theta| \rangle \quad (\text{E.1})$$

$$b' = b'(E_\beta) \equiv b_{\text{Fierz}} \frac{mc^2}{E_\beta}, \quad (\text{E.2})$$

and choose a coordinate system in which the + polarization state is, in some sense, ‘pointing up’ toward the top detector, such that

$$\langle \cos \theta \rangle_{T+} \approx +1 \quad (\text{E.3})$$

$$\langle \cos \theta \rangle_{B+} \approx -1 \quad (\text{E.4})$$

$$\langle \cos \theta \rangle_{T-} \approx -1 \quad (\text{E.5})$$

$$\langle \cos \theta \rangle_{B-} \approx +1. \quad (\text{E.6})$$

This allows us to rewrite the four count rates in simplified notation, as:

$$r_{T+} = \varepsilon_T N_+ (1 + b' + A') \quad (\text{E.7})$$

$$r_{B+} = \varepsilon_B N_+ (1 + b' - A') \quad (\text{E.8})$$

$$r_{T-} = \varepsilon_T N_- (1 + b' - A') \quad (\text{E.9})$$

$$r_{B-} = \varepsilon_B N_- (1 + b' + A') . \quad (\text{E.10})$$

We further define the ‘superratio’, s , to be:

$$s = \frac{r_{T-} r_{B+}}{r_{T+} r_{B-}}. \quad (\text{E.11})$$

We are now in a position to define the ‘superratio asymmetry’, A_{super} , as

$$A_{\text{super}} = A_{\text{super}}(E_\beta) \equiv \frac{1 - \sqrt{s}}{1 + \sqrt{s}}. \quad (\text{E.12})$$

This is explicitly an experimental quantity that is measured directly by the above combination of count rates.

Writing the superratio out explicitly in terms of A' and b' , factors of $\varepsilon_{T/B}$ and $N_{+/-}$ cancel out entirely, and we find that

$$s = \frac{(1 + b' - A')^2}{(1 + b' + A')^2}. \quad (\text{E.13})$$

From here it is immediately clear that in absence of other corrections (*e.g.* backscattering, unpolarized background, ...), if $b' = 0$ it follows that $A_{\text{super}} = A'$. In the case where $b' \neq 0$, we find that

$$A_{\text{super}} = \frac{A'}{1 + b'} \quad (\text{E.14})$$

$$\approx A' (1 - b' + b'^2), \quad (\text{E.15})$$

where we have utilized the assumption that $b' \ll 1$. Thus,

$$A_{\text{super}} \approx A_\beta \frac{v}{c} |\vec{P}| \langle |\cos \theta| \rangle - A_\beta \frac{v}{c} |\vec{P}| \langle |\cos \theta| \rangle \left(b_{\text{Fierz}} \frac{mc^2}{E_\beta} \right) + A_\beta \frac{v}{c} |\vec{P}| \langle |\cos \theta| \rangle \left(b_{\text{Fierz}} \frac{mc^2}{E_\beta} \right)^2. \quad (\text{E.16})$$

Appendix F

Some Corrections to the Superratio Stuff (Old)

We consider further modifications to the rates described in Eqs. (D.4-D.7). In particular, we consider the effect of non-identical polarization magnitudes for the two polarization states and a trap displaced from the center.

We define for the polarization states:

$$P \equiv \frac{1}{2} (|\vec{P}_+| + |\vec{P}_-|) \quad (\text{F.1})$$

$$\Delta P \equiv \frac{1}{2} (|\vec{P}_+| - |\vec{P}_-|) \quad (\text{F.2})$$

and immediately find that

$$|\vec{P}_+| = P + \Delta P \quad (\text{F.3})$$

$$|\vec{P}_-| = P - \Delta P. \quad (\text{F.4})$$

Further, we also define:

$$\langle |\cos \theta| \rangle_T \equiv \langle |\cos \theta| \rangle_{T+} = \langle |\cos \theta| \rangle_{T-} \quad (\text{F.5})$$

$$\langle |\cos \theta| \rangle_B \equiv \langle |\cos \theta| \rangle_{B+} = \langle |\cos \theta| \rangle_{B-}, \quad (\text{F.6})$$

and

$$\langle |\cos \theta| \rangle \equiv \frac{1}{2} (\langle |\cos \theta| \rangle_T + \langle |\cos \theta| \rangle_B) \quad (\text{F.7})$$

$$\Delta \langle |\cos \theta| \rangle \equiv \frac{1}{2} (\langle |\cos \theta| \rangle_T - \langle |\cos \theta| \rangle_B). \quad (\text{F.8})$$

It immediately follows that

$$\langle |\cos \theta| \rangle_T = \langle |\cos \theta| \rangle + \Delta \langle |\cos \theta| \rangle \quad (\text{F.9})$$

$$\langle |\cos \theta| \rangle_B = \langle |\cos \theta| \rangle - \Delta \langle |\cos \theta| \rangle. \quad (\text{F.10})$$

With this new set of variables defined, we can re-write Eqs. (D.4-D.7) as

$$r_{T+}(E_\beta) = \varepsilon_T(E_\beta) N_+ \left[1 + b' + (A_\beta \frac{v}{c})(P + \Delta P) (\langle |\cos \theta| \rangle + \Delta \langle |\cos \theta| \rangle) \right] \quad (\text{F.11})$$

$$r_{B+}(E_\beta) = \varepsilon_B(E_\beta) N_+ \left[1 + b' - (A_\beta \frac{v}{c})(P + \Delta P) (\langle |\cos \theta| \rangle - \Delta \langle |\cos \theta| \rangle) \right] \quad (\text{F.12})$$

$$r_{T-}(E_\beta) = \varepsilon_T(E_\beta) N_- \left[1 + b' - (A_\beta \frac{v}{c})(P - \Delta P) (\langle |\cos \theta| \rangle + \Delta \langle |\cos \theta| \rangle) \right] \quad (\text{F.13})$$

$$r_{B-}(E_\beta) = \varepsilon_B(E_\beta) N_- \left[1 + b' + (A_\beta \frac{v}{c})(P - \Delta P) (\langle |\cos \theta| \rangle - \Delta \langle |\cos \theta| \rangle) \right] \quad (\text{F.14})$$

and the superratio becomes

$$s = \frac{(1 + b' - (A_\beta \frac{v}{c})(P - \Delta P) (\langle |\cos \theta| \rangle + \Delta \langle |\cos \theta| \rangle)) (1 + b' - (A_\beta \frac{v}{c})(P + \Delta P) (\langle |\cos \theta| \rangle - \Delta \langle |\cos \theta| \rangle))}{(1 + b' + (A_\beta \frac{v}{c})(P + \Delta P) (\langle |\cos \theta| \rangle + \Delta \langle |\cos \theta| \rangle)) (1 + b' + (A_\beta \frac{v}{c})(P - \Delta P) (\langle |\cos \theta| \rangle - \Delta \langle |\cos \theta| \rangle))} \quad (\text{F.15})$$

where $\varepsilon_{T/B}$ and $N_{+/-}$ still completely cancel out. After a bit of algebra, this simplifies to:

$$s = \frac{(1 + b' - A' + A_\beta \frac{v}{c} \Delta P \Delta \langle |\cos \theta| \rangle)^2 - (A_\beta \frac{v}{c})^2 (\Delta P \langle |\cos \theta| \rangle - P \Delta \langle |\cos \theta| \rangle)^2}{(1 + b' + A' + A_\beta \frac{v}{c} \Delta P \Delta \langle |\cos \theta| \rangle)^2 - (A_\beta \frac{v}{c})^2 (\Delta P \langle |\cos \theta| \rangle + P \Delta \langle |\cos \theta| \rangle)^2} \quad (\text{F.16})$$

Note that in the superratio ΔP and $\Delta \langle |\cos \theta| \rangle$ have cancelled out to first order, and the remaining dependencies are quadratic only. Eq. (F.16) is exact, but still a huge enough expression to be pretty unwieldy to work with. Let's introduce some

shorthand notation to make this less painful:

$$A'' := A_\beta \frac{v}{c} \quad (\text{F.17})$$

$$c := \langle |\cos \theta| \rangle \quad (\text{F.18})$$

$$\Delta c := \Delta \langle |\cos \theta| \rangle \quad (\text{F.19})$$

$$r' := 1 + b' + A_\beta \frac{v}{c} \Delta P \Delta \langle |\cos \theta| \rangle \quad (\text{F.20})$$

In this notation, we find that

$$s = \frac{(r' - A')^2 - (A'')^2 (\Delta P c - P \Delta c)^2}{(r' + A')^2 - (A'')^2 (\Delta P c + P \Delta c)^2}, \quad (\text{F.21})$$

which hurts a lot less to look at. Then, the superratio asymmetry is

$$A_{\text{super}} = \frac{1 - \sqrt{\frac{(r' - A')^2 - (A'')^2 (\Delta P c - P \Delta c)^2}{(r' + A')^2 - (A'')^2 (\Delta P c + P \Delta c)^2}}}{1 + \sqrt{\frac{(r' - A')^2 - (A'')^2 (\Delta P c - P \Delta c)^2}{(r' + A')^2 - (A'')^2 (\Delta P c + P \Delta c)^2}}} \quad (\text{F.22})$$

$$= \frac{\left[\sqrt{(r' + A')^2 - (A'')^2 (\Delta P c + P \Delta c)^2} - \sqrt{(r' - A')^2 - (A'')^2 (\Delta P c - P \Delta c)^2} \right]^2}{\left[(r' + A')^2 - (A'')^2 (\Delta P c + P \Delta c)^2 \right] - \left[(r' - A')^2 - (A'')^2 (\Delta P c - P \Delta c)^2 \right]} \quad (\text{F.23})$$

$$= \frac{\left(\begin{array}{l} 2 \left[(r')^2 + (A')^2 - (A'')^2 ((P \Delta c)^2 + (\Delta P c)^2) \right] \\ -2 \left[(r' + A')^2 - (A'')^2 (\Delta P c + P \Delta c)^2 \right]^{1/2} \left[(r' - A')^2 - (A'')^2 (\Delta P c - P \Delta c)^2 \right]^{1/2} \end{array} \right)}{4 \left[(r' A') - (A'')^2 (P c \Delta P \Delta c) \right]} \quad (\text{F.24})$$